# Synthesis, Characterization and Redox Properties of Antiaromatic Isophlorin, Confused and Carba Isophlorins

A thesis
Submitted in Partial Fulfilment of the Requirements
for the Degree of

**Doctor of Philosophy**

By

**Panchal Santosh Prakashrao**
ID: 20113127


**Indian Institute of Science Education and Research (IISER), Pune**

**2017**

*Dedicated to*

*My parents*

*Mr. and Mrs. Prakashrao and Sarojadevi*

*and*

*my beloved siblings*

*Dhanaraj, Bhagyashree and Jayshree*

# Certificate

Certified that the work described in this thesis entitled ***"Synthesis, Characterization and Redox Properties of Antiaromatic Isophlorin, Confused and Carba Isophlorins"*** submitted by *Mr. Panchal Santosh Prakashrao* was carried out by the candidate, under my supervision. The work presented here or any part of it has not been included in any other thesis submitted previously for the award of any degree or diploma from any other university or institution.

Date: 19th January, 2018

**Dr. V. G. Anand**
Research Supervisor

# Declaration

I hereby declare that this thesis contains original research work which represents my ideas in my own words and wherever necessary other's ideas have been included, I have adequately cited and referenced the original sources. I have also declare that I have adhered to all principles of academic honesty and integrity and have not misrepresented or fabricated or falsified any idea/data/fact/source in this submission. I understand that violation of the above will result in disciplinary actions by the institute and can also evoke penal action from the sources, which have thus not been taken when needed.

Date: 19th January, 2018

**S. P. Panchal**
ID: 20113127

# Acknowledgements

*"Completion of this doctoral dissertation was possible with the support of several people. I would like to express my sincere gratitude to all of them".*

*Foremost, I would like to express my sincere gratitude to my thesis advisor Prof. V. G. Anand for the continuous support during my Ph.D. study and research, for his scholarly inputs, motivation and enthusiasm that I have received throughout the research work. This notable achievement was possible only because of the unconditional support provided by Sir. I consider it as a great opportunity to do my doctoral programme under his guidance and to learn from his research expertise. Thank you Sir, for all your help and support. Further, I thank him in believing in my abilities and giving work freedom during my Ph.D. It is difficult to compose appropriate sentence to express my gratefulness to him for his guidance and keen interest which made this work possible. I could not have imagined having a better advisor and mentor for my Ph.D study.*

*I am extremely thankful to Prof. K. N. Ganesh for providing excellent research facilities and outstanding research environment.*

*I am also grateful to my research advisory committee (RAC) members Dr. J. Nithyanandhan (NCL, Pune) and Dr. Shabana Khan (IISER, Pune) for their valuable suggestions and advices.*

*I am thankful to Dr. T. S. Mahesh, Dr. R. G. Bhat, Dr. M. Jayakannan, Dr. Jetendra Chug, Dr. Musthafa and Dr. Sunil Nair for their assistance during my research period. In fact, I obliged to pay heartiest thank to every faculty members of IISER-Pune.*

*I am really lucky to have wonderful lab mates. It's my pleasure to thank to all the lovable Dr. VGA lab members Dr. T. Y. Gopalakrishna, Dr. Kiran Reddy, Dr. Santosh C. Gadekar (for their constant help in experimental and theoretical studies), Dr. Neelam Shivran, Dr. Rashmi Nayak, Dr. Jyostna Arora, Dr. Brijesh Chandra, Dr. Sujit P. Chavan, Rakesh Gaur, Madan*

*Ambhore, Ashok kumar B., Udaya H. S., Prachi Gupta, Rajkumar and Swati Deswal as they always maintained a very lively environment inside lab.*

*My sincere thanks to Dr. Rajesh G. Gonnade (NCL, Pune) for his help and his excellent course on crystallography and Dr. Ms. Vrindha V., SAIF department (IIT B) for EPR facility.*

*I thank Dr. V. S. Rao and Santosh Nevse for their precious support and timely help. I thank Dr. Umesha Reddy Kacherki (deputy librarian) and Ms. Anuradha for library support. I thank IISER, Pune administrative staff members especially Mayuresh, Nayana, Tushar, Mahesh, Nitin, Sandip, Yatish and Megha for their generous support.*

*I thank Suresh Prajapat, Syed, Somnath and Pappu from UG lab IISER, Pune. I thank Ms. Neeta Deo and Mr. Salim for IT support.*

*I acknowledge the help from Archana (SCXRD), Pooja Lunawat, Chinmay L. and Deepali J. (NMR), Swati M. Dixit (MALDI), Swathi, Nayana and Sandip (HRMS) for the instrument support.*

*I am also very much thankful to all my friends for their constant love and support for me, specially, Sujata B., Snehal P., Harshal S., Satej D., Pravin S., Govind S., Prashant U. and Sharad V. they are all encouraged me during my weak times.*

*I am also thankful to all my beloved juniors inside and outside IISER Pune for their unconditional love on me and their constant suggestions, support and help because, my field study was made less obstacle ridden due to the presence of a few individuals and I must give special thanks to them specially; Nilesh D., Mahesh N., Ganesh S., Madan A., Suraj T., Vikas K., Amol P., Sujit C., Mangesh B., Ganesh N., Avinash P., Laxman S., Pralhad D., Durgaprasad S., Balaji K., Kapil K., Nagesh D., Ramdas I., Sopan I., Siddharth W., Sharad L., Shiva P., Vijay T., Praful B., Datta K., Arvind G., Pramod S., Shailesh G., Vikas W., Baswaraj K., Suresh B., Madhav J., Rahul J., Priyanka D., Sudhir B., Dnyaneshwar B., Abhay J., Pradeep D., Vishal K., Vaibhav P., and indeed it is difficult to name out all of them whose contribution in my life is enormously valuable.*

*No words can ever convey my sense of gratitude felt for my parents (my father; Mr. Prakashrao and Mother; Mrs. Sarojadevi) and my siblings (Dhanaraj, Bhagayshree and Jayshree).*

*Finally, I am thankful to council of Scientific and Industrial Research (CSIR) for Research Fellowship (JRF and SRF).*

*Above all, I obliged to pay it all to Almighty God "**Lord Krishna**" for granting me the wisdom, health and strength to undertake this research task and enabling me to its completion.*

*Due acknowledgement to them, whose names are unintentionally missed out, despite their unconditional help throughout my life.*

***Santosh***

# Contents

# Synopsis

The present thesis entitled ***''Synthesis, Characterization and Redox Properties of Isophlorins, Confused and Carba Isophlorins''***, describes the successful attempts at the synthesis of stable antiaromatic macrocycles which belong to the class of isophlorinoids. The 20π tetrapyrrolic isophlorin was introduced by Woodward as a hypothetical intermediate during the synthesis of chlorophyll. Till date pyrrole based isophlorins have been found to be unstable under ambient condition due to its rapid oxidation to stable 18π aromatic porphyrin. Substantial efforts were made by Vogel and co-workers to realize such stable 20π macrocycles from other heterocycles such as thiophene, furan and selenophene. However, few other groups were reasonably successful in the synthesis of 20π macrocycles. This thesis focuses on the isophlorin framework, resulting in the synthesis of novel antiaromatic isophlorins and confused isophlorins. Apart from syntheses and structural characterization, electronic and redox properties of these macrocycles have been described with suitable support from quantum mechanical calculations.

In the first chapter the development of synthetic isophlorin chemistry is described. The second chapter describes the synthesis and characterization of the first stable 20π electrons antiaromatic isophlorin containing a pyrrole and three furan rings in the macrocyclic core. The role of core-modification of a porphyrin was analyzed by sequential replacement of individual pyrrole rings. Core-modified porphyrins retain similar structural characteristics with altered electronic properties compared to the parent porphyrin macrocycle. It is observed that replacing two pyrrole units in porphyrin with other five membered heterocycles such as furan/thiophene/selenophene, does not block the 18π electronic framework. Replacing all three or four pyrroles by furans or thiophenes altered the conjugated pathway from the 18π to 20π network, with negligible change in its ring size. Surprisingly, the macrocycle with 20π monopyrrole did not attract sufficient attention of synthetic chemists in spite of its striking antiaromatic structure. A [2+2] Mc Donald condensation strategy was employed with a modified dipyrromethane and meso-phenyl difuran carbinol under acidic conditions followed by oxidation. A detailed analysis confirmed the formation of a highly antiaromatic macrocycle with NH inside the core of the macrocycle. Isophlorins are known to undergo two-electron oxidation which leads to the formation of a stable 18π aromatic porphyrin. The synthesized mono pyrrole 20π antiaromatic macrocycle further underwent two-electron oxidation upon addition of oxidizing agents which gave the corresponding stable 18π aromatic dication. These macrocycles were unambiguously characterized through spectroscopic techniques such as $^{1}$H NMR, UV-Vis, ESR, Cyclic Voltammetry and single crystal X-ray diffraction in addition to computational studies.

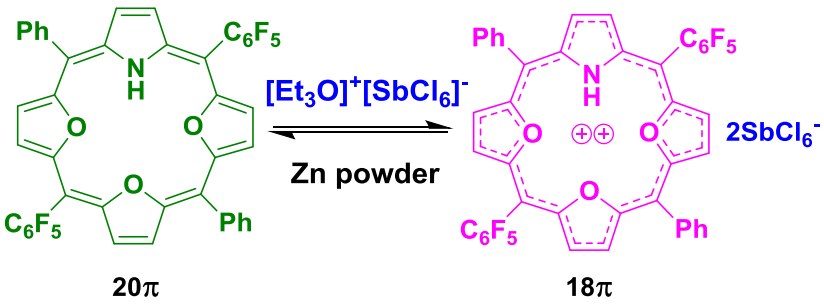


20π 18π

The third chapter describes the synthesis and redox properties of first generation tetrathia S-Confused isophlorins. The reported N-confused porphyrin and neo-confused porphyrin represent structural isomers of porphyrin and have attracted significant interest for the synthesis of porphyrinoid organometallic complexes. These porphyrin skeletons have been obtained by switching the positions of a carbon and nitrogen in a single pyrrole ring. Latos-Grazynski and co-workers reported a confused porphyrin in which a thiophene ring was inverted similar to the confused pyrrole of N-confused porphyrin. Its oxidation yielded an exocyclic keto group on the α-carbon of the confused thiophene ring with enhanced aromaticity. Replacing all the pyrrole units in N-confused porphyrin by thiophene resulted in the formation of a 20π tetrathia S-Confused anti-aromatic isophlorin. Hence, an equimolar ratio of thiophene diol and a confused trithiophene were subjected to condensation in acidic medium under inert conditions followed by oxidation with $FeCl_3$ leading to the formation of α-chlorinated tetrathia S-Confused isophlorin. The two-electron oxidation of this tetrathia S-Confused isophlorin as yielded an expected 18π aromatic mono cation instead of its corresponding 18π macrocyclic dication. The formation of this confused isophlorin was successful only when $FeCl_3$ was employed as the oxidizing agent. When DDQ employed as an oxidizing agent the macrocycle did not undergo complete oxidation and instead it yielded a semi-conjugated macrocycle. To prevent the chlorination of confused thiophene ring, a similar macrocycle having methyl substituent at the alpha position of confused thiophene ring was synthesized. Both the macrocycles displayed weak paratropic ring current effect which is because of the reduced overlap of π orbitals due to the 2,4 link of the thiophene in the 20π electronic framework. Molecular structure obtained from single crystal X-ray diffraction analysis revealed the oxidation of C-Cl bond to C=O on the alpha carbon of the confused thiophene ring. In addition, the macrocycle was associated with a $[SbCl_6]^-$ counter anion, suggesting the oxidation of the macrocycle to a mono cationic species. Further support for this understanding came from the unanticipated resistance of methyl substituted tetrathia S-Confused isophlorin towards two-electron oxidation under similar conditions. Despite structural resemblance to a confused porphyrin, spectroscopic and computational studies reveal weak paratropic ring current effects in 20π tetrathia S-Confused isophlorin. All the macrocycles in this chapter were characterized using $^1H$ NMR, UV-Vis, ESR, Cyclic Voltammetry and single crystal X-ray diffraction studies along with computational studies. Further, theses studies revealed the substituent dependent macrocycle oxidation unfamiliar to the chemistry of anti-aromatic isophlorinoids.

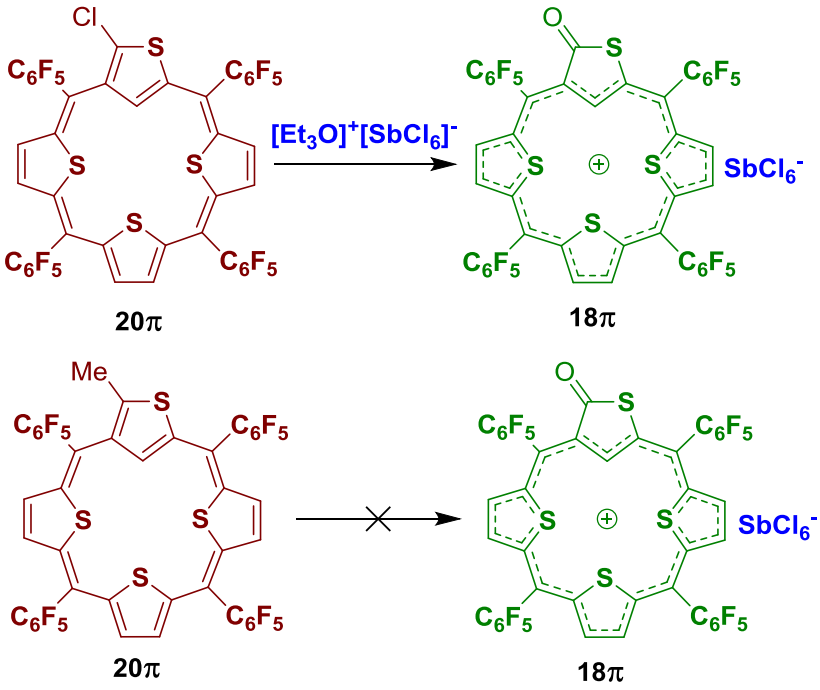


The fourth chapter details the synthesis and structural characterization of azulene expanded 28π expanded isophlorin. It was reported that introduction of an azulene moiety to the porphyrinoid framework is of particular interest because of its redox active nature and employed in the construction large number of redox active molecules. Exploration of this concept led to the synthesis of azuliporphyrins and its hetero analogues, which exhibit borderline macrocyclic aromaticity compared to porphyrins and N-confused porphyrins. These azuliporphyrins have unique electronic features, such as near-infrared absorptions, high extinction coefficients, or small HOMO-LUMO gaps. Latos-Grazynski and co-workers reported the dithiadiazuliporphyrin and dioxadiazuliporphyrin. Further, these non-nitrogenous azuliporphyrins are easily oxidizable to its radical cation or dication and again it was observed that addition of excess DDQ exclusively resulted in the formation of its dication, which can further reduced back to its neutral state macrocycle using suitable reducing agents. Based on this information, it is very well established that expanding the π network of isophlorin is an ideal strategy to synthesize large and stable 4nπ macrocycles and molecules containing such extended π-electron chromophores for their potential in applications such as optoelectronics, electrochromic, or molecular conductivity. These systems are expected to have different properties compared to the aromatic counterparts. If the azulene appended porphyrin is expanded by inserting additional two other heterocycles other than pyrrole such as thiophene, the formed macrocycle will be expected to be a 28π electron macrocycle. Unlike the nitrogen, the chalcogens are not capable of sustaining a double bond with α carbons in the heterocyclic unit and hence, the π circuit is forced to flow only through the carbon atoms. Anticipating analogous macrocycles under identical reaction conditions, catalytic amount of boron trifluoride etherate was added to an equimolar ratio of bithiophene diol and azulene. MALDI-TOF/TOF mass spectrum of the reaction mixture confirmed the formation of the expected

28π macrocycle containing two bithiophene units connected to two azulene rings. The NMR characterization and computational studies revealed weak paratropic ring current effects for this macrocycle. Further, it displayed reversible two-electron oxidation to the aromatic 26π dication using appropriate oxidizing reagents. The formation of dication was confirmed by high resolution mass spectroscopy. It also displayed significant diatropic ring current effects in its $^{1}$H NMR spectrum which was further supported by computational studies. The reversible oxidation of this dication was monitored by electronic absorption spectroscopy and the dication underwent a red shifted absorption compared to free base macrocycle. The molecular structure determined using single crystal X-ray diffraction analysis for free base macrocycle displayed a bowl shaped conformation in which two diagonal azulene units are tilted from the plane of the macrocycle. However, these studies indicated that free base 28π macrocycle displayed a weak paratropic behaviour and its dication showed a significant diatropic ring current effect. In conclusion, the present thesis describes the successful synthesis of stable isophlorins, confused isophlorins, azulene containing expanded isophlorins and their redox properties by controlled core modification of porphyrin, N-confused porphyrins and non-nitrogenous azuliporphyrins.

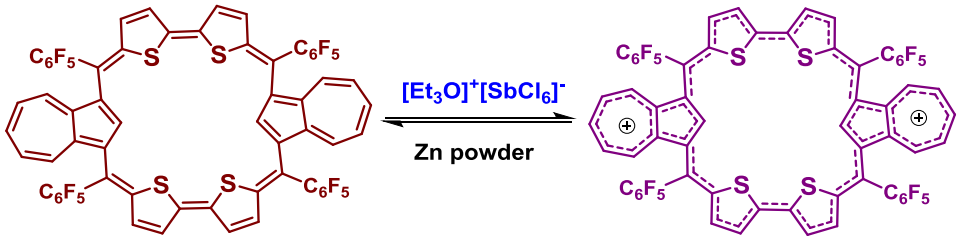


28π 26π

# Publications

- **S. P. Panchal**, S. C. Gadekar, V. G. Anand, *Angew. Chem., Int. Ed.* **2016**, 55, 7797-7800. Controlled Core- Modification of a Porphyrin into an Antiaromatic Isophlorin.

- **S. P. Panchal**, V. G. Anand, *Org. Lett.* **2017**, 19, 4854-4857. Oxidative Transformation of a Tetrathia S-confused Isophlorin into Porphyrin cation.

# Chapter I

# Introduction

## I.1. Introduction:

Porphyrin **I.1**, is a planar aromatic system whose main conjugation pathway contains 18π electrons and thus obeys the Hückel's rule for aromaticity having (4n + 2) number of π electrons that provides ring current effect for the macrocycle. Because of this planar, cyclic π electron conjugation system, the molecule strongly absorbs in the region between 400 and 600nm[1]. The presence of diamagnetic anisotropy in the porphyrin ring is evident from its $^1$H NMR spectral analysis, wherein the *meso* and pyrrolic protons resonate at the downfield region, while the inner NH protons appear in the negative region of the $^1$H NMR spectrum and represent one of the most widely studied of all known macrocyclic ring systems. This versatile family of tetrapyrrolic macrocycles is present at the active site of several bio-molecules owing to their ability to bind variety of metal ions in various oxidation states. Interest in these tetrapyrrolic macrocycles is broadly based on the multiple biological functions which includes electron transfer, oxygen transport and catalytic substrate oxidation[2]. Porphyrin derivatives **I.2**, **I.3** and **I.4** are also known for their ability to form wide variety of metal complexes[3,4]. These interesting chemical properties of porphyrin have inspired the study of a whole range of porphyrin derivatives in the past few decades. Besides their biological importance, the porphyrins have found added applications in almost every research field ranging from materials to medicine[5] and their electronic properties can be precisely analysed even upon subtle structural modification. One such modification is the core-modification by replacing pyrrole units of porphyrin with other heterocyclic units, such as thiophene, furan and selenophene.

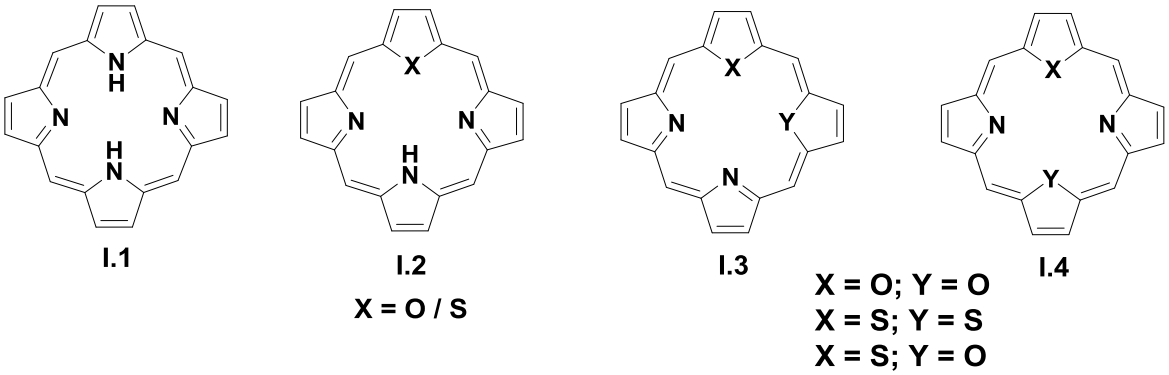


This new class of porphyrin is called core-modified porphyrins or heteroatom-containing porphyrin (**I.2**, **I.3** and **I.4**) which are aromatic macrocycles and display very interesting physicochemical properties quite different compared to the parent porphyrin **I.1**. The properties of heteroatom substituted core modified porphyrins depend upon the number of different heterocycles present in the core of the macrocycle. The mono-heteroatom substituted porphyrin can be synthesized by the replacement of a pyrrole unit by any one of the five-membered heterocycles such as furan, thiophene or selenophene units. The synthetic route for this mono-substituted porphyrin is the widely accepted condensation of 2,5-bis(arylhydroxymethyl)heterocyclopentadiene **I.5**, with benzaldehyde and pyrrole in 1:2:3 ratio under

acidic conditions followed by oxidation with DDQ to get the desired mono-heteroatom substituted porphyrin **I.6**, as its thiophene and furan analogues[6,7].

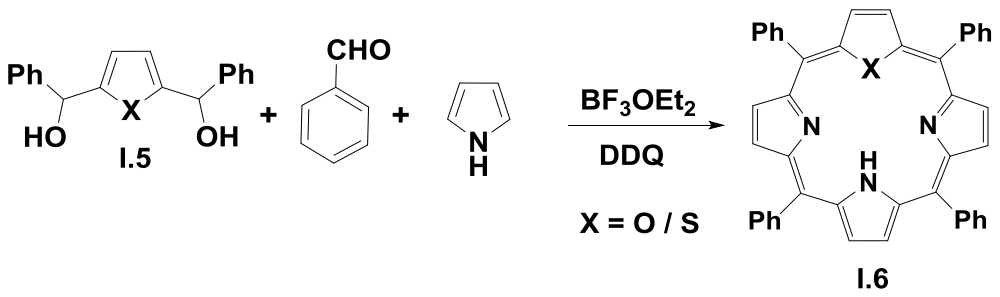


The thia-porphyrins with three pyrrole and one thiophene unit are known to stabilize metal ions, such as Cu and Ni in its +1 oxidation state[8]. Another, class of core modified porphyrin is the dihetero atom substituted porphyrins, in which two of the pyrrole rings were substituted by other heterocyclic rings such as furan or thiophene forming ($N_2X_2$) or ($N_2XY$) inside the core of the macrocycle. These porphyrins containing different heteroatoms display altered properties compared to monohetero porphyrins. There are of two types of such macrocycles based on the presence of heteroatoms at different positions inside the macrocyclic core; 21,22-diheteroporphyrin **I.7**, which corresponds to *cis*- and 21,23-diheteroporphyrin **I.8**, corresponding to *trans*- with respect to same or different hetero atoms.

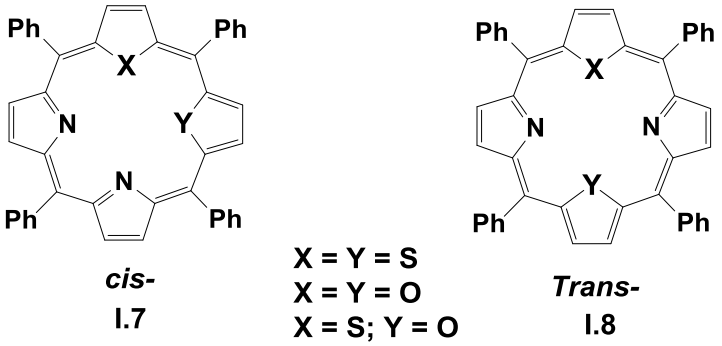


The *cis*- isomer 21,22-diheteroporphyrin having two different heterocyclic units such as furan and thiophene is synthesized by the condensation of appropriate dicarbinol of furan and thiophene units such as 1,9-bis(phenylhydroxymethyl)-5-phenyl-difuryl **I.9a**, or dithienyl **I.9b**, or thienylfuryl dicarbinol **I.9c**, with 5-phenyl-dipyrromethane **I.10**, in equimolar ratio using mild acid catalyst followed by oxidation with 2,3-dichloro-5,6-dicyano-1,4-benzoquinone (DDQ) gave the desired products[9] **I.7a**, **I.7b** and **I.7c**. But there are only few reports on this cis-type of porphyrins and they have not been explored to greater extent as they are found to decompose rapidly because of their unstable nature.

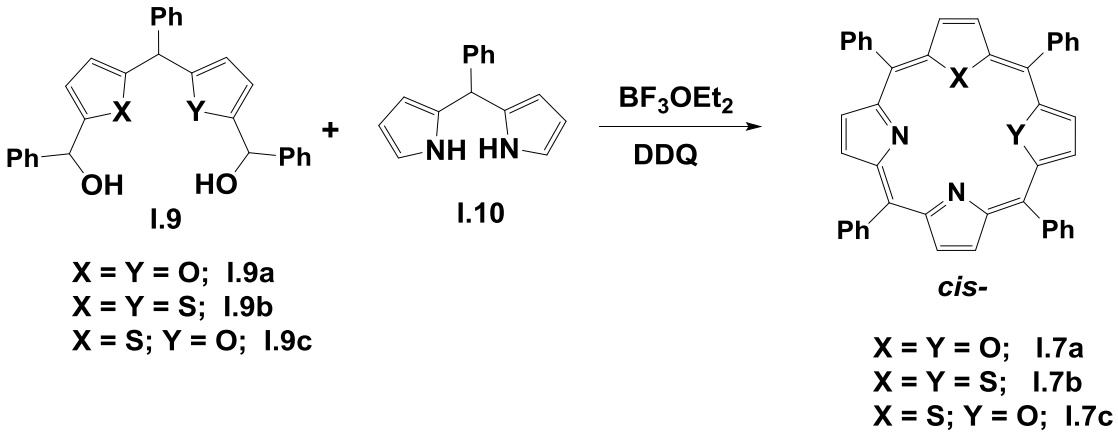


Another class of diheteroporphyrin that resulted from the replacement of two pyrrole units from trans positions led to the formation of 21,23-diheteroporphyrin of $N_2X_2$ or $N_2XY$ type. The *trans*- isomer is synthesized by the condensation of 2,5-bis(aryl-alpha-hydroxymethyl)heterocycle **I.5**, with pyrrole under mild acidic conditions followed by oxidation with DDQ yielded diheteroporphyrin[10] **I.8a** and **I.8b**.

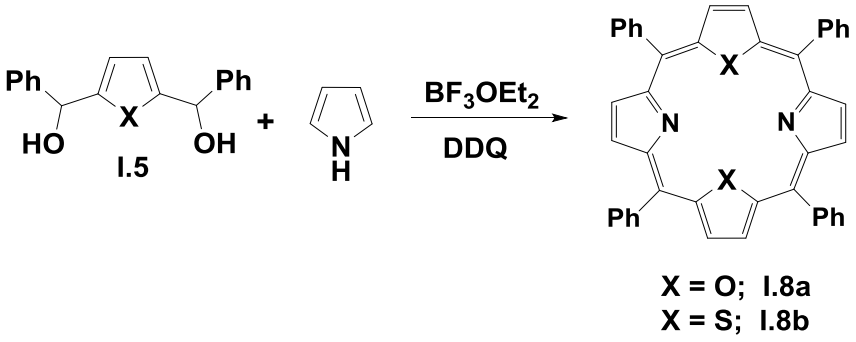


The second mixed diheteroporphyrin isomer has been synthesized by the condensation reaction between appropriate diol of thiophene or furan **I.5a**, with modified tripyrrane **I.11**, followed by oxidation using DDQ to yield **I.11-a**, as the diheteroporphyrin[11].

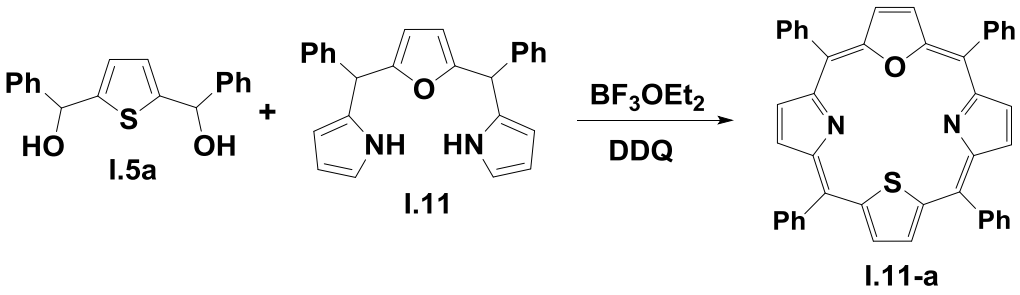


This method is a better choice for the preparation of several *meso*-tetraaryl 21,23-diheteroporphyrin[6,7] of the $N_2X_2$ type and the mixed 21,23-diheteroporphyrin[11] of the $N_2XY$ type **I.11a**.

## I.2. N-Confused Porphyrin:

N-confused porphyrin (NCP) **I.12** and **I.13**, is a structural isomer of porphyrin **I.1**, having same number of 18π electron macrocyclic conjugation as in porphyrin, where one or more nitrogen atoms are outside the ring. These porphyrin isomers having an inner CH and the presence of nitrogens inside and outside the ring have become attractive synthetic targets owing to their potential chemical interest and versatile coordination chemistry towards variety of metal ions.

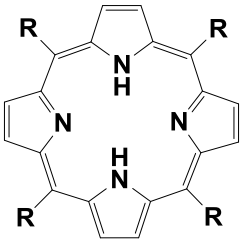

**I.1**
**R = H**

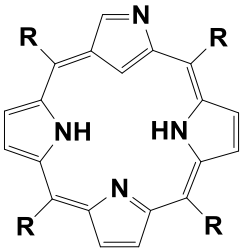

**I.12**
**R = $C_6H_5$**

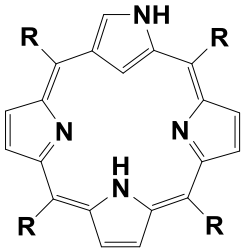

**I.13**

In 1994, Latos-Grazynski[12] et. al. and Furuta[13] et. al. independently reported the N-confused porphyrin 5,10,15,20-tetraaryl-2-aza-21-carbaporphyrin **I.12a**. The availability of an inner CH and an outer nitrogen atom arising from alpha-beta linkage of an inverted pyrrole **I.12a**. **NCP** differed largely from the parent porphyrin in its chemical, structural, and coordination properties. The peripheral nitrogen of N-confused porphyrinoids acts as a binding site for various cation, anion, and neutral species, to form supramolecular architectures. The first confused porphyrin rings reported were 5,10,15,20-tetraphenyl-2-aza-21-carbon porphyrin **I.12a**, or N-confused tetraphenylporphyrins and 5,10,15,20-tetratolyl-2-aza-21-carbon porphyrin **I.12b**, by the condensation of pyrrole and aldehydic partner in the presence of acid catalyst followed by oxidation with *p*-chloranil.

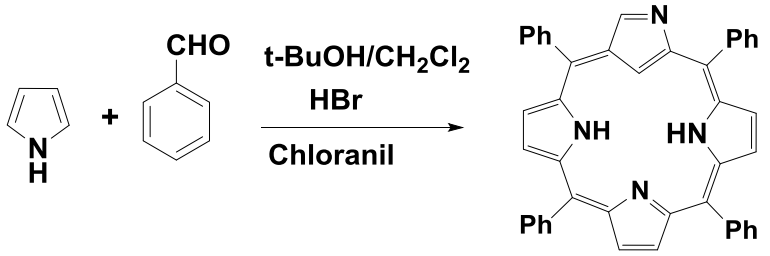


I.12a

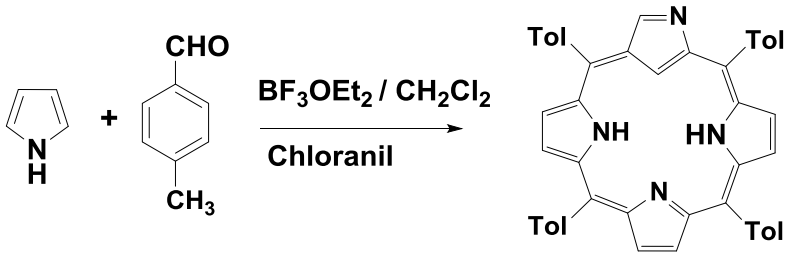


I.12b

Since its invention, the chemistry of NCP has attracted significant research interest, and several new types of confused porphyrins have been synthesized for exploring their metal-coordination properties[14]. NCP isomers containing heteroatoms other than pyrrole units have also been reported by the modification of macrocyclic core. One such core modification wherein the pyrrole of NCP is replaced by other heterocycles such as thiophene **I.14a**, furan **I.14b**, and selenophene **I.14c** results in the formation of core-modified confused porphyrins **I.14**. These analogs were first reported by the three independent groups[15] and they form unusual metal complexes, with interesting properties. There are few reports in the literature on confused heteroporphyrins. The confusion can be due to the pyrrole ring[15] or from the other heterocycle[16], such as thiophene, furan, and selenophene. Thus, these confused heteroporphyrins can be further sub-classified into two types such as N-confused heteroporphyrins **I.14**, and heteroatom- confused heteroporphyrins **I.15** and **I.16**.

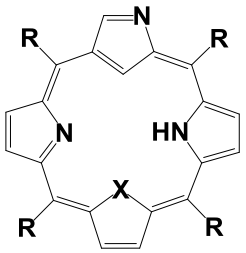

**I.14**

**X = S; I.14a**
**X = O; I.14b**
**X = Se; I.14c**

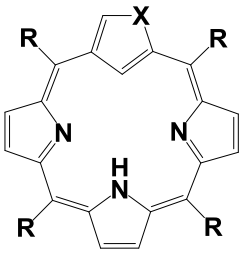

**X = S; I.15**

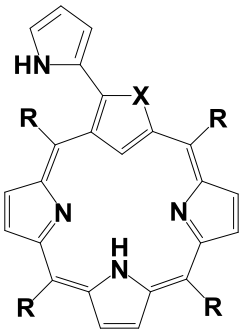

**X = O; I.16**

The first synthesis report on N-confused 21-thiaporphyrins and 21-oxaporphyrins by Lee and co-workers[17-19] described the condensation of 2,4-bis(α-hydroxy-α-phenylmethyl)pyrrole **I.18**, with 16-thiatripyrrane **I.11a**, or 16- oxatripyrrane **I.11b**, under acidic conditions followed by oxidation with DDQ led to yield the N-confused 21-thiaporphyrins **I.14a** and N-confused-21-oxaporphyrins **I.14b**.

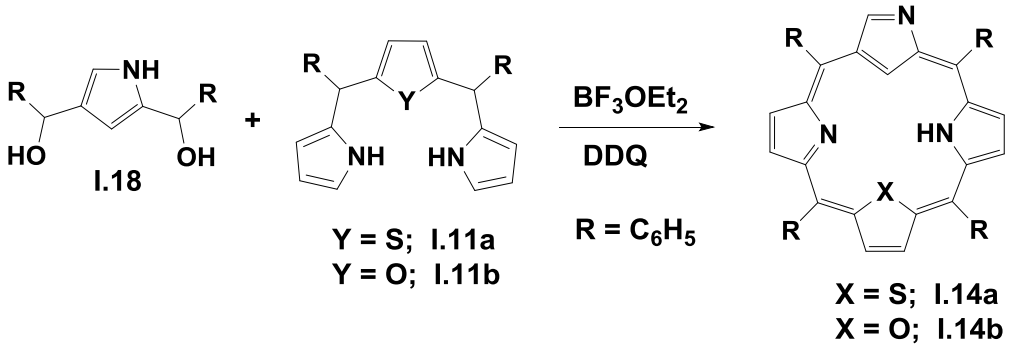


The heteroatom-confused heteroporphyrins such as S-confused porphyrin, 5,10,15,20-tetraphenyl-2-thia-21-carbaporphyrin **I.16a**, was reported for the first time by Latos-Grazynski and co-workers[20,21]. The target molecule can be synthesized either by the condensation of 2,4-bis-(phenylhydroxymethyl)thiophene **I.20**, with benzaldehyde and pyrrole via one-pot, two-step reaction or by condensing the 2,4-bis-(phenylhydroxymethyl)thiophene **I.20**, with 5,10-diphenyltripyrrane **I.21**, followed by oxidation with DDQ or *p*-chloranil to yield the S-confused porphyrin **I.16a**. In the presence of excess oxidant, a new compound **I.22**, was formed.

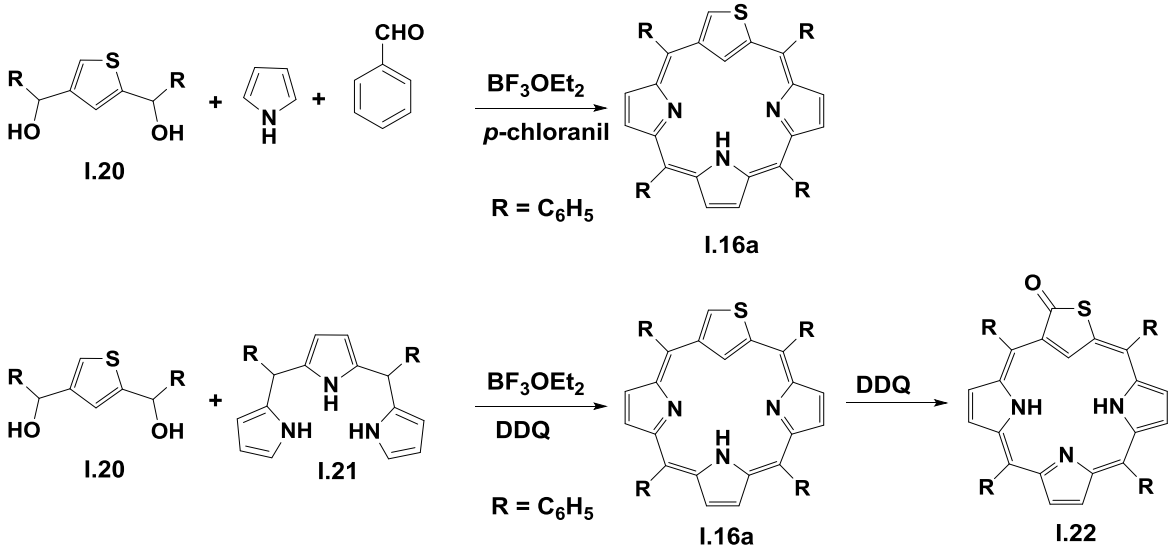


The S-confused porphyrin **I.16a**, displayed borderline aromaticity as analysed from the $^{1}$H NMR resonances of its inner NH proton, which appeared at 5.81 ppm, and the inner CH proton of inverted thiophene, which appeared at 4.76 ppm. However, the new S-confused porphyrin **I.22** derivative exhibited

strong aromatic features with inner CH and two inner NH resonances appearing at −5.31, −3.37, and −2.93 ppm, respectively. The S-confused porphyrin[22] **I.16a**, displayed interesting metal binding properties. Upon treating with metal chlorides such as $CdCl_2$ and $ZnCl_2$ it was observed that the Cd(II) and Zn(II) ions were bound to S-confused porphyrin with three core nitrogen atoms and one axial chloride ligand and, thus, the macrocycle behaved as a monoanionic ligand.

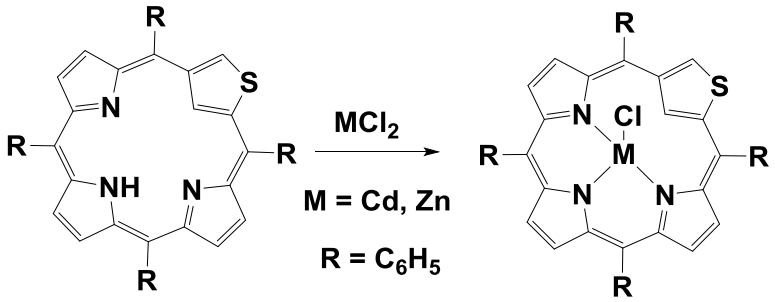


**I.16a** **M = Cd; I.23** **M = Zn; I.24**

A synthetic attempt of another isomer of heteroatom confused porphyrin, such as O-confused porphyrin **I.26**, was reported by Pawlicki and Latos-Grazynski[23] employing identical reaction conditions that was adopted for the synthesis of S-confused porphyrin. The acid catalysed condensation reaction of 2,4-bis(phenylhydroxymethyl)furan **I.25**, with *p*-tolylaldehyde and pyrrole in a 1:2:3 ratio followed by oxidation with DDQ did not yield the desired O-confused 21-oxaporphyrin **I.26**, instead yielded the 3-pyrrole-substituted O-confused porphyrin **I.28**. Actually, the condensation could be purposely directed toward formation of 2-oxa-21-carbaporphyrin derivatives without an appended pyrrole **I.26**. To avoid the formation of 3-pyrrole-substituted O-confused porphyrin **I.28**, a suitable nucleophile was employed, which could compete with the C-3 position of O-confused porphyrin.[24] Several condensations were attempted and ethanol was chosen as the nucleophilic agent and similar condensations were performed in the presence of various ethanol concentrations to afford 3-ethoxy-substituted O-confused porphyrin **I.27**, along with 3-pyrrole-substituted O-confused porphyrin **I.28**, which were subsequently separated by column chromatography. The treatment of 3-ethoxysubstituted O-confused porphyrin **I.27** with TFA and careful titration yielded the true O-confused porphyrin **I.26**, in its diprotonated form.

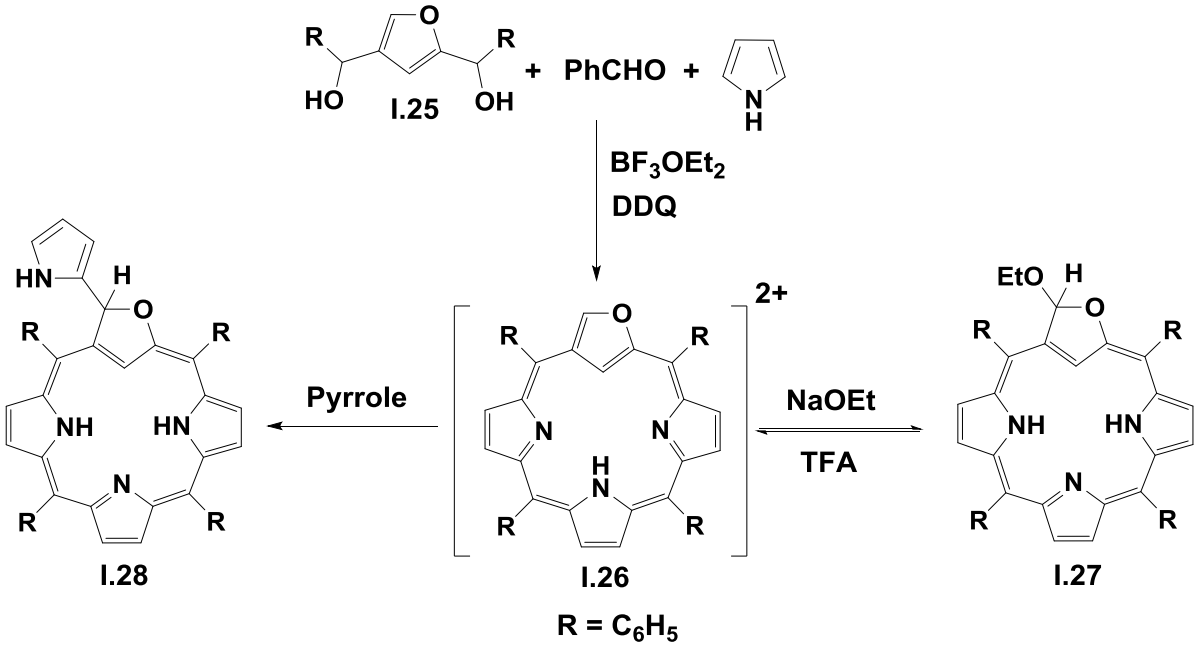


On treatment with sodium ethoxide the O-confused porphyrin **I.26**, gives 3-ethoxy-substituted O-confused porphyrin **I.27**. This process was found to be reversible and hence **I.26** was identified as the common intermediate in the formation of 3-substituted O-confused porphyrins **I.28** and **I.27**. However, when **I.28** was reacted with sodium ethoxide it lead to the formation of an aromatic macrocycle by the substitution of furan's $sp^3$ hydrogen of **I.28** with ethoxy group which could be detached upon reacting with TFA. Further, the coordination chemistry of O-confused porphyrins[23,25] **I.28**, towards variety of metal ions were very interesting as it was found suitable to stabilize the higher oxidation state of metal ions. Based on oxidation state of a central metal ion, the O-confused porphyrin acts as monoanionic, dianionic, and trianionic ligands to form complexes with various metal ions.

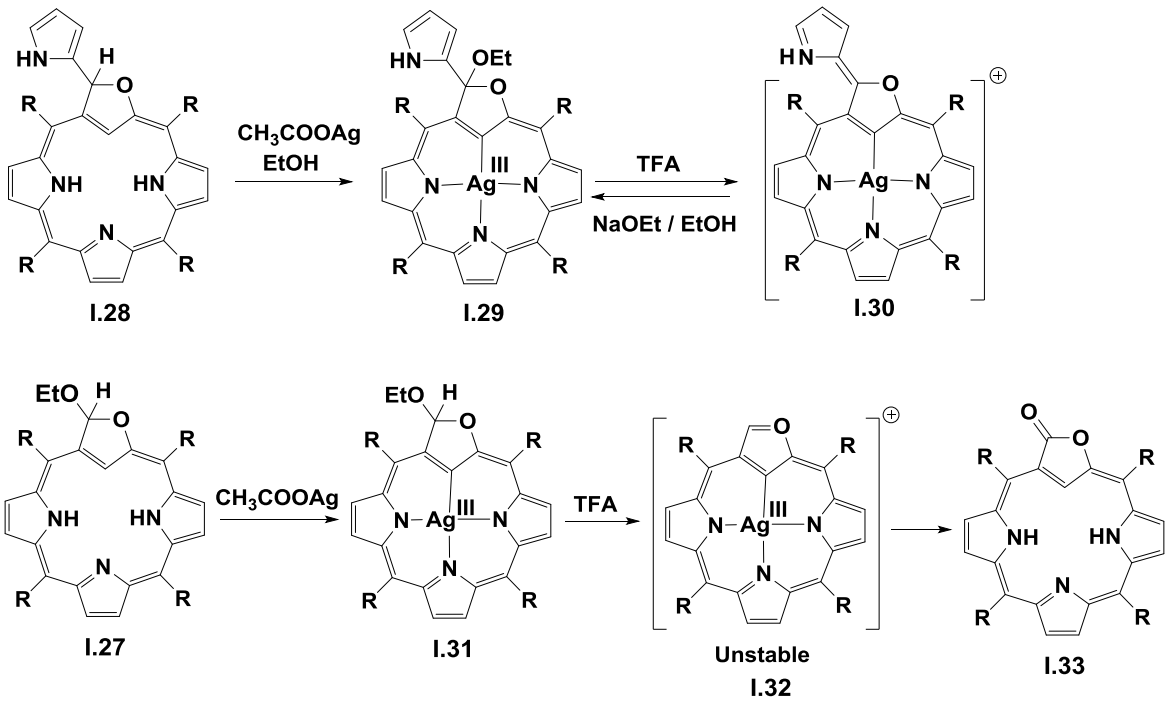


The Ag(III) complexes of two different O-confused porphyrins **I.29** and **I.31** are good examples to represent the O-confused porphyrin as a trianionic ligand.[23,24]. The Ag(III) complex [(OEt,Py)OCP]-Ag(III) **I.29** with ethoxy and pyrrole moieties substituted at the C-3 position of O-confused porphyrin **I.28** was synthesized by using silver(I) acetate in ethanol. It displayed a tetrahedral geometry at C(3) position which had pyrrole and ethoxy substituents. However, the reaction of **I.29** with TFA resulted in the formation of a aromatic Ag(III) complex **I.30** by elimination of the ethoxy group which again converted back to **I.29** when treated with sodium ethoxide in ethanol. The O-confused porphyrin **I.27** containing ethoxy and hydrogen substituents was also converted to Ag(III) complex **I.31** by treating it with silver(I) acetate. However, addition of TFA to **I.31** produced a weakly aromatic complex of the true O-confused carbaporphyrin **I.32** which was unstable and transforms to aromatic carbaporpholactone **I.33** with a lactone functionality. This aromatic carbaporpholactone **I.33** displayed the inner C-H proton at -5.12 ppm and the corresponding six β-H resonances in the region between 8.56−8.74 ppm in its $^{1}$HNMR spectrum.

**I.3. Isophlorin:**

While most of the porphyrin-like macrocycles are generally identified as aromatic species, few macrocycles with identical structural features can be expected to be antiaromatic in nature. Tetrapyrrolic isophlorin, **I.35**, is that foremost amongst the antiaromatic macrocycles. It is a planar structural isomer of porphyrin **I.1,** having 20π electrons with four methine bridges connected through four pyrrole rings in a cyclic fashion. This was first hypothesized by Woodward in 1960 as a possible intermediate between porphyrinogen, **I.34**, and porphyrin, **I.1**, during the biological synthesis of chlorophyll[26]. However, the tetrapyrrolic isophlorin ring was found to be highly unstable and is rapidly oxidized to the more stable 18π

aromatic porphyrin **I.1**. According to Huckel's theory of aromaticity the system having [4n+2] π electrons is aromatic and the system having [4n] π electrons is antiaromatic. Generally aromatic compounds are more stable than its antiaromatic counterpart due to the presence of smaller HOMO-LUMO gap in antiaromatic systems compared to larger gap in HOMO-LUMO for aromatic systems. Interestingly, the $^{1}$HNMR spectrum comparison between aromatic and antiaromatic compounds was found to be different. For example, in the aromatic system the peripheral protons of a cyclic systems resonate in the down field region and protons inside the macrocyclic cavity resonate in up field region due to the presence of strong diatropic ring current effect in [4n+2] π electrons. In contrast, antiaromatic macrocycles display opposite effects such that the outer proton resonates at high field region and inside protons resonate in downfield region due to the presence of strong paratropic ring current effect in [4n] π electrons systems.

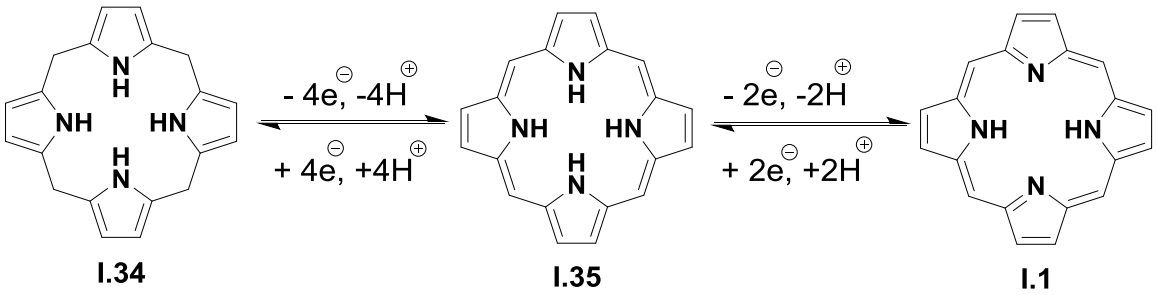


**I.34** **I.35** **I.1**

In contrast to porphyrin **I.1**, the chemistry of isophlorin **I.35** and its analogues has been hindered by lack of straightforward synthesis and also due to unstable nature of this intermediate under ambient conditions which readily oxidizes to stable 18π electron aromatic macrocycle[27,28] **I.1**. Unlike the straight forward synthesis of porphyrin from a one-pot reaction of pyrrole and aldehydic partner, isophlorin is not known to be synthesized under similar reactions conditions. Since then many efforts have been put forth to isolate this fleeting intermediate **I.35** in its stable form. Alternate strategies to synthesize a stable isophlorin were developed by employing nonpyrrolic heterocyclic units such as furan, thiophene and selenophene with the anticipation that they could inhibit the possible oxidation of isophlorin to the aromatic porphyrin. Because of the comparable aromatic features and structural similarity with pyrrole, furan is an attractive choice as a building block for the 20π macrocycle[29]. Vogel and co-workers employed at least three different strategies for the synthesis of tetraoxa isophlorin[29-31] **I.37**. Their primary objective was to obtain neutral antiaromatic 20π electron tetraoxa isophlorin **I.40**.

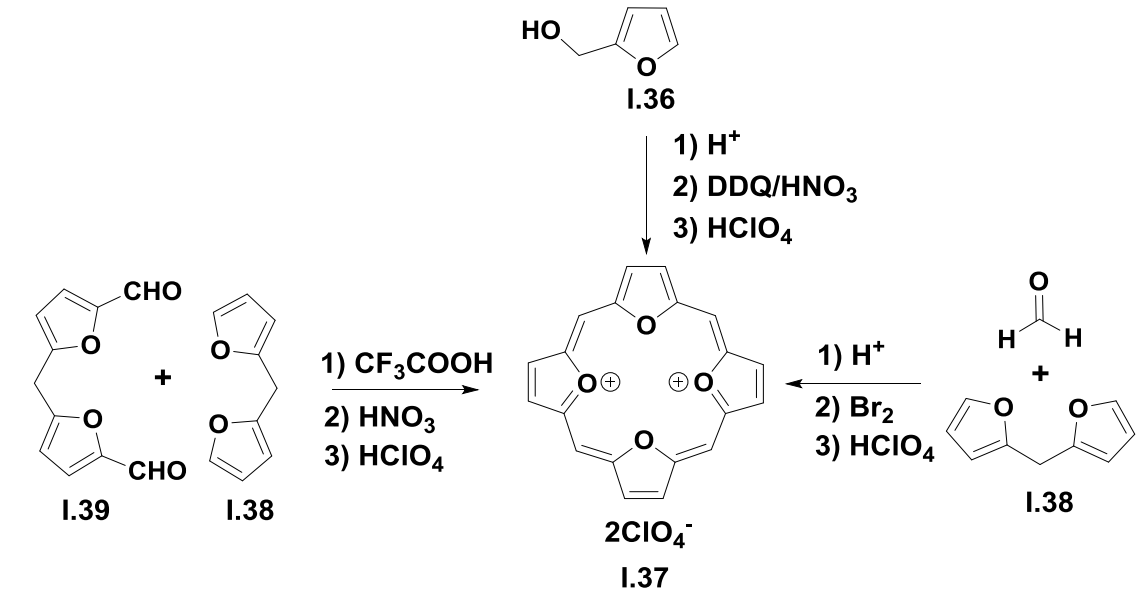


It was apparent that the 20π tetraoxa isophlorin **I.37**, was a fugitive intermediate as suspected for the parent isophlorin (tetrapyrrole) **I.35**, which further drive out the stability of the antiaromatic systems. Even though oxidation of tetraoxaisophlorin to its corresponding dication is parallel to synthesis of porphyrin, the macrocycle didn't lose any of its hydrogens in the process of aromatization. Its tendency for oxidation to a dication by mineral acids is strikingly analogous to the chemical property of metal. Hence, Vogel linked isophlorin to a "pseudo metal" for its ability to undergo ring oxidation with mineral acids[4]. However the reduction of quinone (DDQ) to phenol in the presence of perchloric acid and the undetected isophlorin (tetraoxa), as a source of electrons justified the two-electron oxidation of the macrocycle. Therefore, the possibility of dication reduction to the neutral macrocycles was an expected possibility. Persistent efforts from Vogel and co-workers did not go in vain to isolate the antiaromatic 20π isophlorin. The isolated stable dication **I.37**, was reacted with potassium metal in THF under very rigorous reaction conditions but they could not yield the targeted tetraoxa isophlorin **I.40**. Instead, the reaction proceeded further to give the 22π electron dianionic species **I.41**. Even though the reduction was successful, the dication consumed four electrons to yield the aromatic 22π tetraoxaporphyrin dianion[32] **I.41**.

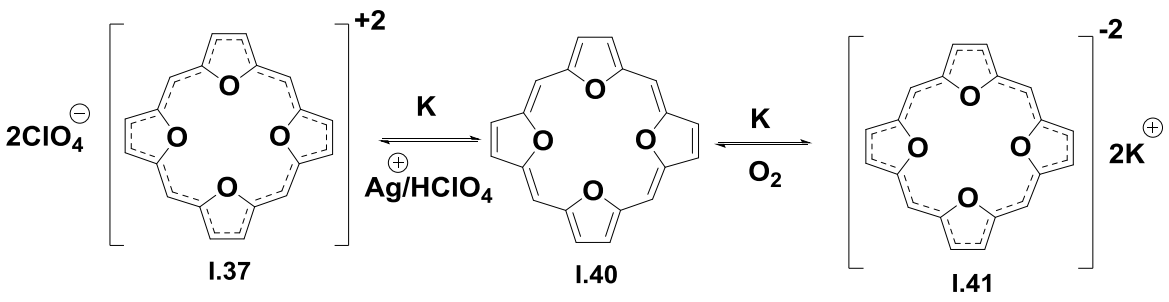

Attempts to synthesize the targeted molecule **I.40** by partial and regulated two-electron oxidation of **I.41** was partially successful by oxidizing with molecular oxygen at low temperatures. However, the obtained crystals of the product was identifies as air sensitive black crystals which can be stored at only -78$^{o}$C. Its single crystal X-ray diffraction analysis confirmed the molecule with a planar structure corresponding to **I.40**. The proton NMR spectrum of **I.40** displayed two sharp singlets at 1.98 and -0.64 ppm corresponding to furan and *meso* protons, respectively. This upfield shift values for the protons exhibited the presence of strong paratropic ring current effect for the [4n] π macrocycle. Similar macrocycles with thiophene and selenophene were also synthesized, but could not support the isolation of a stable isophlorin.

Substituting hydrogen with methyl group on pyrrole nitrogens of **I.35** such as tetra-N-methyl isophlorin is expected to prevent the formation of neutral porphyrin species. In their first successful attempt, Vogel et. al. in 1991, the 18π aromatic macrocycle, **I.42** was treated with a 0.15M solution of anthracene-sodium in THF at -78$^{o}$C for the two electron reduction of dication to yield the 20π electron isophlorin as its octaethyl derivative of *N,N',N'',N'''*-tetramethylisophlorin **I.43** and followed by subsequent partial re-oxidation to *N,N',N'',N'''*-tetramethyloctaethylporphyrin dication **I.42** as its perchlorate salt.[33]

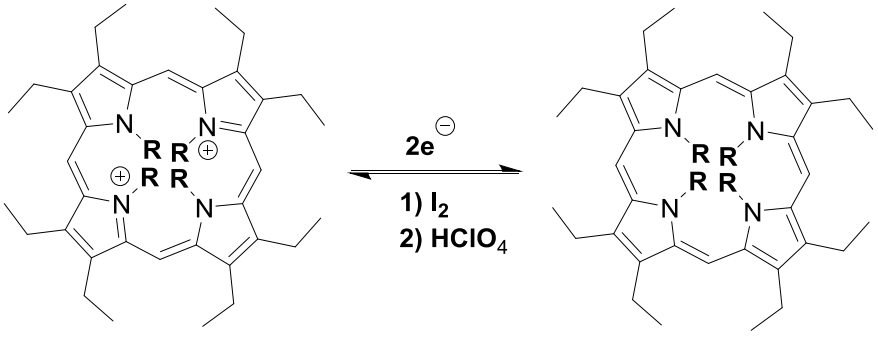


**I.42** **I.43**

It's proton NMR spectrum displayed temperature dependent chemical shift values for inside methyl protons due to partial fluxional behaviour. The presence of four methyl groups inside the core hindered the molecule to adopt the expected planar conformation and hence the macrocycle rendered nonplanar conformation. This macrocycle was found to be moderately stable under ambient conditions compared to the air sensitive tetraoxa isophlorin **I.40**. The single crystal X-ray diffraction analysis of the compound **I.43** displayed a non-planar saddle-shaped macrocycle with *syn*, *anti*, *syn*, *anti* conformation with respect to the N-methyl groups. Mild oxidizing agents such as iodine, iron(III) and silver (I) ions converts **I.43** into **I.42**, bromine is necessary in this reaction which converts *N,N',N'',N'''*-tetramethyloctaethylporphyriogens into **I.42**.

After the discovery of antiaromatic isophlorin and further synthetic developments for stabilizing the antiaromatic isophlorin and its metal complexes using different synthetic protocols were developed to access a variety of *meso* and beta substituted isophlorin. Initial attempts were mainly based on β-substituted

heterocyclic units or without any substituents on the periphery of the macrocycle. It was observed that the effect of substituents did not alter the stability of macrocycles. A silicon(IV) complex **I.44** emerged as a convenient precursor in the design of the Si(IV) complex of isophlorin **I.45**. Vaid et. al. in 2005[34] reported the metal complex of 20π electron isophlorin, wherein they employed an alternative strategy to reduce [Si(IV)(TPP)$Cl_2$], **I.44**, to the antiaromatic 20π electron metal complex [Si(IV)-(tetraphenylisophlorin)](THF)$_2$, **I.45**. They displayed that the porphyrin ring could be reduced from −2 to −4 by addition of two equivalents of sodium amalgam (Na/Hg), to yield **I.45** as an air sensitive dark orange solid. Single crystal X-ray diffraction analysis displayed a ruffled macrocyclic structure because of the smaller size of Si(IV) in contrast to the cavity of the porphyrin compared to aromatic parent **I.44** which is relatively planar and less ruffled. The four nitrogen atoms and silicon in **I.45** were found to be in the same plane leading to a perfect octahedral complex around silicon and the *meso* carbons lie above and below the plane of $SiN_4$. The complex **I.45** has four covalent bonds between Si and four nitrogens at the centre of the macrocycle and coordinated to two THF molecules through the oxygen of THF in the axial positions of the octahedral geometry.

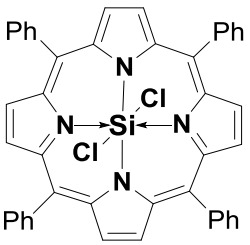


**I.44**

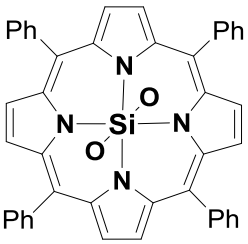


**I.45**

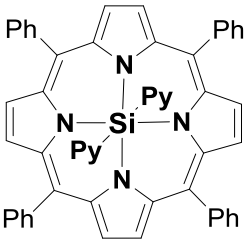


**I.46**

**O = THF**

In both (**I.45** and **I.46**) the metal has +4 oxidation state and the porphyrin ring has -4 oxidation state compared to parent **I.44**, in which the molecule has 18π electron. A well-resolved $^1$H NMR spectrum was obtained upon replacing the THF by pyridine as the axial ligand. The larger chemical shift difference between the protons of the pyrrole rings which appeared as a singlet at δ 1.29 ppm and axial pyridine ring protons at δ 20.35, 10.31, and 9.74 ppm was found to be in agreement with the paratropic ring current effects of a 4nπ system, exhibiting a planar structure in the solution state.

Efforts from the same group revealed that other elements of same group (XIV) were also good enough for coordination. Unlike the silicon complex, Ge yielded a tetracoordinate complex of the porphyrin with a close resemblance to square pyramidal geometry with four nitrogens coordinated the Ge metal little above of the centre of macrocyclic core, exhibiting a dome-like structure rather than distorted macrocycle[35]. Such an observation is generally observed for metal ions, chelated by a porphyrin, in their lower oxidation states and this could not reveal the nature of metal complex with respect to the oxidation state metal ion in its crystal lattice. Spectroscopically, in the proton NMR spectrum significant downfield shifts of the pyrrole

protons and a typical porphyrinic absorption spectrum concluded that Ge is in +2 oxidation state without reducing the porphyrin to isophlorin. The Ge complex, **I.47**, was found to be stable enough without octahedral coordination probably due to the presence of a lone pair of electrons on the central Ge metal ion, where as the silicon complex, **I.45**, could not be isolated without THF coordination.

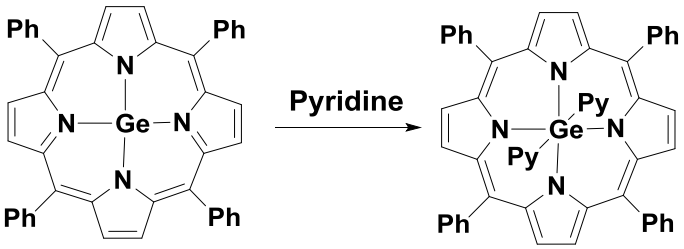


**I.47** **I.48**

Upon dissolving in pyridine it was observed that the Ge complex **I.47** binds two axial pyridine ligands indicated by the subtle change in color from green to red, to yield the hexacoordinate **I.48**. Single crystal X-ray diffraction analysis, revealed a highly ruffled macrocyclic structure similar to that observed for **I.45**. The non planar conformation was observed mainly because of the unusual change in the bond lengths between Ge and the four nitrogen atoms. The significant reduction in bond distance between Ge and all the nitrogen atoms of **I.48** compared to **I.47**, reflects the oxidation of Ge(II) to Ge(IV) upon the coordination of two axial pyridine ligands, which was confirmed by the strong upfield chemical shift of pyrrole protons (δ 0.6 ppm) and low field chemical shift of pyridine protons (δ 21.6 ppm) in its $^{1}$HNMR spectrum of **I.48** as expected from a 20π macrocycle. These significant change in the chemical shift values confirmed the presence of strong paratropic ring current effect corresponding to antiaromatic macrocycle accompanied by pyridine as a reducing agent through the stabilization of a Ge(IV) macrocyclic chelate. The porphyrin complex with Sn(IV) was not found to be feasible even though it belongs to the same group as Si and Ge. It was reasoned that the elements in the top of the group are stabilized by the +4 oxidation state and those at the bottom of the same group choose the +2, expect for Ge which could display unique stabilization in both +4 or +2 states. In this regard, it was observed that pyridine aids the reduction of the aromatic 18π porphyrin to its corresponding antiaromatic 20π isophlorin through the stabilization of a Ge(IV) macrocyclic chelate.

Further synthetic attempts to led to the limited success for a stable isophlorin. Chen et. al. discovered the reduction of a *meso* tetraphenyl porphyrin Cu(II) complex to its corresponding demetalated isophlorin **I.50**, by substituting electron withdrawing groups on the periphery β-positions of the heterocyclic rings[36,37]. The synthesis of β-Tetrakis(trifluoromethyl)-*meso*-tetraphenylporphyrins **I.50** was obtained by the addition of activated zinc powder into the dimethyl sulphoxide (DMSO) solution of **I.49** in an inert atmosphere at room temperature through a serendipitous discovery.


**I.49** **I.50**

The molecule **I.50** was found to be stable under inert conditions, and the single crystal X-ray crystal diffraction analysis displayed a distorted nonplanar saddle-like conformation shown by larger out of the plane distortion because of strong electron withdrawing trifluoromethyl substituted pyrrole rings compared to the unsubstituted pyrrole rings. The reason for nonplanar nature of **I.35** was mainly attributed to the steric hindrance induced by four hydrogens in the macrocyclic cavity. Both spectroscopic evidence and structural details supported the structure induced loss of antiaromatic features in the 20π macrocycle. The presence of four NH's inside the macrocyclic cavity is further confirmed by carrying out the N-methylation reactions of isophlorin **I.50** and it was found that the base used has the great influence on the reactions[37].

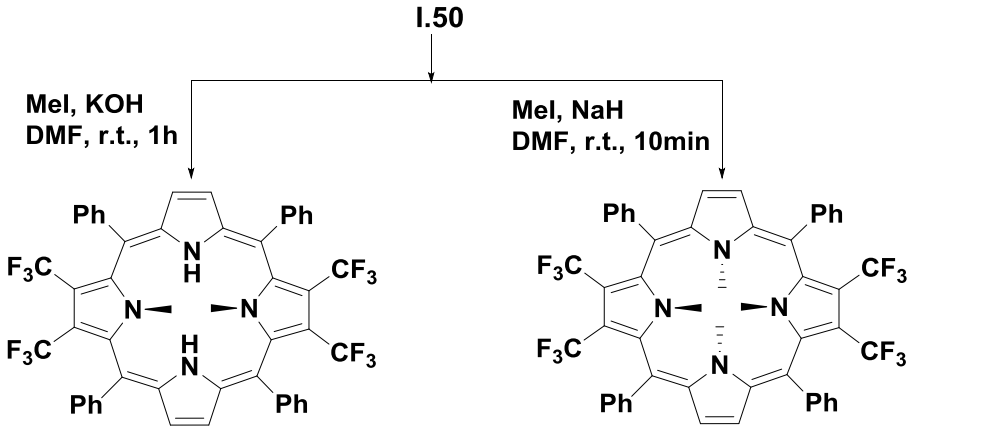


**I.51(98%)** **I.52(64% 52/51 = 4:1)**

When KOH was used with MeI in DMF solution at room temperature for 1h, N-dimethylated isophlorin **I.51** was obtained in quantitative yield. When NaH used as a base with similar reaction condition the reaction proceeds quickly within 10min in good yields and led to the formation of **I.52** (64%) as N-tetramethylated isophlorin in 4:1 ratio of **I.52** and **I.51**. The crystal structures of **I.51** and **I.52** displayed a similar non-planar distorted saddle conformation as in **I.50**. They are found to be more air stable than **I.50** because of the core methyl group's mutual repulsion which hinders the rotation of the pyrrole units into the near planar conformation. Surprisingly, this macrocycle does not undergo reversible oxidation to 18π porphyrin.

Since then many attempts have been made to obtain isophlorin like macrocycles and they have yielded only porphyrin dications of their corresponding macrocycles such as tetrathia/oxa/selena porphyrin dication as their perchlorate salts[38]. In contrast to porphyrins, the lack of straightforward synthesis towards

isophlorin is hindered by its rapid conversion to stable 18π electron aromatic macrocycle due to fast conversion of two of its four amines to imines inside the core at ambient temperature. Replacing pyrrole's nitrogen with other chalcogen atoms were found to avoid the steric hindrance in the centre of the cavity from porphyrin core by other divalent heterocyclic units such as furan/ thiophene and electron withdrawing substituents at the *meso* carbons is another way of stabilizing the 20π electron isophlorin macrocycle. Therefore, chalcogens are better alternatives for NH since they can have similar structural and electronic feature. This was found to be useful towards the synthesis of stable isophlorin analogues of divalent heteroatoms such as furan or thiophene instead of pyrrole units. In 2008 Anand et. al. reported the first stable core modified planar antiaromatic tetraoxa isophlorin by substituting electron withdrawing groups on the meso carbon atoms[39]. The electron withdrawing groups plays a very crucial role in stabilizing this air-stable antiaromatic 20π electron isophlorin which restricts the molecule to be oxidized back to 18π electron aromatic macrocycle as observed for *meso*-free tetraoxa isophlorin dication.

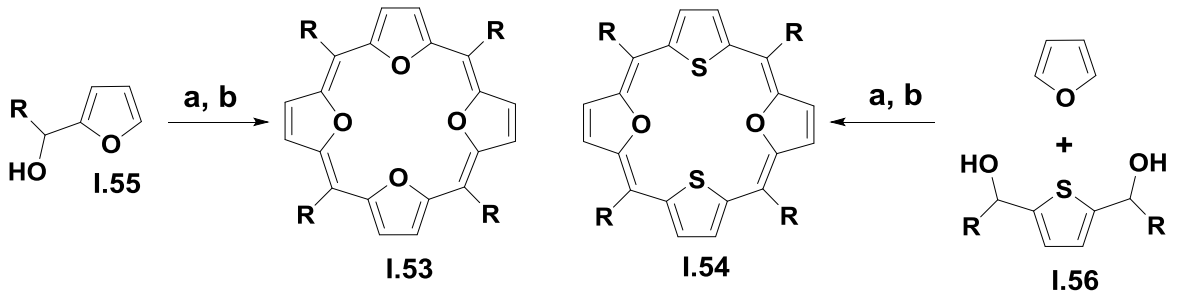


**R = $C_6F_5$**

**a) $BF_3OEt_2$, b) $FeCl_3$**

The 20π electron 21,22,23,24-tetraoxaisophlorin was prepared by the one-pot reaction of self condensation of 2-pentafluorophenylhydroxymethyl furan **I.55** by acid catalysed reaction, followed by oxidation using $FeCl_3$. The macrocycle was purified by column chromatography and found to be stable under ambient conditions and the target molecule **I.53** was isolated in 2.5% yields. Its proton NMR spectrum displayed a singlet at δ 2.49 ppm for the β protons of the four furan rings, suggestive of high symmetry for the molecule. The presence of larger up field chemical shift value for *β*-protons of furan rings supported the presence of strong paratropic ring current effects as expected of a 4nπ cyclic system. Single crystal X-ray diffraction analysis of **I.53** displayed a planar macrocycle with all the furans remaining coplanar with respect to the mean macrocyclic plane. Under the similar reaction conditions, using furan was condensed with 2,5-bis(pentafluorophenylhydroxymethyl)thiophene **I.56** to obtain dithia-dioxa-isophlorin **I.54**, with another higher analogue and the target molecule **I.54** was obtained in 6% yield. The proton NMR of **I.54** displayed upfield chemical shift values at δ 3.37 and 3.33 ppm for the β protons of thiophene and furan. Single crystal X-ray diffraction analysis revealed a planar conformation of this isophlorin. Minor geometrical alterations were observed in the macrocyclic core with decrease in cavity size upon replacing

oxygen by sulphur. Both the **I.53** and **I.54** displayed planar conformation for 20π isophlorin macrocycle with all the heterocyclic rings and *meso* carbon atoms in both the macrocycle in one plane, while the peripheral pentafluorophenyl substituents were perpendicular to the plane of the macrocycle. Unlike the oxidation of tetraoxa isophlorin, **I.40**, to its dication **I.37**, both **I.53** and **I.54** did not display any such tendency to oxidized to the 18π aromatic species, which indicated high stability of these molecules to resist oxidation at ambient temperature.

However, it was observed that they can be oxidized to its dication with high equivalents of perchloric acid to yield the unstable 18π dication under ambient conditions. Shinmyozu and co-workers[40] followed a similar strategy to synthesize the meso-pentafluorophenyl tetrathia isophlorin, **I.59**, from the acid catalyzed condensation reaction of 2-(1-hydroxy-1-(pentafluoro)phenylmethyl) thiophene. In contrast to the planar and antiaromatic features of **I.53** and **I.54**, the tetrathia isophlorin, **I.59**, was found to be nonplanar and non-antiaromatic in nature.

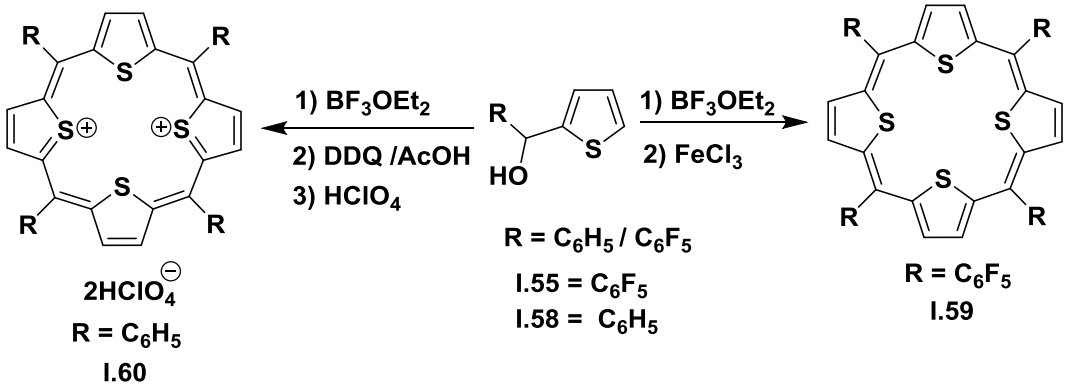


The proton NMR spectrum of **I.59** displayed a singlet at δ 6.19 ppm corresponding to the β protons of thiophene, showing a significant large downfield shift indicating the loss of expected paratropic ring current effects. The single crystal X-ray diffraction analysis revealed its nonplanar structure. Because of steric effects from the bulky sulphur atoms inside the cavity forces a pair of diagonally thiophenes to tilt away from the mean macrocyclic plane that leads to a decrease in the effective π conjugation and structure induced loss of antiaromaticity. Apart from the effect of heteroatoms, the electronic effects of *meso* substituents are significant to the cause of stable isophlorins that hinders the oxidation to its corresponding dication. This was demonstrated when the same group attempted to synthesize *meso* tetraphenyl tetrathia isophlorin. Addition of DDQ/$HClO_4$ as the oxidizing agent to tetraphenyl tetrathia porphyrinogen yielded its corresponding dication, **I.60**, with two $[ClO_4]^-$ as its counter-anions, highlighting the influence of strong electron withdrawing groups in **I.59** to prevent the oxidation of the antiaromatic isophlorin.

Further, Imahori and co-workers reported the synthesis of stable metal−isophlorin complexes, **I.62**, with a heteroporphyrin containing N, N, S, and P as the coordinating atoms of a modified porphyrin, **I.61**[41-43] Reaction of group-10 metals such as Pd, Pt and Ni with heteroporphyrin, **I.61** lead to the formation of the

corresponding metal complexes of the macrocycle, **I.62**. The proton NMR spectrum of these metal complexes displayed slight upfield chemical shift values for the β protons of the macrocycles, while the P-phenyl protons were observed in low field with respect to the parent porphyrin, **I.61**. Single crystal X-ray diffraction analysis of the these complexes revealed the non planar structure in which phosphorous and sulphur atoms were displayed out of the plane with respect to the mean macrocyclic plane due to coordination to metal centre.

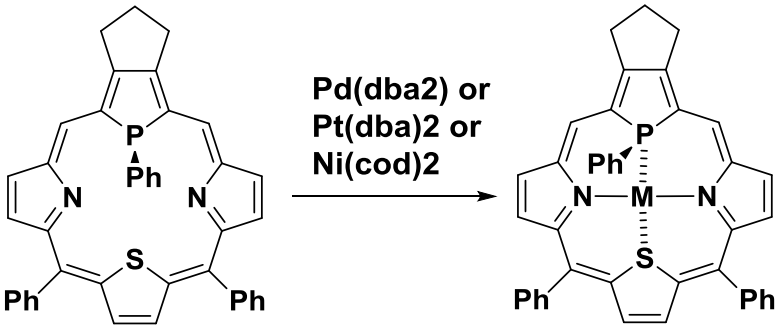


Penelope Brothers and co-workers[44] reported the two-electron reduction of diboron complex of porphyrin, **I.63** to an air and moisture sensitive 20π isophlorin, **I.64**, using magnesium anthracenide as a reducing agent at -30 °C in THF. The macrocycle **I.64**, displayed a +3 oxidation state for boron and a single bond in-between the boron centers. The presence of a single or double bond in **I.64**, was totally dependent on the oxidation state of the macrocycle.

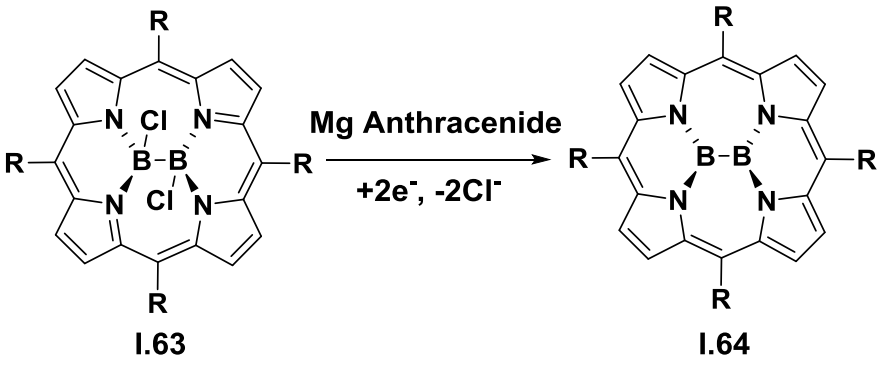


$^{1}$H NMR spectrum of **I.64** displayed upfield chemical shift values of δ 1.05 and 0.51 ppm for the pyrrole protons, and the calculated NICS(1) value of +20.2 ppm further confirmed its antiaromatic character. The computed structure for **I.64** displayed a planar conformation for the macrocycle and a distance of 1.73 Å between the two boron centers.

In summary, the heteroatom-containing porphyrin analogues or core-modified porphyrins that resulted from the replacement of one or two or all the pyrrole rings with other five-membered heterocycle units such as furan, thiophene and selenophene results in the formation of core modified porphyrins or isophlorins and these molecules exhibit quite different physicochemical properties compared to regular azaporphyrins. The properties of these heteroatom-containing porphyrins depend on the nature and number of different heterocycles present in place of pyrrole rings. Thus, significant progress has been made in last few decades on core-modified porphyrins in terms of their synthesis, their use in building multi-porphyrin arrays for light harvesting applications, their use as ligands to form unusual metal complexes and also their use for several other studies. Unlike core modified porphyrins, attempts to make isophlorin-like macrocycles using core modification have yielded only tetrathia/oxa/selena porphyrin dications. In contrast to porphyrin, the evolution of isophlorin and its analogues has been hindered by lack of straightforward synthesis and also due to their unstable nature under ambient conditions which rapidly transform itself into a stable aromatic 18π system due to the fast conversion of two of its four cyclic amines to imines. Replacing nitrogen with divalent oxygen or sulphur in the macrocyclic core and with electron withdrawing substituents on the *meso* carbons was found to be an efficient way to the synthesis of stable isophlorin analogues of thiophene/furan with *meso* pentafluorophenyl substituents. Antiaromatic [4n]π systems are clearly different in their reactivity with oxidizing agents in comparison to the aromatic counterparts which has the potential to be employed as a source of electrons in organic redox transformations and expected to be better organic conductors in comparison to diamagnetic aromatic species. In addition, the pyrrole NH also plays a key role in the proton-coupled, two-electron oxidation of isophlorin to the aromatic porphyrin. Replacement of one of the nitrogen atoms within the porphyrin core with a carbon produces a N-confused porphyrins or carbaporphyrins. This new class retains its aromatic properties which exhibit unusual reactivity and the ability to form stable organometallic derivatives. A variety carbaporphyrinoid systems have been synthesized and investigated with other heteroatoms such as thiophene, furan, and selenophene which also results in the formation of core-modified confused porphyrins analogues with “confused” furan or thiophene units. They exhibit different properties such as development of components of catalytic systems, supramolecular systems and in the development of fluorescence sensors and may exist as aromatic, nonaromatic, or even antiaromatic systems. Considering these unique and different properties of core-modified porphyrins and isophlorins compared to regular azaporphyrins, it is desirable to direct efforts towards the development of novel synthetic methods to synthesize different stable, new core-modified isophlorins and their derivatives. In this thesis, the synthetic aspects of stable core-modified antiaromatic isophlorin and its derivatives ever since its invention, with its structural, electronic, and redox properties will be highlighted. It is expected that the chemistry of core-modified isophlorin and their derivatives will be further used to a greater advantage in the future to understand their complete potential for various applications as a replacement for aza analogues.

## I.4. References


[1] D. Dolphin, *The Porphyrins*, Academic Press: **1978**.

[2] H. Nishide, T. Suzuki, H. Kawakami, E. Tsuchida, *J. Phys. Chem*. **1994**, 98, 5084-5088.

[3] K. M. Kadish, K. M. Smith, R. Guilard, *The porphyrin Handbook*, Academic Press, San Diego, **2000**, Vol. 1-10.

[4] L. Latos-Grazynski, *The porphyrin Handbook*, K. M. Kadish, K. M. Smith, R. Guilard, Eds. Academic Press, New York, **2000**, 361-416.

[5] (a) K. M. Kadish, K. M. Smith, R. Guilard, Eds.; *The Porphyrin Handbook*, Academic press: New York, Applications: Past, Present and Future. **2006**, 6. (b) Z. Zhou, Z. Shen, *J. Mater. Chem. C* **2015**, 3, 3239-3251. (c) T. Higashino, H. Imahori, *Dalton Trans.* **2015**, 44, 448-463. (d) Y. Ding, W. Zhu, W. -H, Y. Xie, *Chem. Rev*. **2016**, DOI: 10.1021/acs.chemrev.6b0021

[6] L. Latos-Grazynski, J. Lisowski, M. M. Olmstead, A. L. Balch, *J. Am. Chem. Soc*. **1987**, 109, 4428-4429.

[7] Z. Gross, I. Saltsman, R. P. Pandian, C. M. Barzilay, *Tetrahedron Lett.* **1997**, 38, 2383-2386.

[8] L. Latos-Grazynski, *The Porphyrin Handbook*, K. M. Kadish, K. M. Smith, R. Guilard, Eds. Academic press: New York, **2000**, 361-416.

[9] (a) W. S. Cho, C. H. Lee. *Bull. Korean Chem. soc.* **1998**, 19, 314-319. (b) C. H. Lee, W. S. Cho, *Tetrahedron Lett*. **1999**, 40, 8879-8882.

[10] (a) A. Ulman, J. Manassen, *J. Am. Chem. Soc*. **1975**, 97, 6540-6544. (b) A. Ulman, J. Manassen, *J. Chem. Soc. Perkin Trans*.1, **1979**, 1066-1069. (c) P. H. Heo, K. Shin. C. H. Lee, *Tetrahedron Lett.* **1996**, 37, 197-200. (d) P. H. Heo, C. H. Lee, *Bull. Korean Chem. soc.* **1996**,17, 515-520.

[11] A. Ulman, J. Manassen, F. Frolow, D. Rabinovich, *Tetrahedron Lett.* **1978**, 19, 167-170.

[12] P. J. Chmielewski, L. Latos-Grazynski, K. Rachlewicz, T. Glowiak, *Angew. Chem. Int. Ed. Engl*. **1994**, 33, 779-981.

[13] H. Furuta. T. Asano, T. Ogawa, *J. Am. Chem. Soc*. **1994**, 116, 767-768.

[14] (a) M. Toganoh, H. Furuta, *Chem. Commun*. **2012**, 48, 937-954. (b) J. D. Harvey, C. J. Ziegler, *Coordination Chemistry Reviews*, **2003**, 247,1-19.

[15] (a) D. W. Yoon, C. H. Lee, *Bull. Korean Chem. Soc*. **2000**, 21, 618-622. (b) E. Pacholska, L. Latos-Grazynski, L. Szterenberg, Z. Ciunik, *J. Org. Chem.* **2000**, 65, 8188-8196. (c) S. K. Pushpan, A. Srinivasan, V. G. Anand, T. K. Chandrashekar, A. Subramanian, R. Roy, K. Sugiura, Y. Sakata, *J. Org. Chem*. **2001**, 66, 153-161.

[16] (a) N. Sprutta, L. Latos-Grazynski, *Tetrahedron Lett.* **1999**, 40, 8457-8460. (b) L. Szterenberg, N. Sprutta, L. Latos-Grażyński, *J. Inclusion Phenom.* **2001**, *41*, 209.

[17] C. H. Lee, H. J. Kim, *Tetrahedron Lett.* **1997**, 38, 3935-3938.

[18] C. H. Lee, H. J. Kim, D. W. Yoon, *Bull. Korean Chem. Soc.***1999**, 20, 276-280.

[19] D. W. Yoon, C. H. Lee, *Bull. Korean Chem. Soc*. **2000**, 21, 618-622.

[20] N. Sprutta, L. Latos-Grazynski, *Tetrahedron Lett.* **1999**, 40, 8457-8460.

[21] L. Szterenberg, N. Sprutta, L. Latos-Grażyński, *J. Inclusion Phenom.* **2001**, *41*, 209

[22] M. J. Chmielewski, M. Pawlicki, N. Sprutta, L. Szterenberg, L. Latos-Grazynski, *Inorg. Chem.* **2006**, 45, 8664-8671.

[23] M. Pawlicki, L. Latos-Grazynski, *Chem. Eur. J.* **2003**, 9, 4650-4660.

[24] M. Pawlicki, L. Latos-Grazynski, *Chem Review*, **2006**, 6, 64

[25] M. Pawlicki, L. Latos-Grazynski, L. Szterenberg, *Inorg. Chem*. **2005**, 44, 9779-9786.

[26] R. B. Woodward, *Angew Chem.* **1960**, 72, 651

[27] K. G. Untch, D. C. Wysocki, *J. Am. Chem. Soc*. **1966**, 88, 2608-2610

[28] J. A. Pople, K. G. Untch, *J. Am. Chem. Soc*. **1966**, 88, 4811-4815.

[29] E. Vogel, W. Haas, B. Knipp, J. Lex, H. Schmickler, *Angew. Chem. Int. Ed.* **1988**, 27, 406-409.

[30] W. Haas, B. Knipp, M. Sicken, J. Lex, E. Vogel, *Angew. Chem. Int. Ed.* **1988**, 27, 409-4411.

[31] E. Vogel, P. Rohrig, M. Sicken, B. Knipp, A. Herrmann, M. Pohl, H. Schmickler, J. Lex, *Angew. Chem. Int. Ed.* **1989**, 28, 1651-1655.

[32] E. Vogel, *Pure Appl. Chem.* **1993**, 65, 143-152.

[33] M. Pohl, H. Schmickler, J. Lex, E. Vogel, *Angew. Chem. Int. Ed*. **1991**, 30, 1693-1697.

[34] J. A. Cissell, T. P. Vaid, A. L. Rheingold, *J. Am. Chem. Soc*. **2005**, 127, 12212-12213.

[35] J. A. Cissell, T. P. Vaid, G. P. Yap, *J. Am. Chem. Soc*. **2007**, 129, 7841-7847.

[36] C. Liu, D. M. Shen, Q. Y. Chen, *J. Am. Chem. Soc*. **2007**, 129, 5814-5815.

[37] Q. Y. Chen, X. G. Chen, C. Liu, D. M. Shen, *Synthesis.* **2009**, 2009, 3860-3868.

[38] E. Vogel, P. Rohrig, M. Sicken, B. Knipp, A. Herrmann, M. Pohl, , H. Schmickler, J. Lex, *Angew. Chem. Int. Ed.* **1989**, 28, 1651-1655.

[39] J. S. Reddy, V. G. Anand, *J. Am. Chem. Soc*. **2008**, 130, 3718-3719.

[40] M. Kon-no, J. Mack, N. Kobayashi, M. Suenaga, K. Yoza, T. Shinmyozu, *Chem. Eur. J.* **2012**, 18, 13361-13371.

[41] Y. Matano, T. Nakabuchi, S. Fujishige, H. Nakano, H. Imahori, *J. Am. Chem. Soc.* **2008**, 130, 16446-16447.

[42] Y. Matano, H. Imahori, *Acc. Chem. Res*. **2009**, 42, 1193-1204.

[43] Y. Matano, T. Nakabuchi, H. Imahori, *Pure. Appl. Chem*. **2010**, 82, 583-593.

[44] A. Weiss, M. C. Hodgson, P. W. D. Boyd, W. Siebert, P. J. Brothers, *Chem. Eur. J.* **2007**, 13, 5982-5993.

# Chapter II

# Synthesis, Characterization and Redox Properties of 20π Isophlorins containing *mono*-pyrrole

## II.1. Introduction:

Heteroatom-containing porphyrin analogues or core-modified porphyrins that resulted from the replacement of one or two pyrrole rings with other heterocycles such as furan, thiophene and selenophene exhibit ability to bind metals in various oxidation states. They also displayed physicochemical properties different from the parent tetrapyrrolic porphyrin[1] and have potential for applications in research fields ranging from materials to medicine[2]. As observed, replacing all pyrrole rings by other heterocycles such as furan/thiophene/selenophene not only modified the conjugated pathway, but also inverted the ring current effect of the parent aromatic porphyrin. Such a contrasting effect is mainly attributed to the extension of π conjugation from 18π to 20π electrons and consequent establishment of an antiaromatic macrocycle. Macrocycles obtained by partial core-modification of the porphyrin core, such as mono/di-hetero porphyrins, does not disturb the aromatic 18π conjugation. Hence, it can be presumed that the extent of core-modification dictated the electronic property of the resulting porphyrin core. Interestingly, the mono-pyrrole porphyrin was the missing link between the partial and complete core-modification of a porphyrin ring. In this chapter the design, synthesis, electronic and redox behaviour of the first mono pyrrole porphyrin will be described in detail.

## II.2. Monoheteroporphyrins:

The mono heteroporphyrins resulting from the replacement of one pyrrole with a range of other five-membered heterocycles can be synthesized by different synthetic strategies. A common synthetic strategy involves the condensation of one equivalent of an appropriate 2,5-bis(arylhydroxymethyl)heterocyclopentadiene with two equivalents of benzaldehyde and three equivalents of pyrrole under mild acidic conditions to afford the monoheteroporphyrins[3,4] **(Scheme-II.1)**.

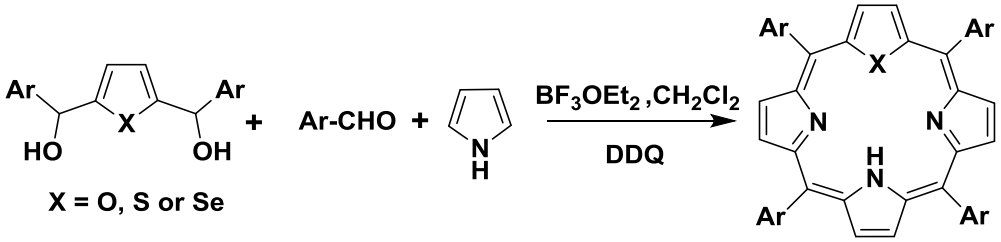


**Scheme-II.1:** Acid catalysed condensation reaction of core modified porphyrin

The same methodology is employed to synthesize functionalized monoheteroporphyrins[5] by introducing one or more functional groups on the meso-aryl carbon atoms.

## II.3. Diheteroporphyrins:

The diheteroporphyrins corresponding to the replacement of two pyrrole rings with other heterocycles such as thiophene/furan or selenophene results in the formation of macrocycle of the type ($N_2X_2$) or ($N_2XY$).

The diheteroporphyrins containing the same heteroatoms[6] were synthesized by condensing an appropriate 2,5-bis(aryl-α- hydroxymethyl)heterocycle with pyrrole under conditions similar to monohetero porphyrins **(Scheme-II.2)**. Porphyrins with a combination of three different heteroatoms (N, S and O) have been synthesized employing suitable precursors under similar conditions. However, there are very few reports on 21,22-diheteroporphyrins[7,8] as these porphyrins were found to be unstable and decompose rapidly **(Scheme-II.2)**.

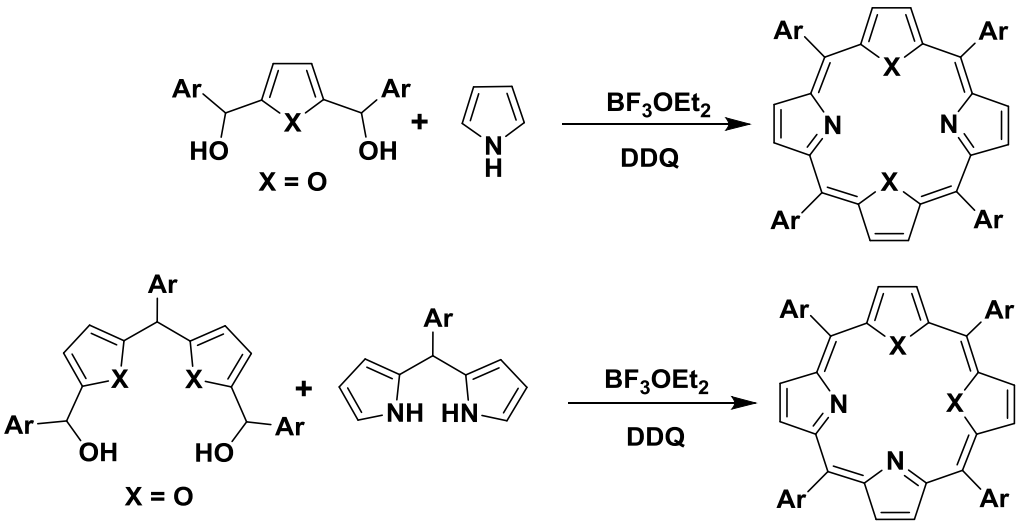


**Scheme-II.2:** One pot synthesis of diheteroatom -substituted porphyrins.

## II.4. Synthesis:

There have been sustained efforts towards the synthesis of core-modified porphyrins[9,10] except for the synthesis of a monopyrrole derivative. Interest in mono-pyrrole derivative of porphyrins was chiefly due to the anticipated anti-aromatic character of the macrocycle. In the scheme described below, it was expected that a mono pyrrole derivative should resemble the properties of the parent 20π isophlorin. Furthermore, it also could be the first derivative of a pyrrole isophlorin to exhibit the unobserved, but expected, reversible two-electron oxidation of the macrocycle.

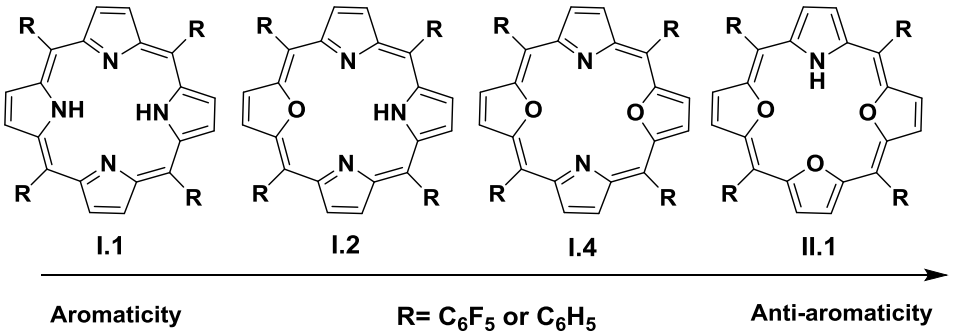


Core-modified porphyrin to isophlorin

The synthesis of core-modified isophlorin **II.1** was achieved by a MacDonald-type condensation of the *meso*-phenyl difuran carbinol with a modified dipyrromethane **(Scheme-II.3)**. An equimolar ratio of the reactants in dichloromethane was condensed under dark and acidic conditions. The reaction was catalyzed by the addition of boron trifluoride ethereate and stirred for an hour and few drops of triethylamine was added to the reaction mixture. DDQ was then added with continued stirring for two hours in a flask open to the atmosphere. MALDI-TOF/TOF mass spectrometry of the reaction mixture confirmed the formation of macrocycle **II.1.**

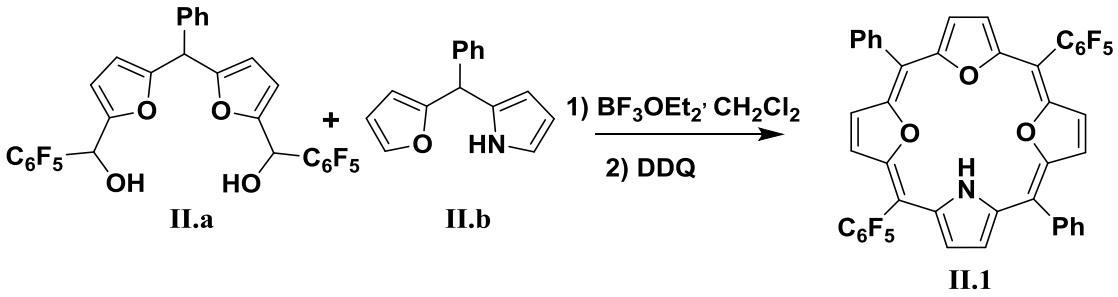


**Scheme II.3:** Acid catalysed one pot synthesis of 20p isophlorin.

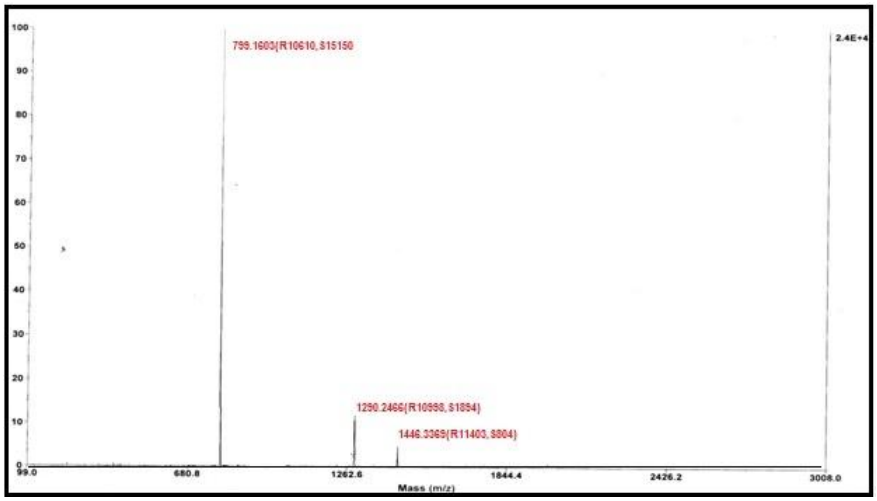


**Figure-II.1:** MALDI-TOF/TOF mass spectrum of reaction mixture (scheme II.3).

**II.5: Isolation and characterization of (II.1)**.

The reaction mixture was passed through a short pad of basic alumina and concentrated under reduced pressure. After column chromatography on basic alumina a yellowish-green band that separated with $CH_2Cl_2$ / petroleum ether (5%) corresponded to the expected 20π electron macrocycle **II.1**. *m/z* value of 799.1194 (Cald. for $C_{44}H_{19}F_{10}NO_3$; 799.1205) obtained from the ESI-TOF high-resolution mass spectrum confirmed the composition of this macrocycle **(Figure-II.3)**. In its electronic absorption the molecule displayed a relatively intense and split absorption for the Soret-like band at λ= 359 nm (ε =108700) and 369 nm (10700) with three weak absorptions in the region between λ=430–500 nm **(Figure-II.2)**.

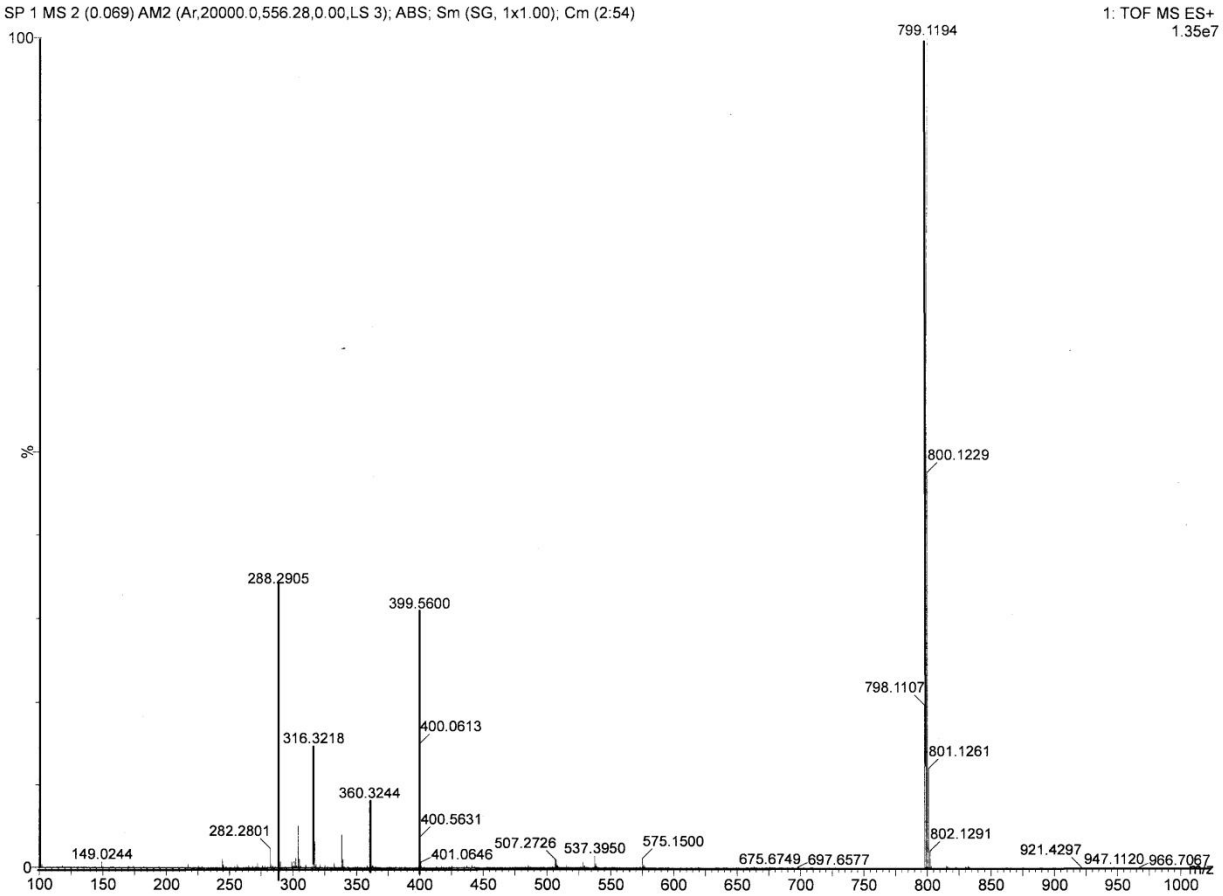


**Figure-II.3:** High resolution mass spectrum (HRMS) of **II.1** spectrum.

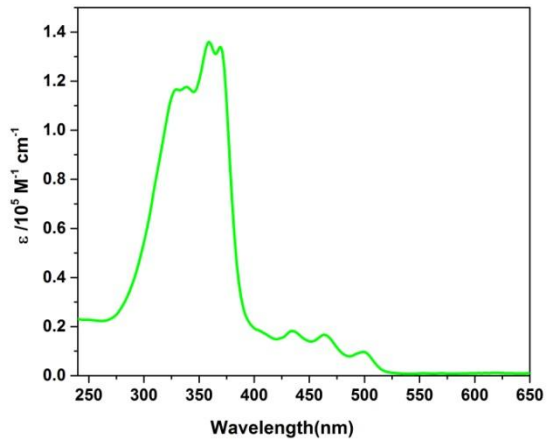


**Figure-II.2:** Electronic absorption spectrum **II.1** in $CH_2Cl_2$.

The $^1$H NMR analysis of **(II.1)** did not result in a well-resolved spectrum and was broadened at room temperature **(Figure-II.4)**. Interestingly, at room temperature this macrocycle exhibited a weak paramagnetic behaviour in the solution state which was confirmed from Electron Paramagnetic Resonance

(ESR) spectroscopy **(Figure-II.4)** and this observed NMR broadening can only be explained by the thermal population from diamagnetic singlet ground state to paramagnetic triplet excited state at room temperature due to the presence of smaller singlet-triplet energy gap[11, 12].

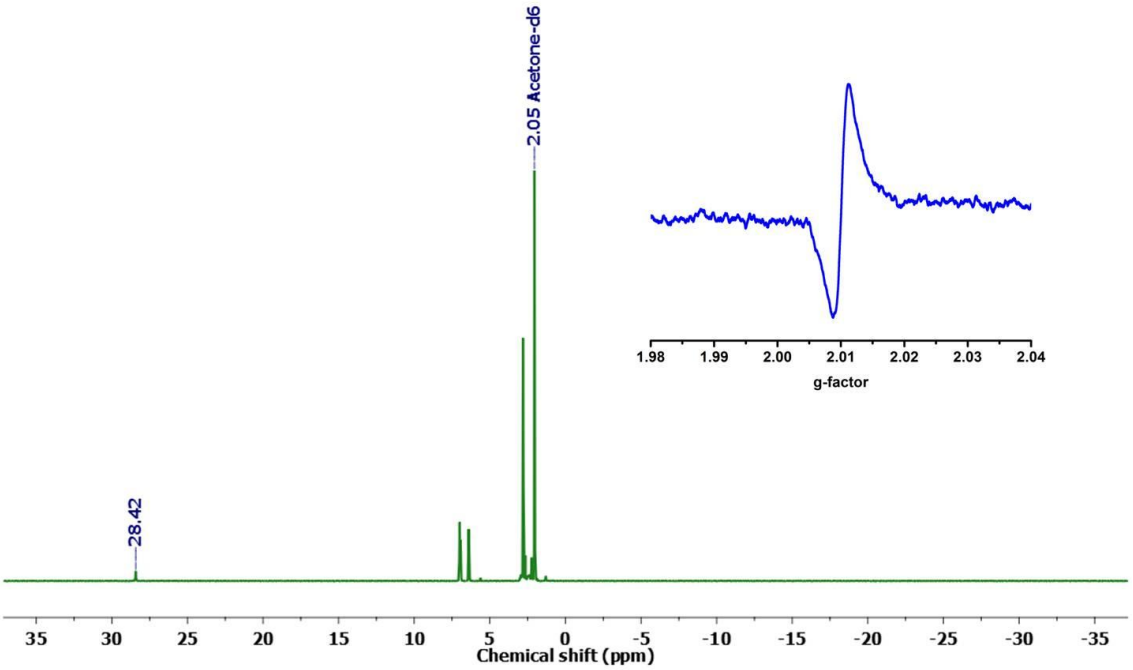


**Figure-II.4:** Room temperature $^{1}$H NMR in acetone-$d_6$ and EPR spectrum (blue) in toluene at 298K of **II.1**.

However, a typical paratropic ring current effect was observed in its $^{1}$H NMR spectrum at 213K **(Figure-II.5)**. The molecule displayed eight doublets in its proton NMR spectrum in acetone-$d_6$, corresponding to the eight β-protons of three furan and one pyrrole, in the region between δ = 3–1.8 ppm **(Figure-II.6)**. More number of signals for this macrocycle can be expected from the reduced symmetry of mono pyrrole porphyrins despite a flat topology expected for [4n] π systems. The $^{1}$H-$^{1}$H 2D COSY spectrum revealed four sets of correlations amongst these eight doublets **(Figure-II.7)**.

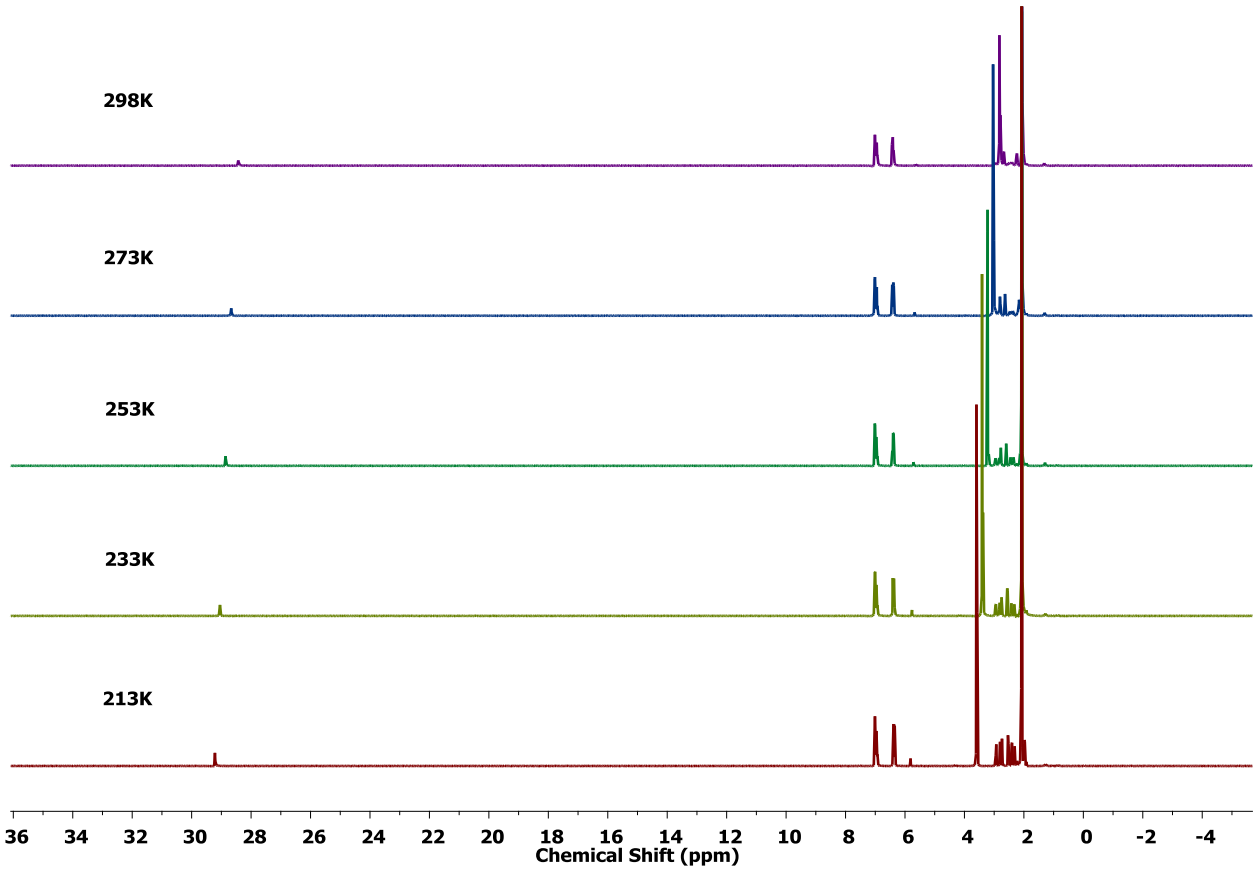


**Figure-II.5:** Variable temperature $^{1}$H NMR spectrum of II.1 in acetone-$d_6$.

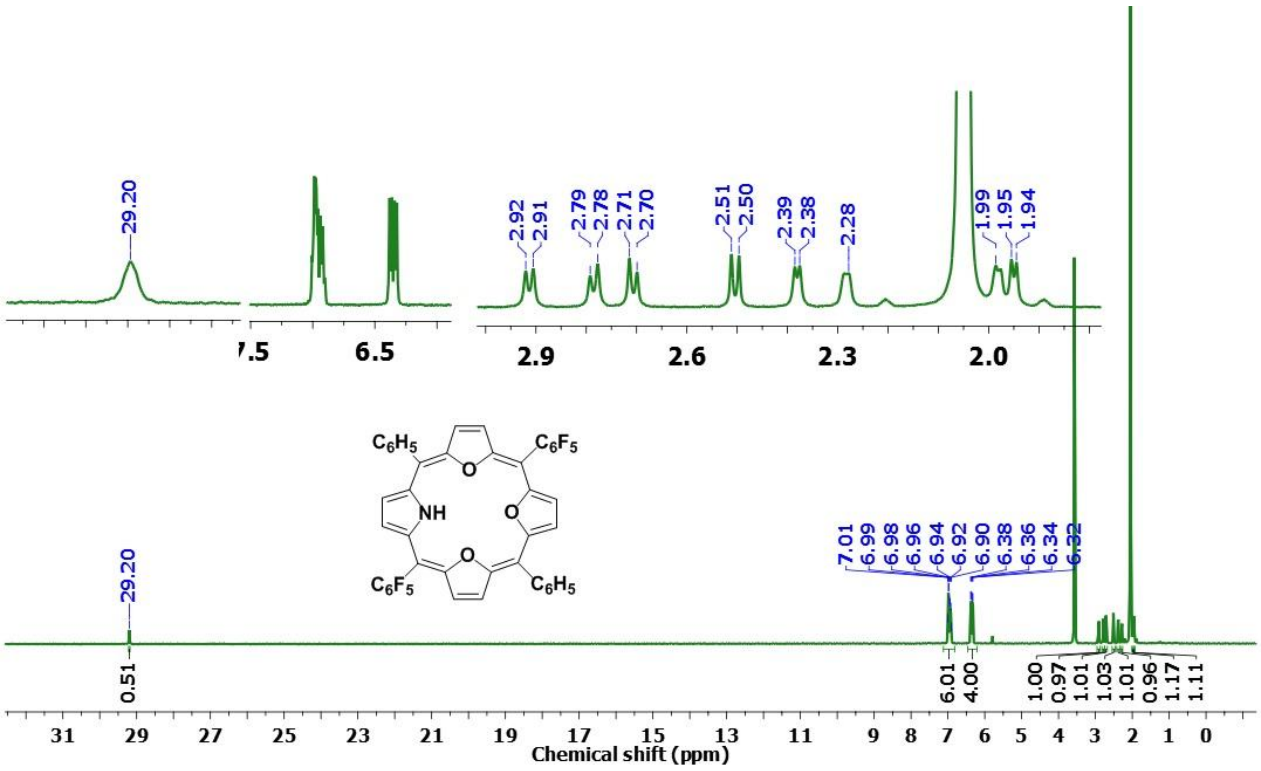


**Figure-II.6:** $^{1}$H NMR spectrum of **II.1** in acetone-$d_6$ at 213K.

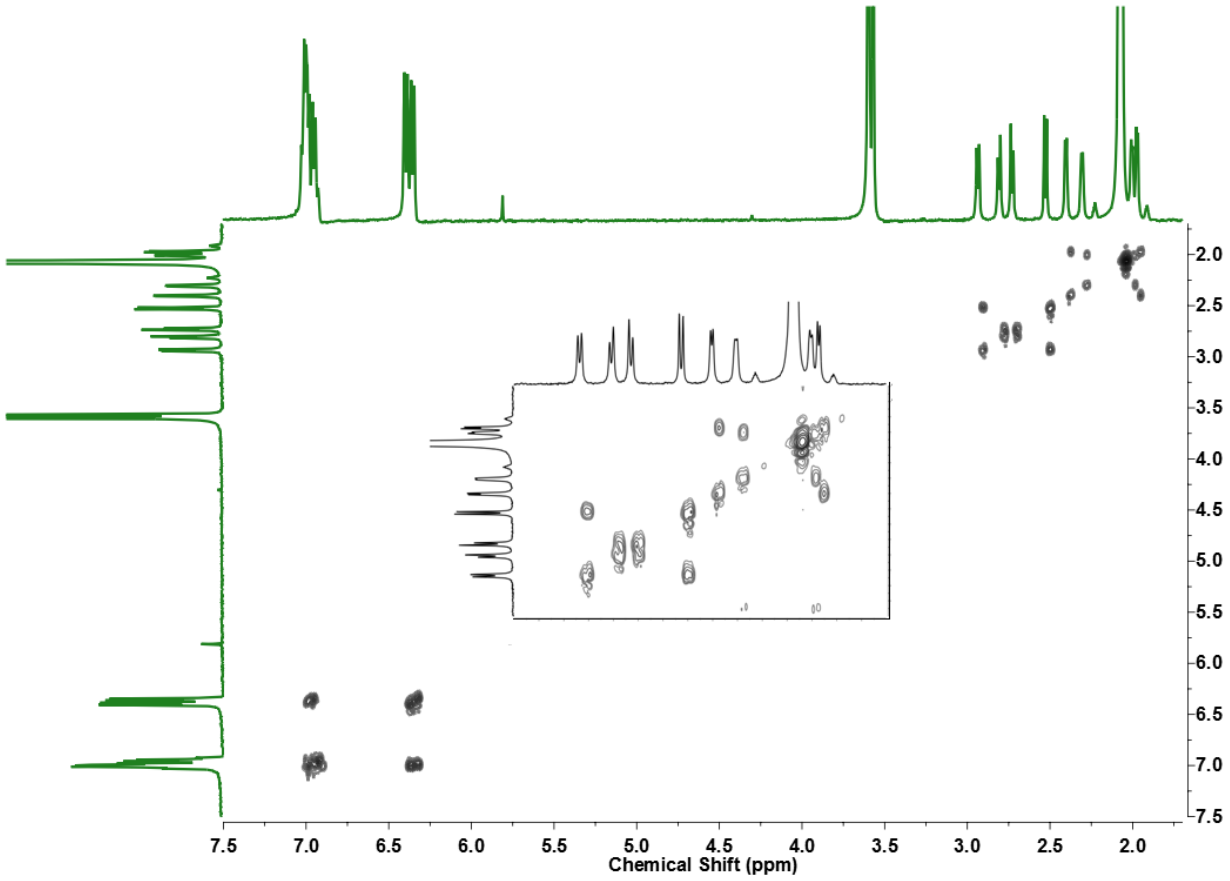


**Figure-II.7:** $^{1}$H-$^{1}$H 2D COSY spectrum of II.1 in acetone-$d_6$ at 213K.

In addition to these upfield signals, a broad singlet was observed at δ = 29.2 ppm corresponding to the pyrrole NH in the core of the 20π macrocycle which implied the effect of paratropic ring current effect. This large difference in the chemical shift values signified strong paratropic ring current effects attributed to antiaromatic character marked by typical upfield shifts for the protons on the periphery of the macrocycle, and unusually large downfield signals for the protons at the center of the macrocycle. The unusual low-field resonance for the pyrrole NH at the center of the macrocycle further supported the strong paratropic ring current effect because of the delocalization of 20π electrons throughout the macrocycle. In addition to the two different *meso* substiutents, the lone pyrrole reduces the symmetry of the macrocycle which was supported by the eight distinct doublets for the protons on the four heterocyclic rings. This far downfield shifted NH singlet was further supported by deuterium exchange experiment upon the addition of $D_2O$. Addition of $D_2O$ led to the disappearance of downfield NH signal which exchanged with deuterium **(Figure-II.8)**. The $^{19}$F NMR spectra displayed three different signals at -143.8 ppm, -157.3 ppm and -162.9 ppm corresponding to *ortho*, *meta* and *para* substituted fluorines of pentafluoro groups recorded at 213K **(Figure-II.9)**.

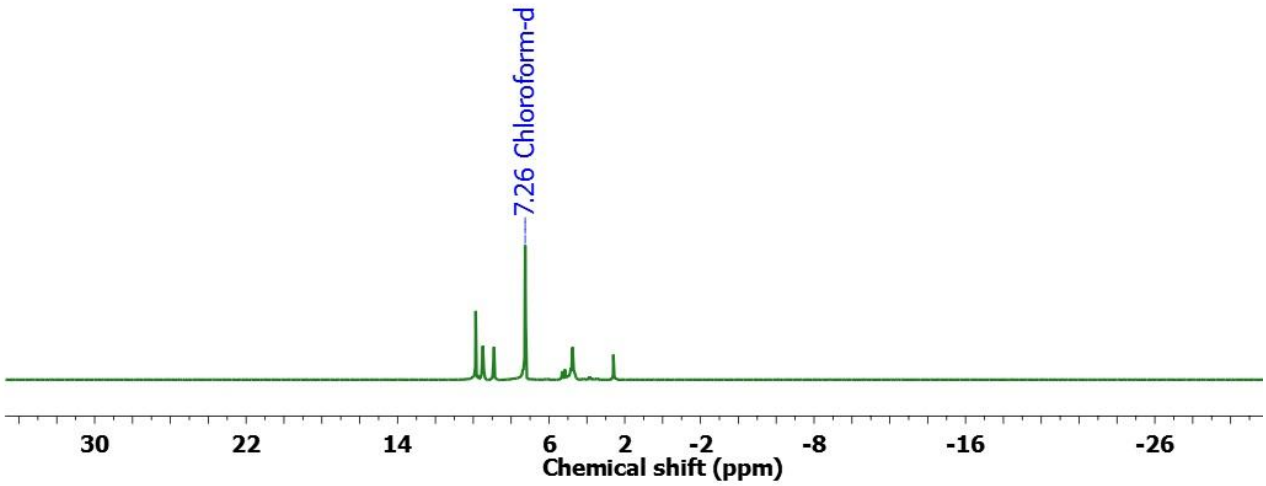


**Figure-II.8:** $^{1}$H NMR spectrum of **II.1** after $D_2O$ exchange in $CDCl_3$ at 213K

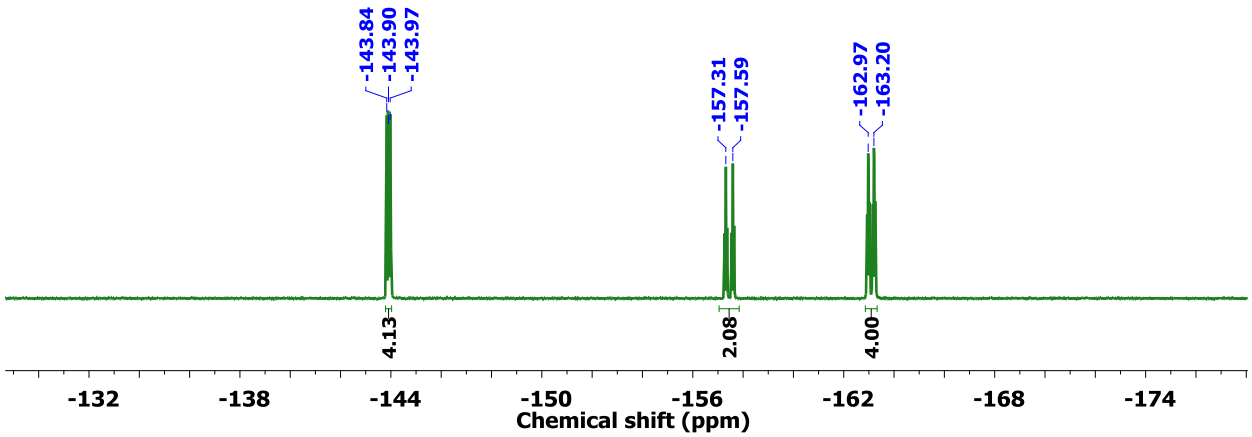


**Figure-II.9:** $^{19}$F NMR spectrum of **II.1** in acetone-$d_6$ at 213K.

The molecular structure of the 20π antiaromatic macrocycle **(II.1)** was established by single crystal X-ray diffraction analysis. The molecule displayed a complete planar conformation for the antiaromatic 20π isophlorin **(Figure-II.10)**. All the heteroatoms are pointed towards the center of the macrocycle, while the *meso* substituted phenyl and two pentafluoro phenyl rings are at a near-orthogonal orientation with respect to the mean macrocyclic plane.

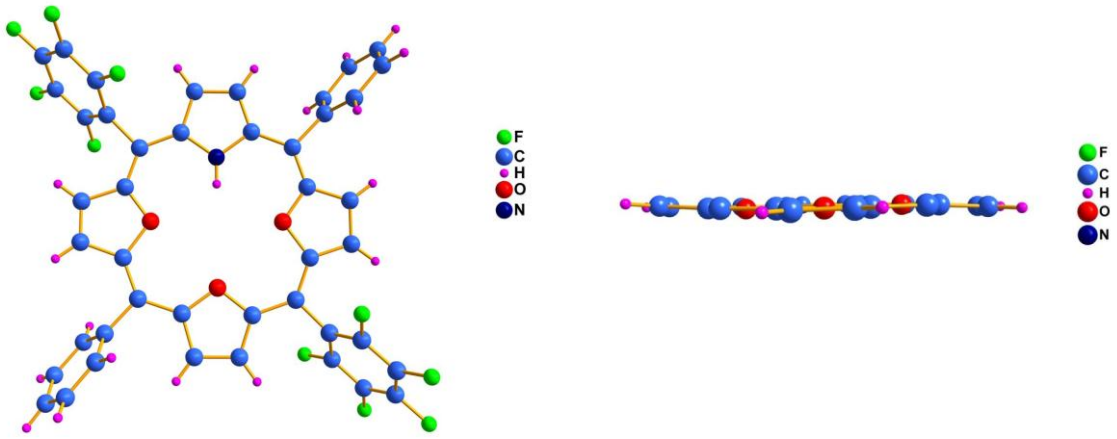


**Figure-II.10:** Molecular structure of **II.1** top view (left). In the side view (right) the *meso* substituents are omitted for clarity.

## II.6. Redox properties of [4n]π electron macrocycle (II.1):

The macrocycle **II.1** was characterized as [4n]π antiaromatic systems with 20π electrons. Preliminary cyclic voltammetry studies for **II.1** revealed redox properties with two reversible reduction waves at -1.54 V and -1.31 V respectively and two oxidation waves at +0.13 V and +0.44 V **(Figure-II.11)**,. The calculated $\Delta_{redox}$ value of 1.18 V was found to be much lesser than the 18π aromatic porphyrin. More importantly, **II.1** displayed a relatively lower oxidation potential compared to that of the tetraphenyl porphyrin **(Figure-II.12)** and *meso*-tetra(pentafluorophenyl)tetraoxaisophlorin[18]. These lower oxidation values were found to be quasi-reversible in nature.

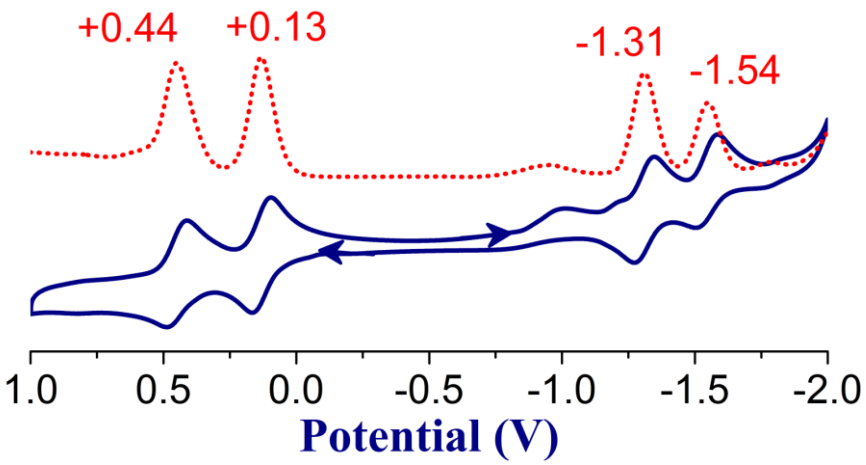


**Figure-II.11:** Cyclic voltammograms (blue line) and differential pulse voltammogram (dotted red line) of **II.1** recorded in dichloromethane ($CH_2Cl_2$) containing 0.1 M tetrabutylammonium perchlorate as the Supporting electrolyte at 50 $mVs^{-1}$ scan rate.

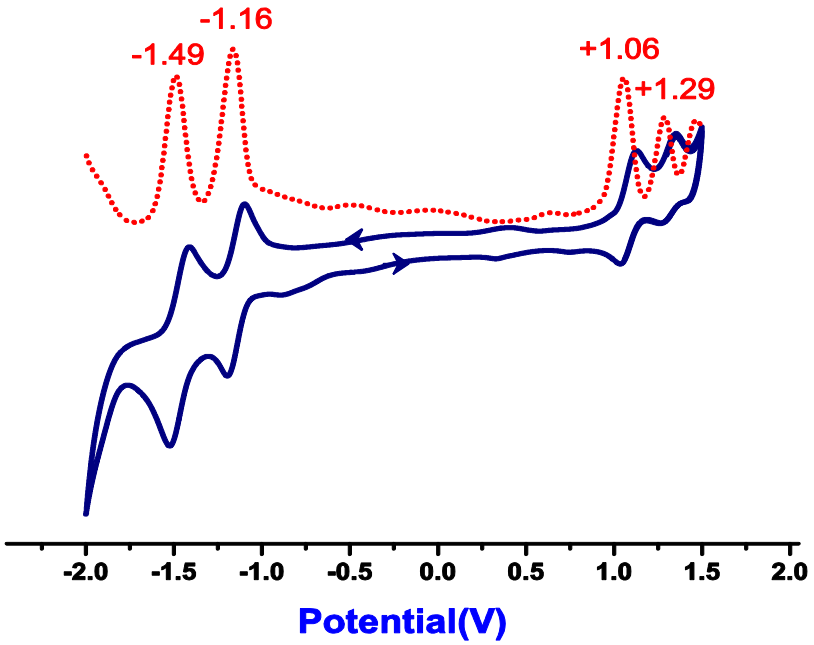


**Figure-II.12:** Cyclic voltammograms (blue line) and differential pulse voltammogram (dotted red line) of Tetra Phenyl Porphyrin (TPP).

### II.7. Two electron oxidation of macrocycle (II.1):

In support of the electrochemical studies, the molecule could be chemically oxidized to the corresponding dication with oxidizing agents such as meerwein's salt $[Et_3O]^+[SbCl_6]^-$ or $[NO^+][BF_4^-]$. It is well known that the oxidation of aromatic systems is known to yield a radical cation, while antiaromatic macrocycles tend to undergo two-electron oxidation to the corresponding the dication species[13]. Meerwein's salt such as $[Et_3O]^+[SbCl_6]$ act as an effective one electron-oxidizing agents for conjugated systems[14]. As observed earlier[15], the pyrrole NH is prone to oxidation so as to accommodate the nitrogen atom of the pyrrole in the conjugated **(Scheme-II.4)** pathway of the macrocycle. It can be envisaged that the two-electron oxidation of **II.1** can yield either the diamagnetic 18π radical dication **II.2** either directly or via two one-electron steps via the paramagnetic radical 19π cation **II.3**.

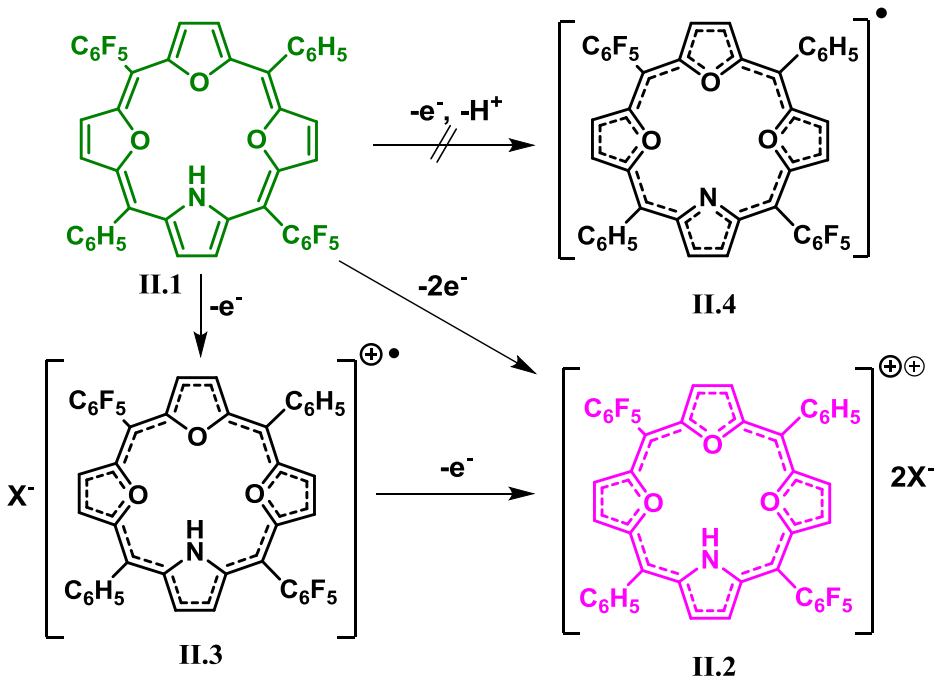


**Scheme-II.4:** Stepwise one-electron oxidation of **II.1** to **II.2** when three pyrroles are replaced by furan. $X^-$ corresponds to the counter anion ($[SbCl_6]^-$or $[BF_4]^-$).

In earlier reports, it was observed that salts such as $[Et_3O]^+[SbCl_6]$ and $[NO]^+[BF_4]^-$ act as excellent two-electron oxidizing agents for antiaromatic systems.[16] Hence, three to four equivalents of $[Et_3O]^+[SbCl_6]$ was added to a solution of **II.1** in dichloromethane and stirred for ten minutes under nitrogen atmosphere. The solution displayed an immediate change from a yellowish green to pink color suggestive of the expected oxidation **(Scheme-II.5)**. Pink-colored crystals were obtained in quantitative yield upon the evaporation of the solvent.

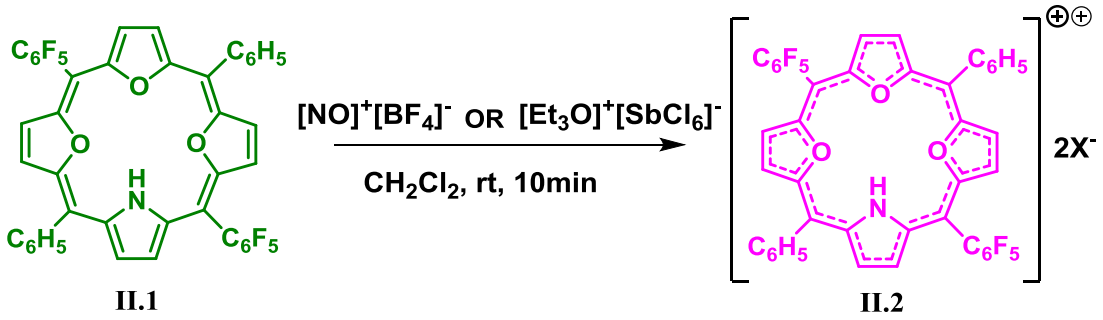


**Scheme-II.5:** Two electron oxidation of **II.1** to **II.2.** $X^-$ is the counter anion ($[SbCl_6]^-$or $[BF_4]^-$).

The ESI-TOF high-resolution mass spectrum of these pink coloured crystals displayed an *m/z* value of 399.5598 (Cald. for $[C_{44}H_{19}F_{10}NO_3]^{2+}$: 399.5602) corresponding to the dication formation of the macrocycle **II.2. (Figure-II.13)**. Interestingly, this value suggested an oxidative process without altering

the chemical composition of the macrocycle. The oxidation of the macrocycle by two electrons suggested the formation of an 18π aromatic dication. This pinkish coloured crystals solution of **II.2** displayed a red shifted Soret-like absorptions as a split band at $\lambda_{max}$ = 426 nm (ε =223 550), with weak bands in the region between λ = 540 to 625 nm **(Figure-II.14)**. This change in the absorption is found to be similar to that observed for the 20π tetraoxaisophlorins, thus supporting the two-electron oxidation to the aromatic 18π dication. It was also observed that **II.1** exhibited significant emission at $\lambda_{max}$ = 410 and 434 nm when excited either at λ = 360 or 370 nm, with a quantum yield (Φ) of 2.2% in dichloromethane, and **II.2** displayed a weak (Φ =1.2%) but strong red-shifted emission at $\lambda_{max}$ = 650 nm, which is very much similar to that observed for tetraphenyl porphyrins **(Figure-II.15)**.

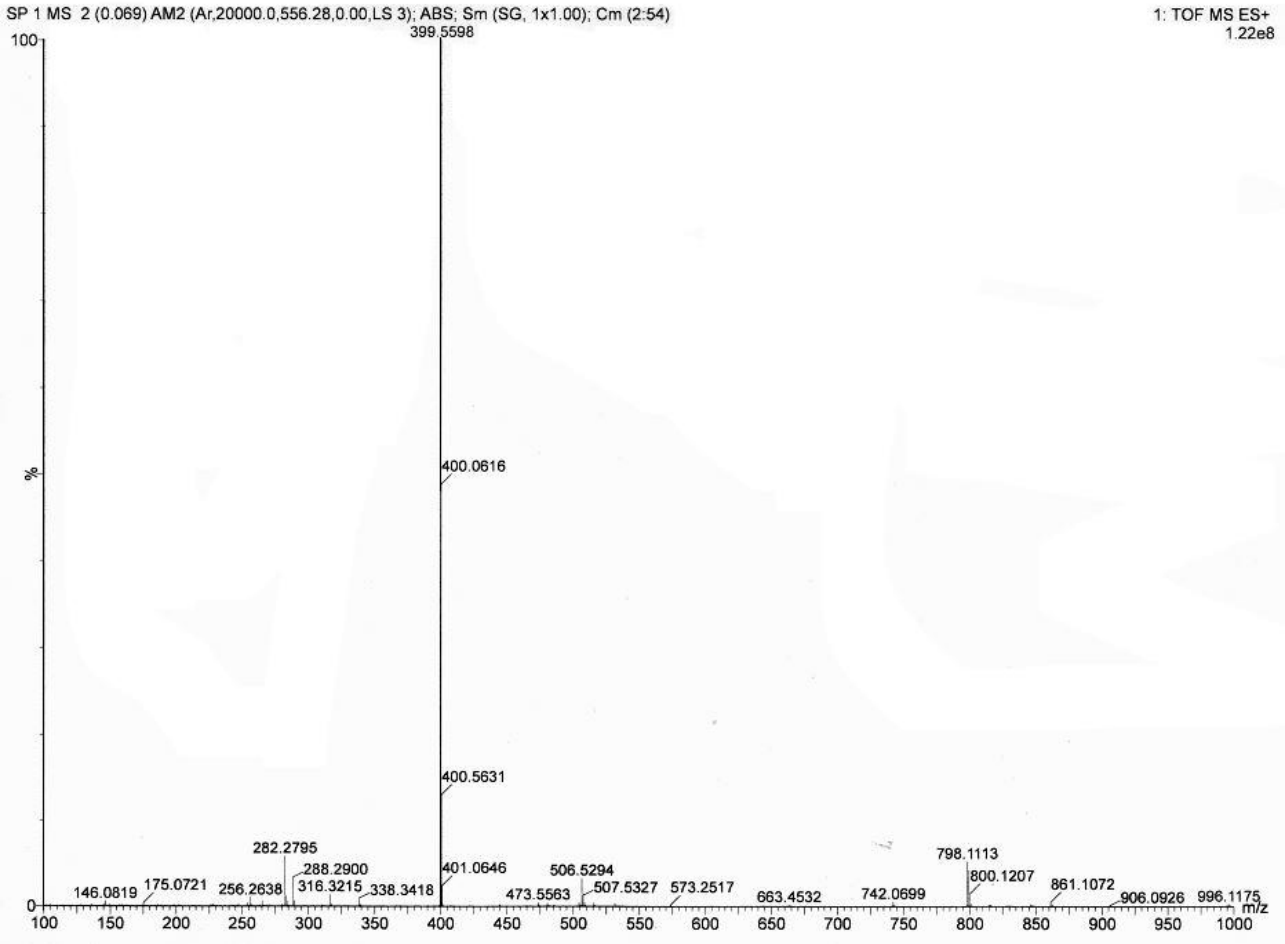


**Figure-II.13:** High resolution mass spectrum (HRMS) of **II.2**.

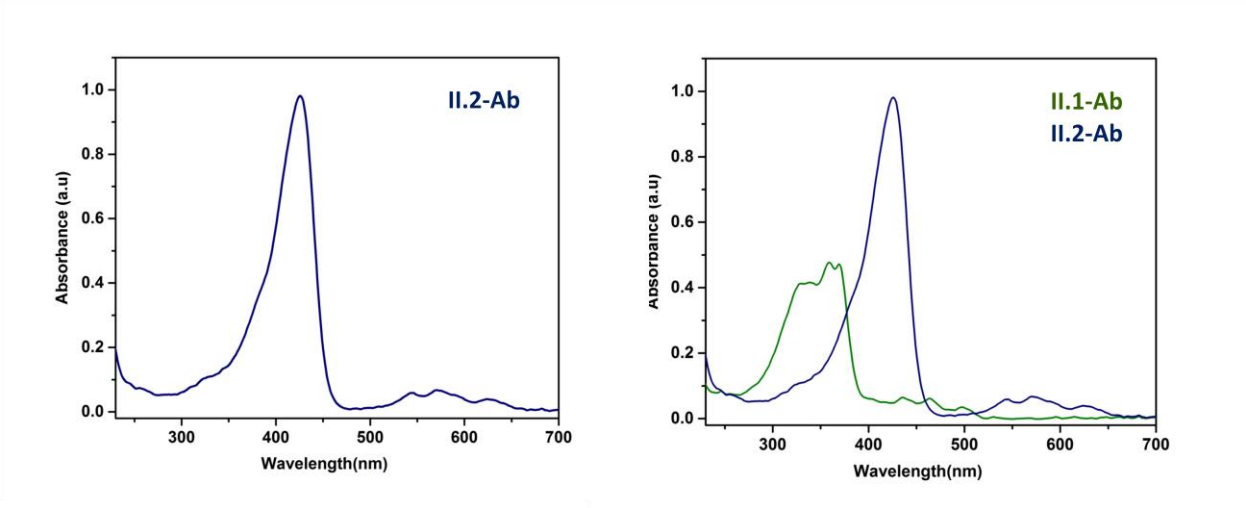


**Figure-II.14:** Electronic absorption spectrum of **II.1** and **II.2** in dichloromethane at room temperature**.**

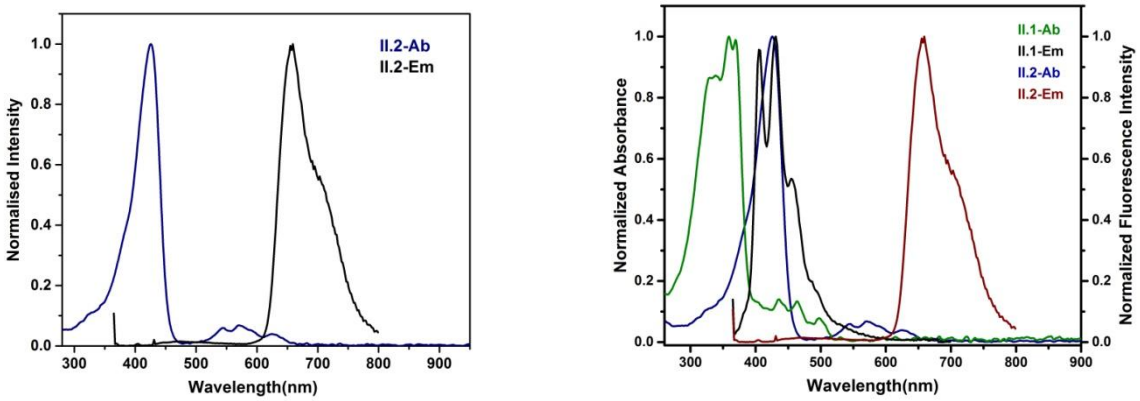


**Figure-II.15:** Electronic absorption and emission spectrum of **II.1** and **II.2** in dichloromethane at room temperature.

The dication **II.2** displayed a well-resolved $^{1}$HNMR spectrum in deuterated acetonitrile-$d_3$ ($CD_3CN$) at room temperature. Even though it displayed the same number of signals as for the anti-aromatic 20π electron macrocycle **II.1**, the chemical-shift values for the protons of the four heterocyclic rings varied significantly with respect to the neutral molecule **II.1.** In stark contrast to the upfield signals for **II.1**, the dication **II.2** displayed eight signals for the four heterocyclic rings in the low- field region between δ = 10.6 and 9.6 ppm **(Figure-16)**. All the eight signals resonated as doublets and their multiplicity was confirmed from the $^{1}$H–$^{1}$H 2D COSY spectrum **(Figure-17)**. The appearance of the NH in the high field region confirmed the 18π aromatic character of the macrocycle as observed in mono-oxa/thia porphyrins[17]. More importantly, the inner NH signal for the pyrrole ring displayed an amazing shift by nearly Δδ = 34 ppm from δ = +29.2 ppm in **II.1** to δ = -4.6 ppm in **II.2**.

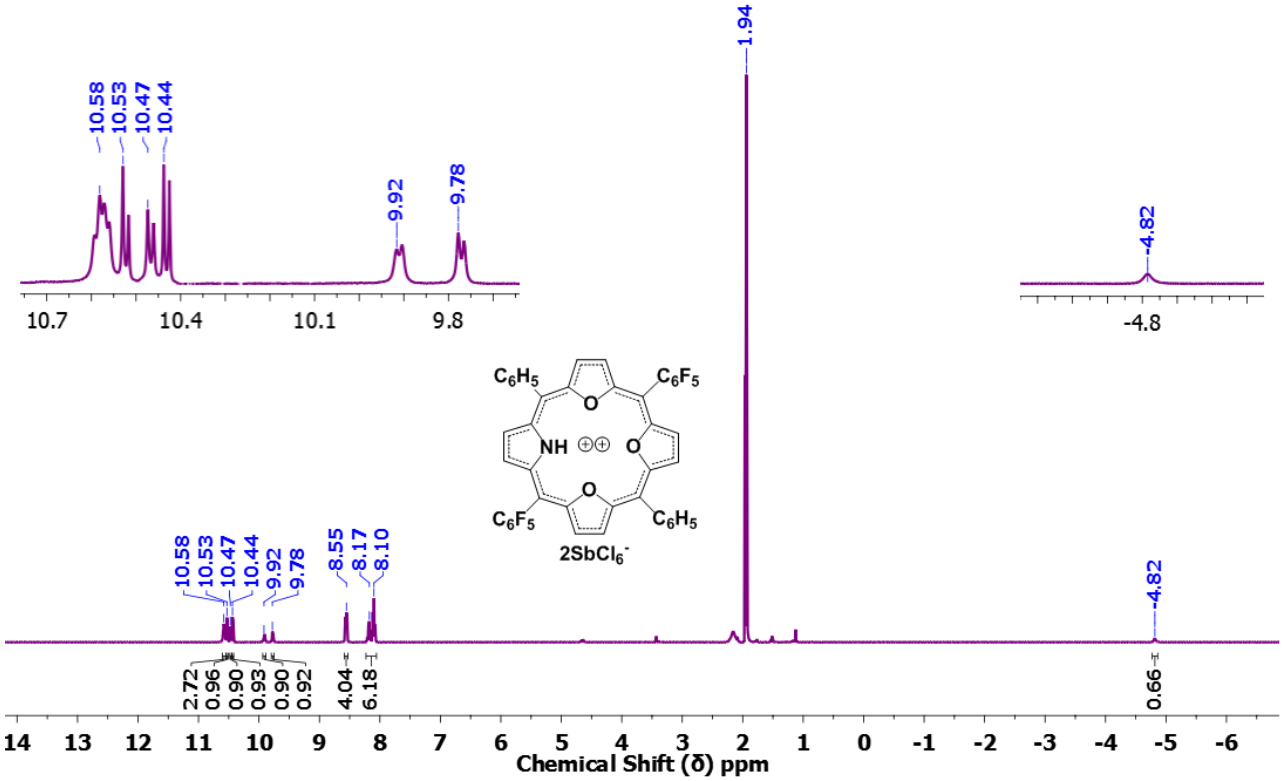


**Figure-II.16:** $^{1}$H NMR spectrum of II.2 in acetonitrile-$d_3$ at 298K.

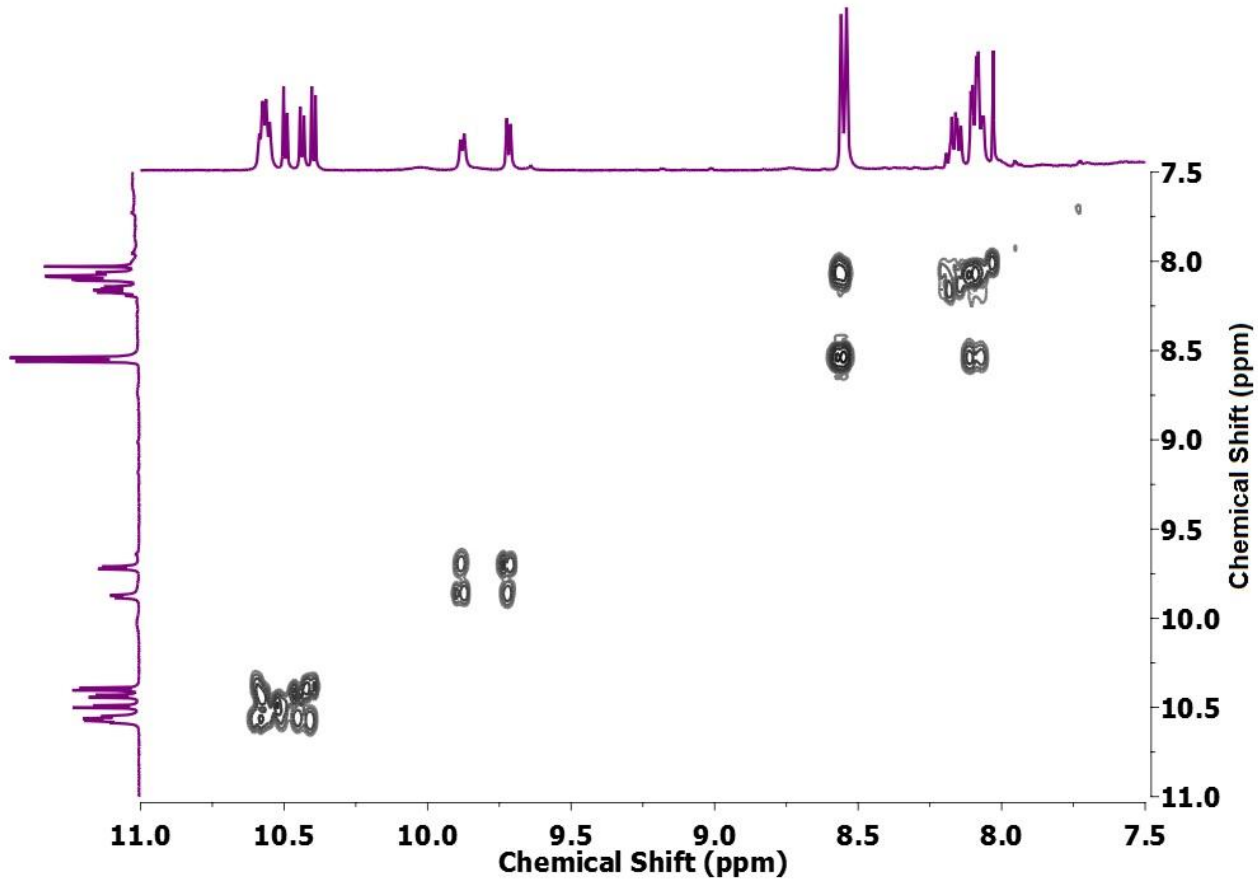


**Figure-II.17:** Partial $^{1}$H-$^{1}$H 2D COSY spectrum of II.2 in acetonitrile-$d_3$ at 298K.

This value is perhaps the largest difference between the 20π and 18π states for the NH signal amongst all the known core-modified porphyrins. The formation of this dication can be envisaged through two one-electron oxidations, with the intermediate formation **II.3** rather than the 19π radical **II.4**. Such a mechanism provides evidence in favour of resonance stabilization for an antiaromatic isophlorin even in the presence of pyrrole rings. This structure represents the first example for ring oxidation of a stable pyrrole derivative of a 20π isophlorin to an 18π dication without deprotonating the pyrrole NH. Even though such a two-electron oxidation is known for other 20π isophlorins, both states for any given isophlorin could not be characterized comprehensively, as only one of them was found to be stable under ambient conditions. The β-substituted thia/oxa/selena isophlorins were found to be stable as porphyrin dications[18], whereas the tetraphenyl (or pentafluorophenyl) tetraoxaisophlorin was found to resist oxidation to the corresponding 18π dication[19]. The molecular structure of **II.2** was unambiguously determined by single-crystal X-ray diffraction studies **(Figure-II.18)**. The macrocycle was found to sustain a planar conformation. Its dicationic behaviour was further confirmed by the presence of two $[SbCl_6]^-$ as counter anions, one above and one below the plane of the macrocycle.

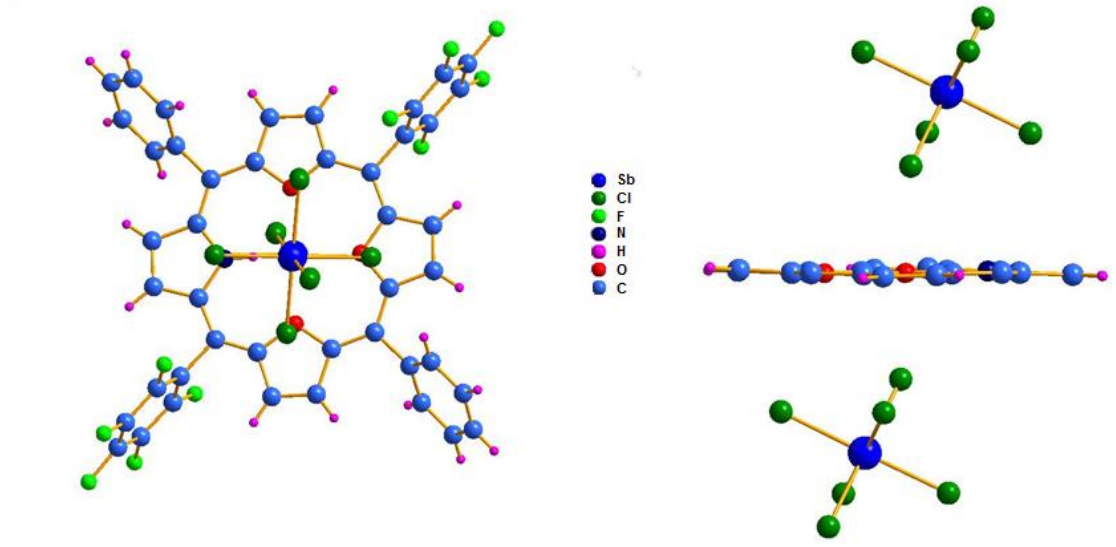


**Figure-II.18:** Molecular structure of **II.2**, top view (left) and side view (right) *meso*-pentafluorophenyl rings are omitted for clarity.

## II.8: Chemical reversibility between II.1 and II.2:

The oxidation of 20π electron macrocycle **II.1** to the dicationic species **II.2** was achieved by either $[Et_3O]^+[SbCl_6]$ or $[NO]^+[BF_4]^-$ as a one electron oxidant as evidenced by the subtle change in the colour of the solution from yellowish-green to pink upon oxidation. This pink colour solution displayed red-shifted absorption compared to neutral species and this change in absorption of Soret-like band from 359 nm in **II.1** to 426 nm in **II.2** confirmed the formation of dicationic species. In an attempt to reduce the dication

back to the 20π antiaromatic isophlorin, **II.2** was treated with reducing agents such as $FeCl_2$ and sodium. Neither of them yielded **II.1**. However, it could be reduced to **II.1** by the addition of zinc dust. This redox change was observed by electronic absorption spectroscopy **(Figure-II.19)**. Based on the earlier reports[20], it was envisaged that the fluorines of the pentafluorophenyl groups might interfere with sodium metal in the reduction mechanism. It was also observed that the dication of $[SbCl_6]^-$ undergoes a quick reduction in comparison to the $[BF_4]^-$ salt.

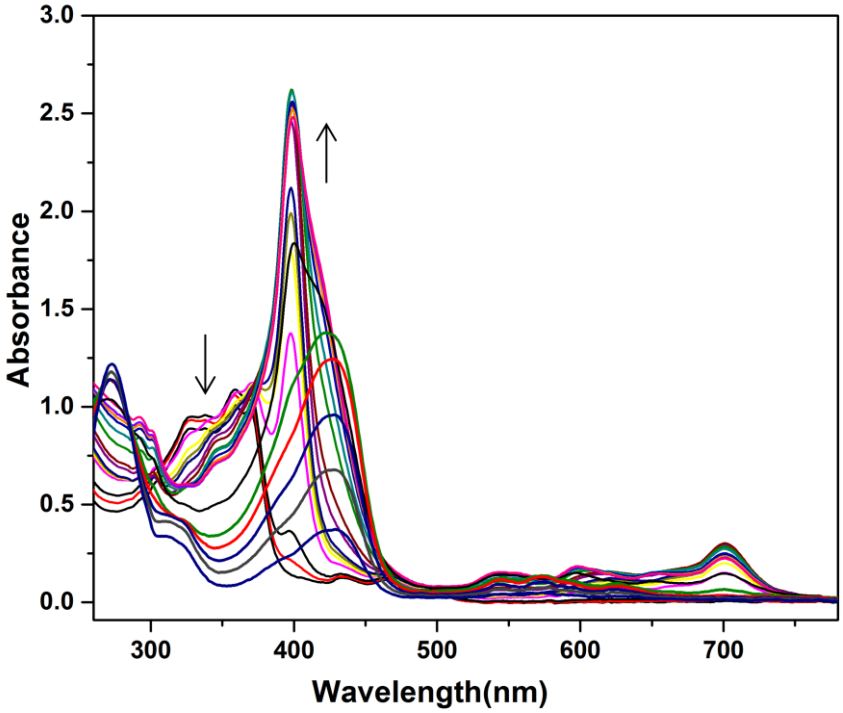


**Figure-II.19:** Changes in absorption spectrum upon addition of $[NO]^+[BF_4]^-$ to the dichloromethane solution of **II.1.**

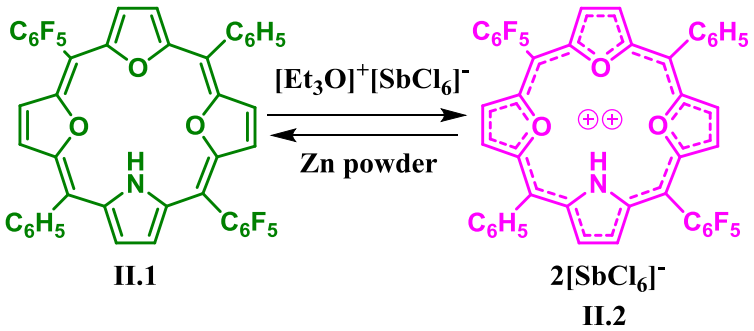


**II.1** **2[SbCl$_6$]$^-$** **II.2**

**Scheme-II.6:** Reversible redox reaction between **II.1** to **II.2.**

## II.9: Quantum mechanical calculations:

The measure of aromaticity and antiaromaticity of **II.1** and **II.2**, through quantum mechanical calculations were performed with the help of Gaussian09 rev D programme[21] The required calculations were carried out by employing Density Functional Theory (DFT) with Becke's three-parameter hybrid exchange functional and the Lee-Yang-Parr correlation functional (B3LYP) and 6-31G(d,p) basis set for all the atoms in the molecule that were subjected to these calculations. Molecular structure obtained from single crystal X-ray diffraction analysis were employed to obtain the geometry-optimized structures. Recently, Schleyer et al[22-24] introduced the use of the negative of the calculated magnetic shieldings at the ring center, which he referred as " nucleus-independent chemical shift" (NICS) as a simple magnetic criterion to measure the aromaticity and antiaromaticity (or non-aromaticity) in the cyclic conjugated systems. The magnetic properties results from the presence of ring current effects in aromatic cyclic conjugated systems when the species is placed in magnetic field. The negative NICS values indicate the aromaticity and positive NICS values for antiaromatic systems as shown in table.

| Molecule | NICS | Magnetism | Ring Current | Aromaticity |
|---|---|---|---|---|
| II.2 | -13.8 ppm | Shielding | Diatropic | Aromatic |
| II.1 | 27.6 ppm | Deshielding | Paratropic | Antiaromatic |

**Table-II.1:** NICS and ring currents.

NICS values were obtained with gauge independent atomic orbital (GIAO) method based on optimized geometries. The global ring centres for the NICS(0) values were designated at the non-weighted mean centres of the macrocycles. The large positive NICS(0) value of +27.6 ppm estimated for **II.1**, is in strong agreement with the antiaromatic character as established by the presence of strong paratropic ring current effect in its $^{1}$H NMR spectrum. The high negative NICS (0) value of -13.8 ppm for the **II.2** supports the strong aromatic character as observed in the $^{1}$H NMR spectrum of dication **II.2**.

Another criterion to determine the ring current effects in aromatic and anti-aromatic systems is the Anisotropy of Induced-Current Density (AICD)[25]. It was used to visualize the ring currents due to presence of delocalised π electrons. The magnitude and the direction of the induced ring current in the systems can be directly displayed by AICD plots when an external magnetic field is applied orthogonal to the macrocycle plane. It displays current density plots which were obtained by employing the continuous set of gauge transformations (CSGT) method to calculate the current densities, and the obtained results were plotted using POVRAY 3.7 software for Windows. In AICD plot, the clockwise ring current represents aromatic molecules whereas anticlockwise ring currents are representative of antiaromatic molecules which is similar to the NICS representations of aromatic and antiaromatic systems. Apart from the direction of

ring currents, it also helps in determining the path of the delocalized π-electrons in cyclic conjugated systems using arrows. As in **II.1** and its dicationic species **II.2**, it displayed the anti-clockwise direction of arrows for **II.1** and clockwise direction of arrows for **II.2**, suggesting the delocalization of π-electrons **(Figure-II.20)**. In both the neutral and dication species, the electron flow was observed only through the carbon perimeter.

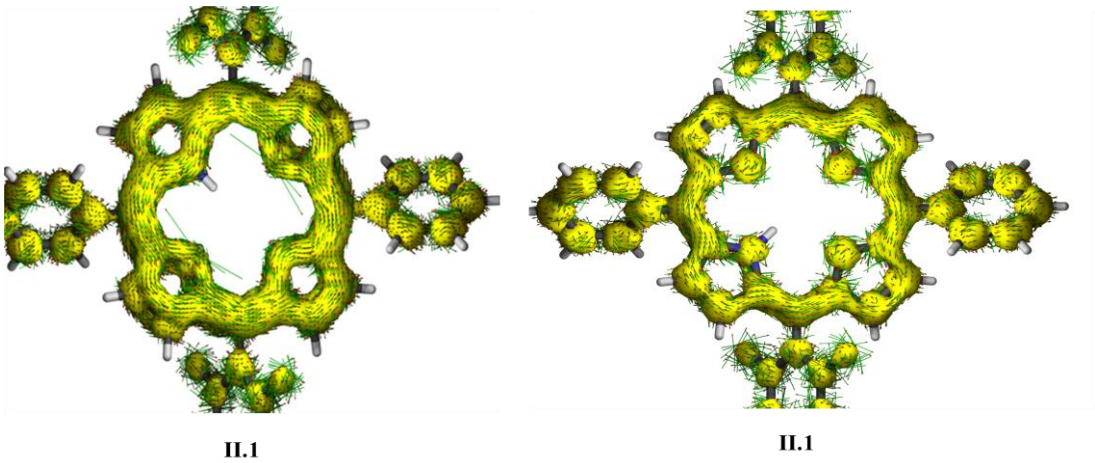


**Figure-II.20:** AICD plot of II.1 (left) and II.2 (right).

Time-dependent TD-DFT calculations were employed to study the steady-state absorption spectra, on the optimized structures. The absorption spectra for the **II.1** matched with the experimental results. The smallest HOMO-LUMO gap of 1.45 eV and 2.14 eV **(Figure-II.21)** for macrocycle **II.1** and **II.2** supported the antiaromatic and aromatic character[26] using selected molecular orbitals **(Figure-II.22)**. A relatively higher HOMO-LUMO gap of 2.14 eV for the dicationic species **II.2** supported the aromatic nature of cationic state with its absorption spectra (**Figure-II.23)**.

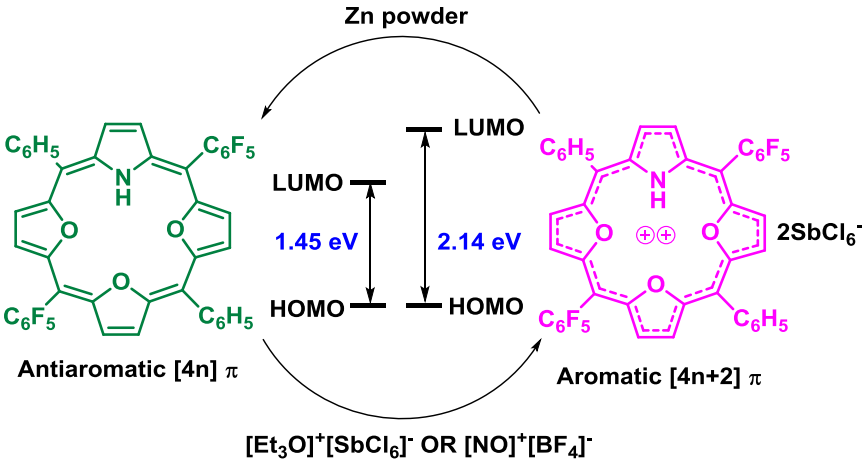


**Figure-II.21:** HOMO-LUMO gap between **II.1** and **II.2** calculated at the B3LYP/6-31G(d,p) level.

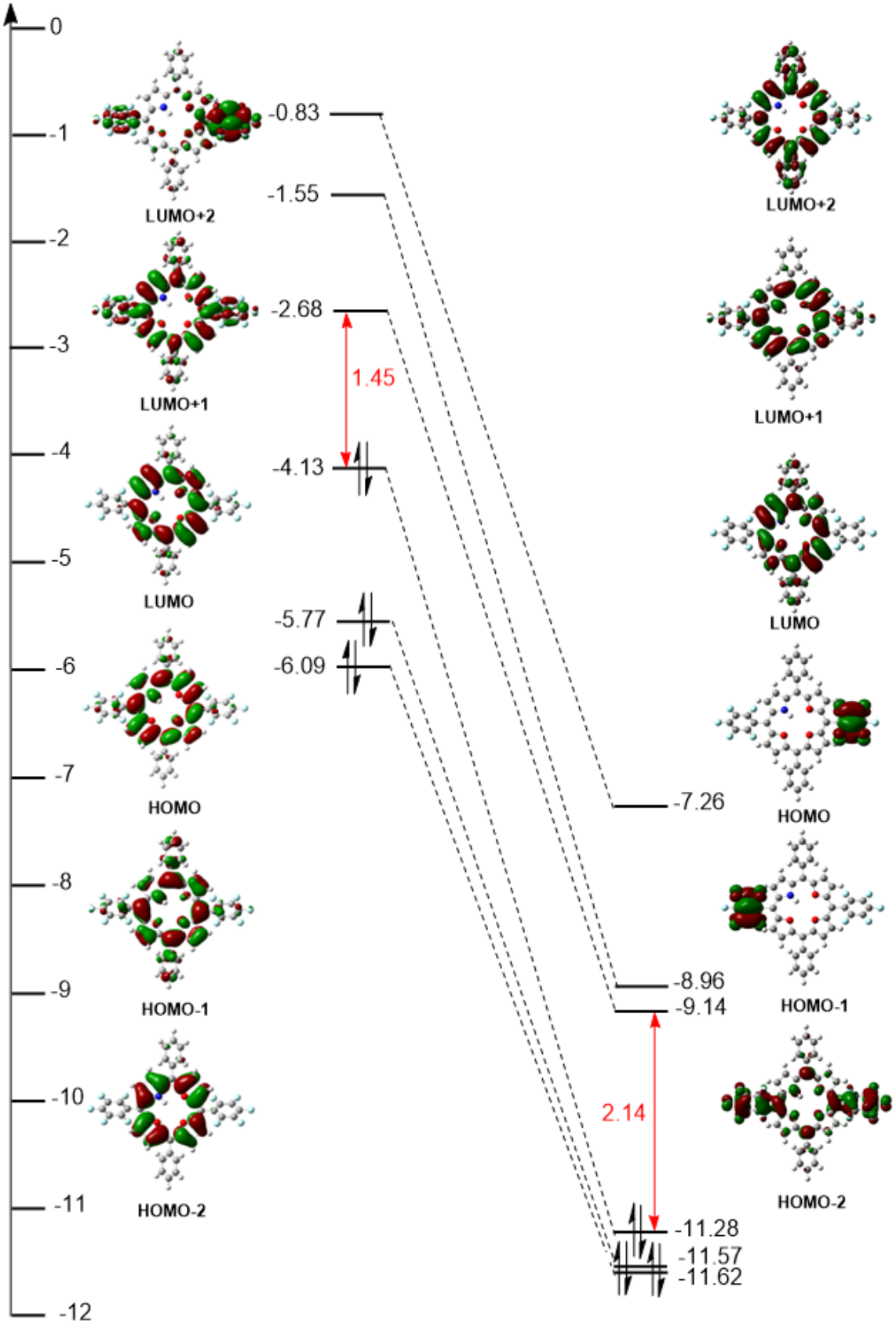


**Figure-II.22:** Selected frontier MOs of **II.1** and **II.2** calculated at the B3LYP/6-31G(d,p) level.

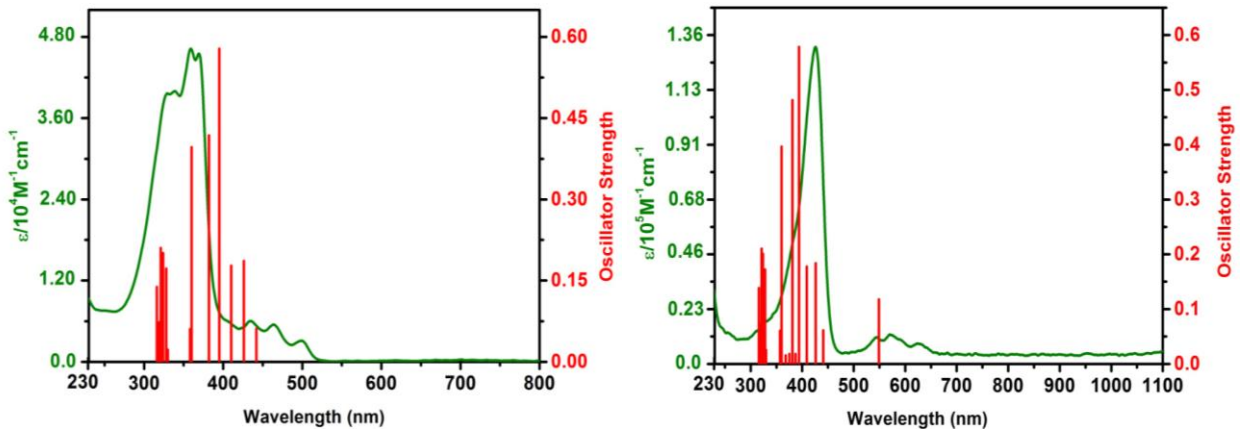


**Figure-II.23:** The steady state absorption spectra along with the theoretical vertical excitation energies (red bar) obtained from TD-DFT calculations which were carried out using B3LYP/6-31G(d,p) level of **II.1** (left) and **II.2** (right).

## II.10: Synthesis and characterization of antiaromatic dimer (II.5):

In continuation of the interesting redox properties of 20π mono pyrrole isophlorin, it could be expected that the antiaromatic dimer **II.5** similar to *meso-meso* linked tetraoxa dimer [27] would be an ideal system for four electrons oxidation

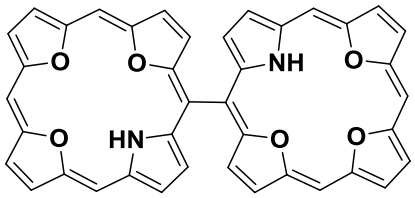


**II.5**

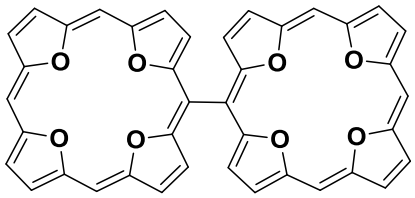


**II.6**

## II.11: Synthesis:

The synthesis of this dimer was attempted through the condensation of an equimolar ratio of difuran diol **II.a** and hetero dipyrromethane **II.c** in dry dichloromethane solution under dark condition using catalytic amount of boron trifluoride etherate. The reaction mixture was stirred for an hour followed by oxidation using DDQ with additional one hour stirring. **(Scheme-II.7)**. The MALDI-TOF/TOF mass spectrum of the reaction mixture displayed the formation of expected dimer **II.5** and the expected *meso* free four membered macrocycle **II.7** as a major product.

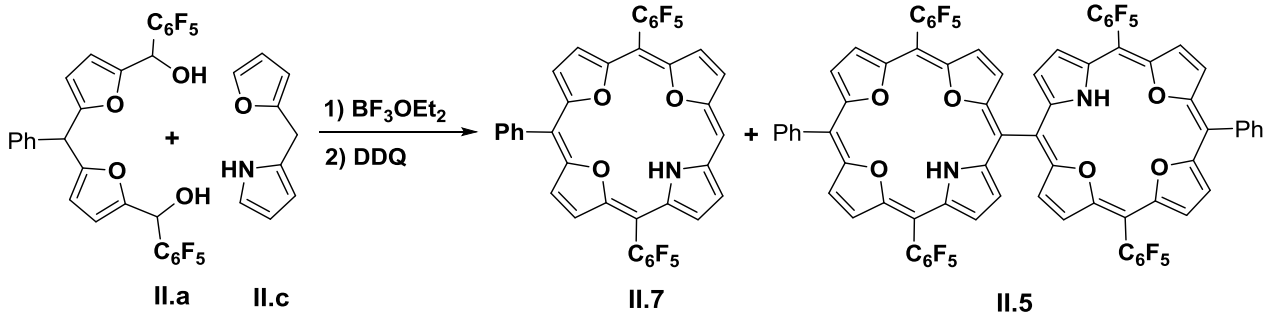


**Scheme-II.7:** Synthesis of **II.7** and **II.5.**

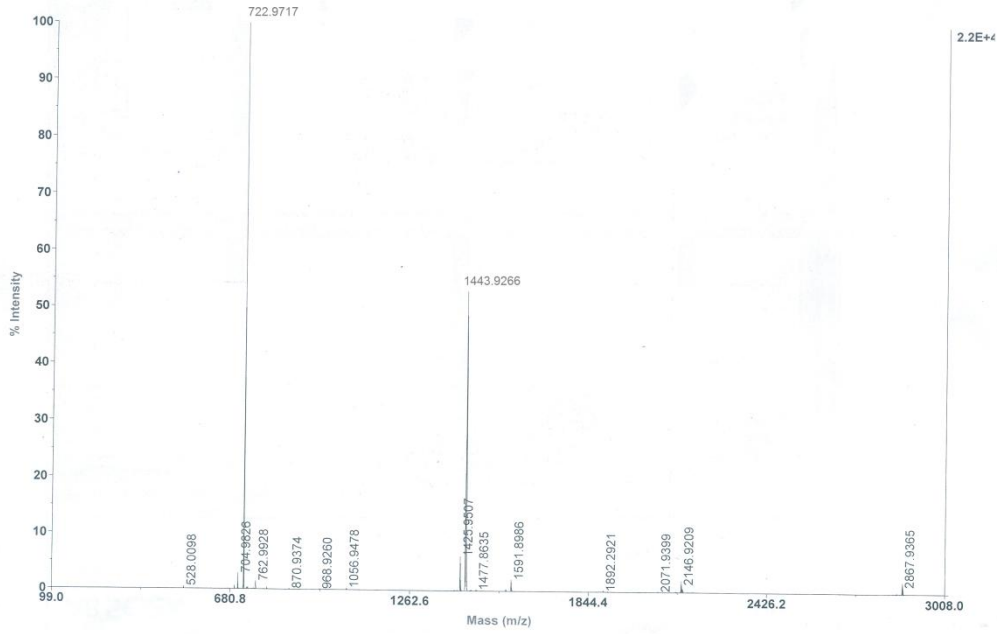


**Figure-II.23:** MALDI-TOF/TOF mass spectrum of reaction mixture (Scheme II.7).

## II.12: Isolation and characterization of meso-free macrocycle (II.7):

Further purification through column chromatography using basic alumina led to the isolation of **II.7** as a green solid which displayed $\lambda_{max}$ of 331nm in its UV-vis absorption spectrum in dichloromethane solution (**Figure-II.24**). It's molecular structure determined from single crystal X-ray diffraction analysis (**Figure-II.25**), displayed an unexpected three membered macrocycle **II.8**. instead of the expected four membered macrocycle. It confirmed that one of the furan rings was connected to the *meso* carbon (**Scheme-II.8**). In its high-resolution mass spectrum (HRMS) an *m/z* value of 723.0884 (**Figure-II.26**) further confirmed the formation of three membered 16π electron antiaromatic macrocycle (**II.8**). Even though the molecular mass of the expected **II.7** and **II.8** are the same, they represent structural isomers for a given elemental composition, which could not be distinctly distinguished from mass spectrometry. In $^{1}$H NMR spectrum of **II.8**, the inner NH proton in this case was found to resonate in the far downfield region at 30 ppm similar to **II.1** (**Figure-II.27**). Six β-protons corresponding to two furan rings and one pyrrole ring of three membered macrocycle were found to resonate in the upfield region between 3.5 to 4.5ppm. On the other hand, the

peripheral *meso* substituted protons for phenyl and furan rings were found to resonate in the downfield region (5.5 to 7.5ppm) compared to ring protons of the macrocycle. Further, these chemical shift values for the protons indicate the presence of strong paratropic ring current effects in **II.8** akin to **II.1**. The calculated NICS(1) at ring centre (29.77ppm) further confirmed the strong paratropic ring current effect.

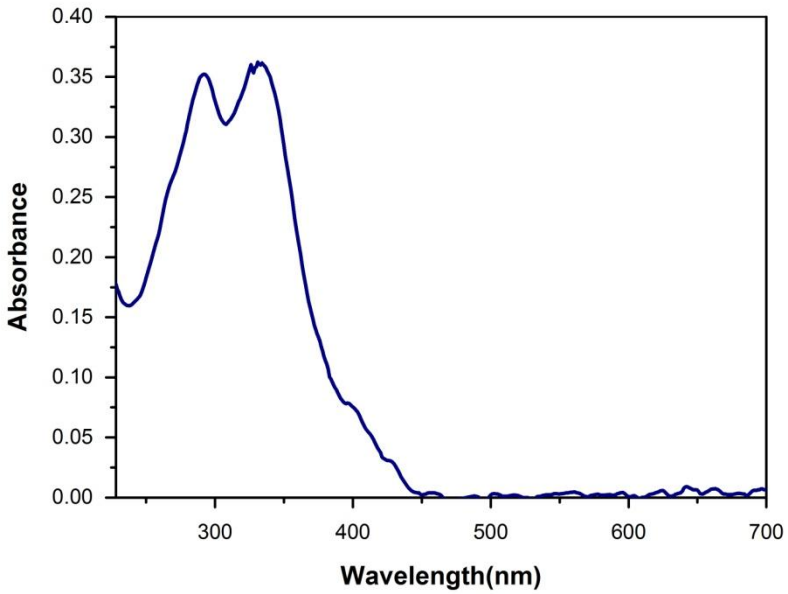


**Figure-II.24:** UV-Visible spectrum of **II.8**.

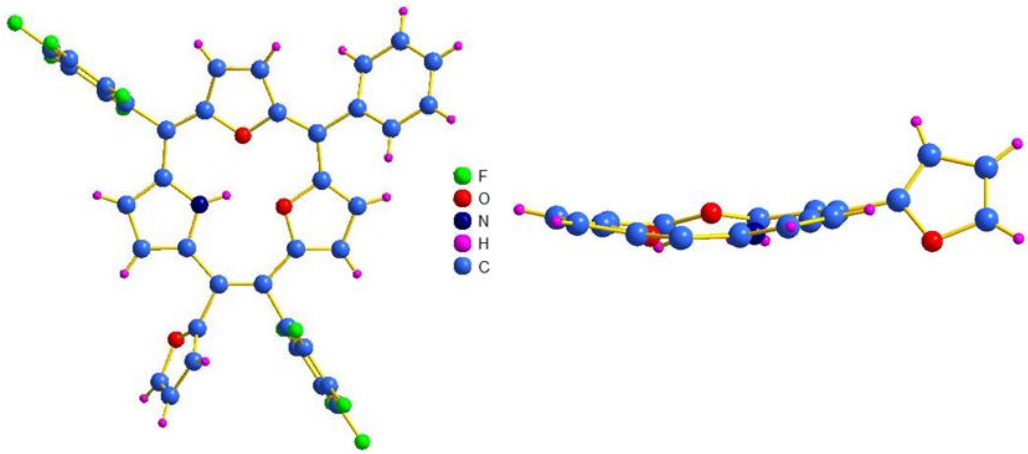


**Figure-II.25:** Molecular structure of **II.8** top view (left) and side view (right).

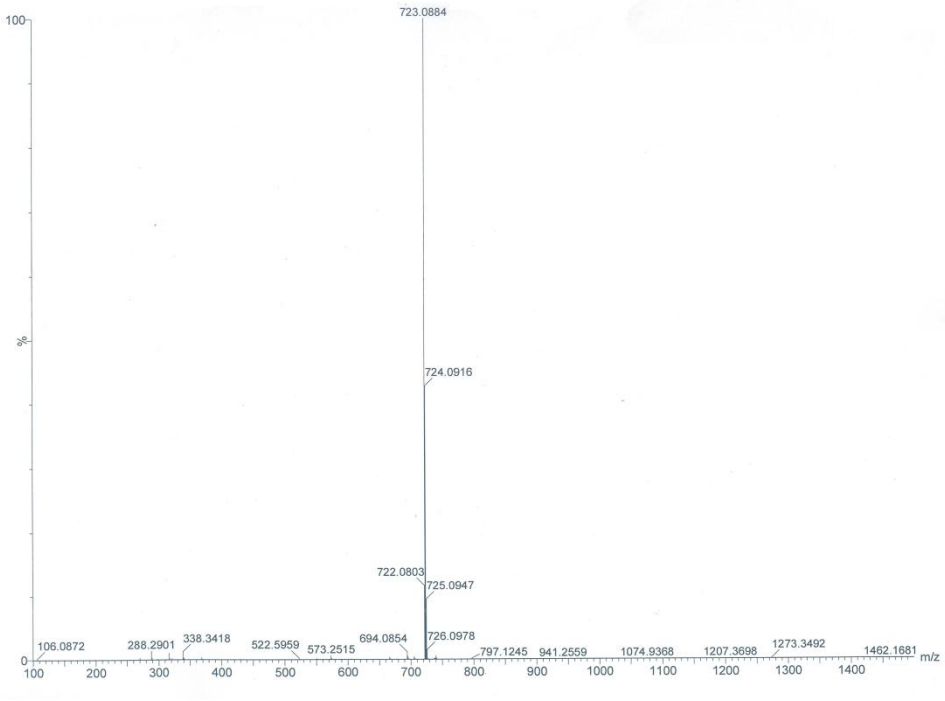


**Figure-II.26:** High resolution mass spectrum of **II.8.**

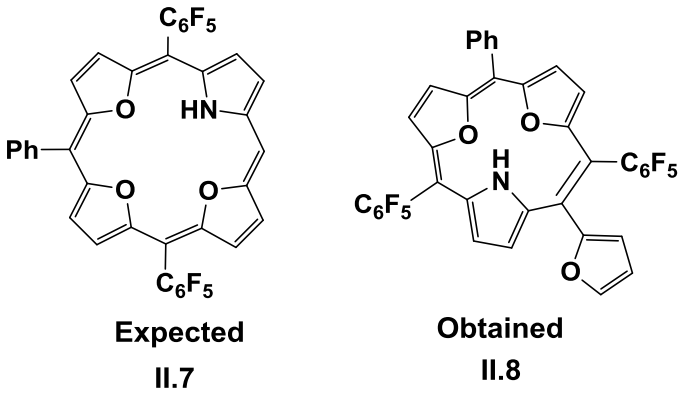


**Scheme-II.8:** Unexpected formation of **II.8** instead of **II.7**.

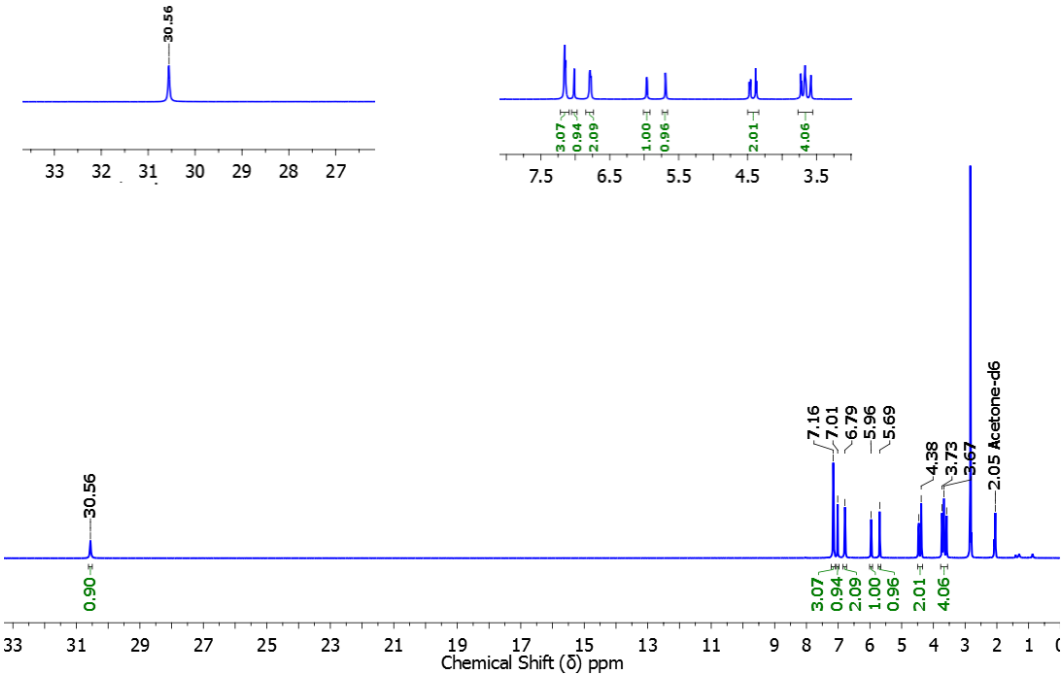


**Figure-II.27:** $^{1}$H NMR spectrum of **II.8** in Acetone-$d_6$ at 298K.

All the six signals for β-protons (two furans and one pyrrole) of three membered macrocycle **II.8** resonated as doublets and their multiplicity was confirmed from the $^{1}$H–$^{1}$H 2D COSY spectrum **(Figure-28)** and the remaining protons correspond to the *meso* phenyl and furan rings.

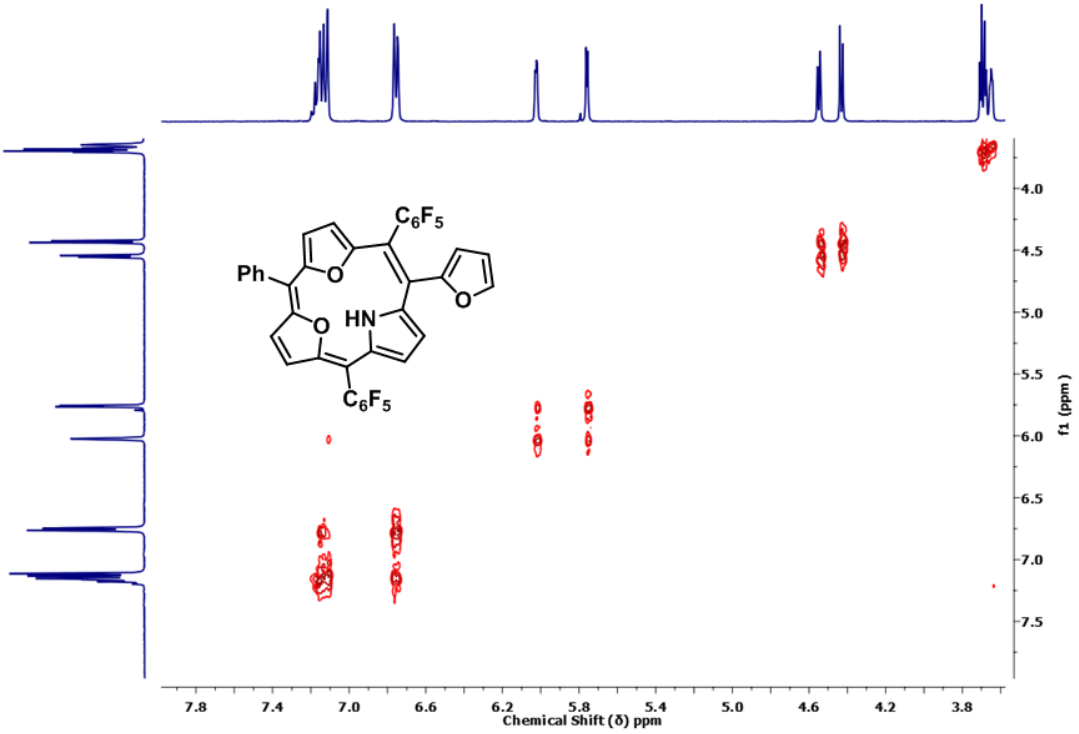


**Figure-II.28:** Partial $^{1}$H-$^{1}$H 2D COSY spectrum of **II.8** in Acetone-$d_6$ at 298K.

Based on the obtained three membered macrocycle, the expected dimer of this macrocycle could be of the structure **II.9 (Figure-II.29)**. However, the poor yields of this dimer prevented the isolation and the structural characterization of this unusual dimer.

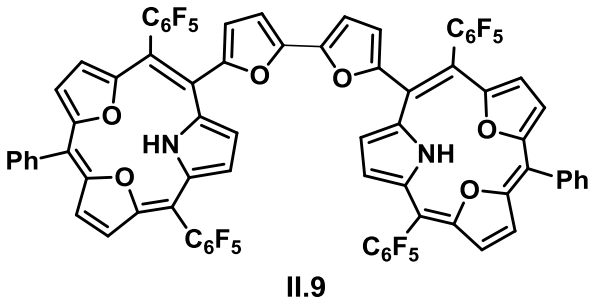


**II.9**

**Figure-II.29:** Expected dimer of **II.8** having structure **II.9**.

## II.13: Conclusion:

This successful synthesis of the first stable derivative of *mono*-pyrrole based 20π electron antiaromatic isophlorin was achieved by the partial core modification of porphyrin. It can be employed as a convenient synthetic strategy to obtain various other isomers of this isophlorin. When an equimolar ratio of *meso*-phenyldifuran carbinol was condensed with modified dipyrromethane through a MacDonald-type condensation under acidic conditions, followed by oxidation with DDQ, it yielded the 20π electron antiaromatic macrocycle. Variable temperature $^{1}$H NMR studies strongly supported the antiaromatic behaviour of neutral macrocycle, and further supported by single crystal X-ray diffraction studies. In contrast to the tetra-, tri-, and dipyrrole derivatives of a porphyrin, a monopyrrole porphyrin exhibits antiaromatic characteristics. It undergoes a reversible two-electron ring oxidation to yield the 18π aromatic dication. $^{1}$H NMR analysis provides distinct evidence of the altered electronic characteristics through typical paratropic and diatropic ring current effects for the [4n] and the [4n+2]π electrons systems, respectively. The two-electron oxidation of the antiaromatic macrocycle to the aromatic dication has been uniquely proven and these observations were studied through experiments including $^{1}$H NMR, EPR, UV-Vis, Cyclic voltammetry and single crystal X-ray crystallography and computational studies using TD-DFT, NICS and AICD. These results represent a macrocycle with a structural resemblance to the parent tetrapyrrole isophlorin, which undergoes a reversible two-electron oxidation. The chemical reversibility of the two-electron oxidation of an isophlorin to a porphyrin has been established for the first time with *mono*-pyrrole derivative of core modified porphyrin. To conclude, this *mono*-pyrrole derivative of core modified porphyrin to isophlorin appears to be a suitable building block for the synthesis of variety of core modified antiaromatic macrocycles. Further, it is observed that the reactivity and properties of antiaromatic macrocycles are found to be different than that of aromatic macrocycles. Therefore, such variety of core

modified antiaromatic molecules appear as novel ligands to ligate different metal ions. Further, the unexpected formation of three membered 16π electron antiaromatic macrocycle obtained by condensing equimolar ratio of difuran diol and *meso* free hetero dipyrromethane under catalytic amount of boron trifluoride etherate in dry dichloromethane using similar reaction conditions signifies an altered reactivity of the *meso* free dipyrromethanes. The molecular structure determined using single crystal X-ray diffraction analysis further confirmed the formation of three membered macrocycle. In its $^{1}$H NMR spectrum, the inner NH proton was found to resonate at 30 ppm and the ring β-protons of two furan and one pyrrole rings were resonating in the region between 3.5 to 4.5 ppm. The remaining eight protons corresponding to *meso* phenyl and furan resonated in the region between 7.3 to 5.6 ppm in the downfield region. The molecule exhibited the presence of strong paratropic ring current effects which was proved through experimental ($^{1}$H NMR) and computational (NICS) studies.

## II.14: Experimental Section:

All reagents and solvents were of commercial reagent grade and were used without further purification except where noted. Dry $CH_2Cl_2$ was obtained by refluxing and distillation over $P_2O_5$. Column chromatography was performed on basic alumina and silica gel (100-200mesh) in glass columns. $^{1}$H NMR and $^{19}$F NMR spectra were recorded on a Bruker 400 MHz spectrometer. Chemical shifts were reported as the delta scale in ppm relative to $(CH_3)_2CO$ 1H (δ = 2.05 ppm), or $CH_3CN$ (δ = 1.94 ppm). Electronic spectra were recorded on a Perkin-Elmer λ-35 ultraviolet−visible (UV−vis) spectro-photometer. Electron Paramagnetic Resonance (EPR) spectra were recorded using a Bruker ESP 300 EPR spectrometer. High Resolution Mass spectra were obtained using WATERS G2 Synapt Mass Spectrometer. Single-crystal diffraction analysis data were collected at 100K with a BRUKER KAPPA APEX II CCD Duo diffractometer (operated at 1500 W power: 50 kV, 30 mA) using graphite-monochromated Mo Kα radiation (λ = 0.71073 Å). More information on crystal structures can also be obtained from the Cambridge Crystallographic Data Centre, CCDC 1443655 for **7** and CCDC 1445017 for **10**. Cyclic voltammetry (CV) and Differential pulse voltammetry (DPV) measurements were carried out on a BAS electrochemical system using a conventional three-electrode cell in dry $CH_2Cl_2$ containing 0.1 M tetrabutylammonium perchlorate (TBAP) as the supporting electrolyte. Measurements were carried out under an Argon atmosphere. A glassy carbon (working electrode), a platinum wire (counter electrode), and silver (reference electrode) were used.

## II.15: Density Functional Theory (DFT) Calculations:

Quantum mechanical calculations were performed with the Gaussian 091 program suite using a High Performance Computing Cluster facility of IISER PUNE. All calculations were carried out by Density functional theory (DFT) with Becke's three-parameter hybrid exchange functional and the Lee-Yang-Parr correlation functional (B3LYP) and 6-31G (d,p) basis set for all the atoms were employed in the

calculations. The molecular structures obtained from single crystal analysis were used for geometry optimization. To simulate the steady-state absorption spectra, the time-dependent TD-DFT calculations were employed on the optimized structures. Molecular orbital contributions were determined using GaussSum 2.2.Program package. The global ring centers for the NICS (0) values were designated at the non-weighted mean centers of the macrocycles. The NICS (0) value was obtained with gauge independent atomic orbital (GIAO) method based on the optimized geometries. We calculated the Anisotropy of the current-induced density (ACID) to visualize delocalized electrons. The AICD plots can directly display the magnitude and direction of the induced ring current when an external magnetic field is applied orthogonal to the macrocycle plane. Current density plots were obtained by employing the continuous set of gauge transformations (CSGT) method to calculate the current densities, and the results were plotted using POVRAY 3.7 for Windows. The molecular orbitals were visualized using Gauss View 4.1

.

## Synthetic procedure for Isophlorin II.1:

An equimolar concentration of compound **II.a** (200 mg, 0.3246 mmol, 1 equiv.) and **II.b** (72 mg, 0.3246 mmol, 1 equiv.) were dissolved in dry 100 ml dichloromethane and stirred for five minutes under $N_2$ atmosphere. Catalytic amount of Boron trifluoride ethrate (0.040 ml, 0.3246 mmol, 1 equiv.) was added in the dark, the resulting solution was stirred for additional 1 hour. Few drops of triethyl amine was used to quench the reaction. Then, (221 mg, 0.9738 mmol, 3 equiv.) of 2,3-Dichloro-5,6-dicyano-1,4-benzoquinone (DDQ) was added and the solution stirred for further 2 hours. Finally solution was passed through short pad of basic alumina column. This crude mixture was purified by basic alumina column chromatography under $CH_2Cl_2$/petrolium ether as eluent, the greenish yellow colored, **II.1** were obtained. The resulting solid was recrystallized from $CH_2Cl_2$/hexane. Yield (10%).

**$^1$H NMR:** (400 MHz, Acetone-$d_6$, 213K) δ 29.20 (s, 1H), 7.01-6.32 (m, 10H), 2.92-2.91 (d, *J* = 4.0 Hz, 1H), 2.79-2.78 (d, *J* = 4.0 Hz, 1H), 2.70-2.71 (d, *J* = 4.0 Hz, 1H), 2.51-2.50 (d, *J* = 4.0 Hz, 1H), 2.39-2.38 (d, *J* = 4.0 Hz, 1H), 2.28 (d, 4.0 Hz, 1H), 1.99 (d, 4.0 Hz, 1H), 1.94-1.95 (d, *J* = 4 Hz, 1H). **$^{19}$F NMR:** (376 MHz, Acetone-*d*6, 298K) δ -143.91 (ddd, *J* = 24.0, 15.9, 7.1 Hz), -157.45 (dt, *J* = 105.0, 20.7 Hz), -163.09 (dtd, *J* = 27.5, 21.8, 6.6 Hz). **HRMS** (ESI-TOF)**:** *m/z*= 799.1205 (calculated for $C_{44}H_{19}F_{10}NO_3$); Observed: 799.1194 (100.0%). **UV/Vis** ($CH_2Cl_2$): $\lambda_{max}$ (ε) L mol$^{-1}$cm$^{-1}$ = 330 nm (9320.5), 359 nm (108737), 369 nm (10705), 435 nm (1453.24), 463 nm (1330.1), and 499 nm (773.54). **EPR:** g = 2.0099. **Redox:** $E^{1\text{-red}}$ = -1.54mV, $E^{2\text{-red}}$ = -1.31mV, $E^{1\text{-oxd}}$ = +0.13mV and $E^{2\text{-oxd}}$ = +0.44mV. **Crystal data:** $C_{44}H_{19}F_{10}NO_3$(*M*r = 799.60), triclinic, space group *P* 1 (no. 1), *a* = 10.128(3), *b* = 12.159(3), *c* = 15.035(4) Å, *α* = 68.086(5)°, *β* = 89.921(6)°, γ = 89.944(5)°, *V* =1717.7(8) Å$^3$, *Z* = 2, *T* = 100 K , $D_{calcd}$ = 1.546 g cm$^{-3}$, $R_{int}$ (all data) = 0.0521, $R_1$ (all data) = 0.1349, $R_w$ (all data) = 0.1392, GOF = 0.921.

## Synthetic procedure for Isophlorin II.2:

The dication **II.2**, was generated by the addition of $[Et_3O]^+[SbCl_6]^-$ or $NOBF_4$ to a solution of the macrocycle, **II.1** (10 mg) in dry dichloromethane and the resulting solution was stirred for 10 minutes under nitrogen atmosphere at room temperature. The yellowish-green coloured solution immediately changes to pink colour and this solution was further stirred for additional 15min and the solution was cooled to -30 to -60 $^oC$ in dry ice-acetone bath. This cooled solution then layered with diethyl ether and kept for additional one hour. The pink coloured crystals were formed after keeping this solution undisturbed. This pink colored crystals are submitted directly to NMR.

**$^1$H NMR**: (400 MHz, Acetonitrile-$d_3$, 298 K) δ -4.60 (s, 1H), 8.56-8.06 (m, 10H), 9.72-9.71 (d, *J* = 4.0 Hz, 1H), 9.88-9.87 (d, *J* = 4.0 Hz, 1H), 10.39-10.40 (d, *J* = 4.0 Hz, 1H), 10.44-10.43 (d, *J* = 4.0 Hz, 1H), 10.50-10.49 (d, *J* = 4.0 Hz, 1H), 10.59-10.55 (m, 3H). **HRMS** (ESI-TOF): *m/z* = 399.560 calculated for $(C_{44}H_{19}F_{10}NO_3)^{2+}$ **II.2**; Observed: 399.559 (100.0%). **UV/Vis** ($CH_2Cl_2$): $\lambda_{max}$ (ε) L $mol^{-1}cm^{-1}$ = 426 nm (223568) and Q Bands at 545 nm, 570 nm and 624 nm. **Crystal data:** $C_{48}H_{25}Cl_{12}F_{10}N_3O_3Sb_2$(*Mr* = 1550.63), triclinic, space group P 1 (no. 1), *a* = 9.9605(5), *b* = 11.3825(6), *c* = 13.7354(8) Å, *α* = 65.5920(10)°, *β* = 80.763(2)°, *γ* = 81.905(2)°, V =1394.88(13)$Å^3$, Z = 1, T = 150 K , $D_{calcd}$ = 1.846 g $cm^{-3}$, $R_{int}$ (all data) = 0.0459, $R_1$ (all data) = 0.0516, $R_w$ (all data) = 0.1430, GOF = 1.113.

## Synthetic procedure for II.8:

The synthetic procedure is similar to **II.1**. Yield: <1.5%

**$^1$H NMR:** (400 MHz, Acetone-$d_6$, 298K) δ 30.56 (s, 1H), 7.16-5.69 (*meso* phenyl and furan, 8H), 4.47-4.46 (d, *J* = 4.0 Hz, 1H), 4.38-4.37 (d, *J* = 4.0 Hz, 1H), 3.73-3.58 (m, *J* = 60Hz, 4H). **$^{19}$F NMR:** (400 MHz, Acetone-*d*6, 298K) δ -140.07 (dd, *J* = 20 Hz), -143.57 (dd, *J* = 16 Hz), -157.49 (tt, *J* = 160 Hz). **HRMS** (ESI-TOF)**:** *m/z*= 723.0892 (calculated for $C_{38}H_{15}F_{10}NO_3$); Observed: 723.0884 (100.0%). **UV/Vis** ($CH_2Cl_2$): $\lambda_{max}$ = 292nm and 331 nm. **Crystal data:** $C_{38}H_{15}F_{10}NO_3$ (*M*r = 723.51), triclinic, space group *P* -1 (no. 1), *a* = 7.588(4), *b* = 14.296(7), *c* = 14.818(7) Å, *α* = 75.860(9)°, *β* = 81.850(11)°, γ = 74.937(11)°, *V* =1499.9(13) $Å^3$, *Z* = 2, *T* = 100 K , $D_{calcd}$ = 1.602 g $cm^{-3}$, $R_{int}$ (all data) = 0.0756, $R_1$ (all data) = 0.2141, $R_w$ (all data) = 0.2209, GOF = 0.915.

## II.15. References:


[1] (a) K. M. Kadish, K. M. Smith, R. Guilard, Eds.; *The Porphyrin Handbook*, Academic press: New York, **2000**, Vol. 1. (b) K. M. Kadish, K. M. Smith, R. Guilard, Eds.; *The Porphyrin Handbook*, Academic press: New York, **2000**, Vol. 2. (c) K. M. Kadish, K. M. Smith, R. Guilard, Eds.; *The Porphyrin Handbook*, Academic press: New York, **2000**, Vol. 3. (d) K. M. Kadish, K. M. Smith, R. Guilard, Eds.; *The Porphyrin Handbook*, Academic press: New York, **2000**, Vol. 4. (e) K. M. Kadish, K. M. Smith, R. Guilard, Eds.; *The Porphyrin Handbook*, Academic press: New York, **2000**, Vol. 6.

[2] (a) K. M. Kadish, K. M. Smith, R. Guilard, Eds.; *The Porphyrin Handbook*, Academic press: New York, **2000**, Vol. 6. (b) Z. Zhou, Z. Shen, *J. Mater. Chem. C* **2015**, 3, 3239-3251. (c) T. Higashino, H. Imahori, *Dalton Trans.* **2015**, 44, 448-463. (d) Y. Ding, W. Zhu, W. -H, Y. Xie, *Chem. Rev.* **2016**, DOI: 10.1021/acs.chemrev.6b0021.

[3] L. Latos-Grazynski, J. Lisowski, M. M. Olmstead, A. L. Balch, *J. Am. Chem. Soc*. **1987**, 109, 4428-4429.

[4] Z. Gross, I. Saltsman, R. P. Pandian, C. M. Barzilay, *Tetrahedron Lett.* **1997**, 38, 2383-2386.

[5] S. Punidha, N. Agarwal, M. Ravikanth, *Eur. J. Org. Chem*. **2005**, 2500-2517.

[6] (a) A. Ulman, J. Manassen, *J. Am. Chem. Soc*. **1975**, 97, 6540-6544. (b) A. Ulman, J. Manassen, *J. Chem. Soc. Perkin Trans.* 1 **1979**, 1066-1069. (c) P. Y. Heo, K. Shin, C. H. Lee, *Tetrahedron Lett.* **1996**, 37, 197-200. (d) P. Y. Heo, C. H. Lee, *Bull. Korean Chem. Soc*. **1996**, 17, 515-520. (e) W. S. Cho, C. H. Lee, *Bull. Korean Chem. Soc*. **1998**, 19, 314-319.

[7] W. S. Cho, C. H. Lee, *Bull. Korean Chem. Soc*. **1998**, 19, 314-319.

[8] C. H. Lee, W. S. Cho, *Tetrahedron Lett.* **1999**, 40, 8879-8882.

[9] L. Latos-Grazynski in *The porphyrin Handbook*, (Eds.: K. M. Kadish, K. M. Smith, R. Guilard), Academic, New York, **2000**.

[10] (a) A. Srinivasan, B. Sridevi, M. V. Reddy, S. J. Narayanan, T. K. Chandrashekar, *Tetrahedron Lett*. **1997**, 38, 4149. (b) M. Ravikanth, T. K. Chandrashekar, *Struct. Bonding (Berlin)* **1995**, 82, 105–188. (c) B. Sridevi, S. J. Narayanan, A. Srinivasan, M. V. Reddy, T. K. Chandrashekar, *J. Porphyrins Phthalocyanines* **1998**, 1, 69. (d) P. Y. Heo, K. Shin, C. H. Lee, *Tetrahedron Lett*. **1996**, 37, 197. (e) C. H. Lee, W. S. Cho, *Tetrahedron Lett*. **1999**, 40, 8879. (f) N. Sprutta, L. Latos-Grazynski, *Org. Lett*. **2001**, 3, 1933.

[11] Hejian Zhang, Hoa Phan, Tun Seng Herng, Tullimilli Y. Gopalakrishna, Wangdong Zeng, Jun Ding, and Jishan Wu, *Angew. Chem. Int. Ed*. **2017**, 56, 13484.
[12] (a) Z. Sun, S. Lee, K. H. Park, X. Zhu, W. Zhang, B. Zheng, P. Hu, Z. Zeng, S. Das, Y. Li, C. Chi, R. W. Li, K. W. Huang, J. Ding, D. Kim, J. Wu, *J. Am. Chem. Soc*. **2013**, 135, 18229 (b) Z. Zeng, X. Shi, C. Chi, J. T. L. Navarrete, J. Casado, J. Wu, *Chem. Soc. Rev*. **2015**, 44, 6578.

[13] (a) T. Y. Gopalakrishna, V. G. Anand, *Angew. Chem. Int. Ed*. **2014**, 53, 6678, *Angew. Chem. Int. Ed.* **2014**, 126, 6796. (b) B. Franck, A. Nonn, *Angew. Chem. Int. Ed*. **1995**, 34, 1795, *Angew.Chem. Int. Ed* **1995**, 107, 1941. (c) V. Markl, T. Knott, P. Kreitmeier, T. Burgemeister, F. Kastner, *Helv. Chim. Acta* **1998**, 81, 1480. (d) G. Markl, R. Ehrl, H. Sauer, P. Kreitmeier, T. Burgemeister, *Helv. Chim. Acta* **1999**, 82, 59.

[14] R. Rathore, A. S. Kumar, S. V. Lindeman, J. K. Kochi, *J. Org. Chem.* **1998**, 63, 5847-5856.

[15] a) K. M. Kadish, K. M. Smith, R. Guilard, Eds.; *The Porphyrin Handbook*, Academic press: New York, **2000**, Vol. 1. (b) K. M. Kadish, K. M. Smith, R. Guilard, Eds.; *The Porphyrin Handbook*, Academic press: New York, **2000**, Vol. 2. (c) K. M. Kadish, K. M. Smith, R. Guilard, Eds.; *The Porphyrin Handbook*, Academic press: New York, **2000**, Vol. 3. (d) K. M. Kadish, K. M. Smith, R. Guilard, Eds.; *The Porphyrin Handbook*, Academic press: New York, **2000**, Vol. 4. (e) K. M. Kadish, K. M. Smith, R. Guilard, Eds.; *The Porphyrin Handbook*, Academic press: New York, **2000**, Vol. 6.

[16] T. Y. Gopalakrishna, V. G. Anand, *Angew. Chem. Int. Ed.* **2014**, 53, 6678, *Angew. Chem. Int. Ed.* **2014**, 126, 6796.

[17] E. Vogel, P. Rohrig, M. Sicken, B. Knipp, A. Herrmann, M. Pohl, H. Schmickler, J. Lex, *Angew. Chem. Int. Ed*. 28, **1989**, 1651-1655.

[18] (a) E. Vogel, *Pure Appl. Chem*. **1993**, 65, 143. (b) M. Pohl, H. Schmickler, J. Lex, E. Vogel, *Angew. Chem. Int. Ed*. **1991**, 30, 1693, *Angew. Chem. Int. Ed*. **1991**, 103, 1737. (c) W. Haas, B. Knipp, M. Sicken, J. Lex, E. Vogel, *Angew. Chem. Int. Ed.* **1988**, 27, 409, *Angew. Chem. Int. Ed.* **1988**, 100, 448. (d) E. Vogel, C. Frçde, A. Breihan, H. Schmickler, J. Lex, *Angew. Chem. Int. Ed.* **1997**, 36, 2609, *Angew. Chem. Int. Ed.* **1997**, 109, 2722. (e) E. Vogel, P. Rohrig, M. Sicken, B. Knipp, A. Herrmann, M. Pohl, H. Schmickler, J. Lex, *Angew. Chem. Int. Ed.* **1989**, 28, 1651, *Angew. Chem. Int. Ed.* **1989**, 101, 1683.

[19] J. S. Reddy, V. G. Anand, *J. Am. Chem. Soc.* **2008**, 130, 3718-3719.

[20] (a) T. Y. Gopalakrishna, V. G. Anand, *Angew. Chem. Int. Ed*. **2014**, 53, 6678, *Angew. Chem. Int. Ed.* **2014**, 126, 6796, (b) B. Franck, A. Nonn, *Angew. Chem. Int. Ed.* **1995**, 34, 1795, *Angew. Chem. Int. Ed*.

**1995**, 107, 1941, (c) V. Markl, T. Knott, P. Kreitmeier, T. Burgemeister, F. Kastner, *Helv. Chim. Acta* **1998**, 81, 1480, (d) G. Markl, R. Ehrl, H. Sauer, P. Kreitmeier, T. Burgemeister, *Helv. Chim. Acta* **1999**, 82, 59.

[21] Gaussian 09, Revision D.01, M. J. Frisch, G. W. Trucks, H. B. Schlegel, G. E. Scuseria, M. A. Robb, J. R. Cheeseman, G. Scalmani, V. Barone, B. Mennucci, G. A. Petersson, H. Nakatsuji, M. Caricato, X. Li, H. P. Hratchian, A. F. Izmaylov, J. Bloino, G. Zheng, J. L. Sonnenberg, M. Hada, M. Ehara, K. Toyota, R. Fukuda, J. Hasegawa, M. Ishida, T. Nakajima, Y. Honda, O. Kitao, H. Nakai, T. Vreven, J. A. Montgomery, Jr., J. E. Peralta, F. Ogliaro, M. Bearpark, J. J. Heyd, E. Brothers, K. N. Kudin, V. N. Staroverov, R. Kobayashi, J. Normand, K. Raghavachari, A. Rendell, J. C. Burant, S. S. Iyengar, J. Tomasi, M. Cossi, N. Rega, J. M. Millam, M. Klene, J. E. Knox, J. B. Cross, V. Bakken, C. Adamo, J. Jaramillo, R. Gomperts, R. E. Stratmann, O. Yazyev, A. J. Austin, R. Cammi, C. Pomelli, J. W. Ochterski, R. L. Martin, K. Morokuma, V. G. Zakrzewski, G. A. Voth, P. Salvador, J. J. Dannenberg, S. Dapprich, A. D. Daniels, Ö. Farkas, J. B. Foresman, J. V. Ortiz, J. Cioslowski, and D. J. Fox, Gaussian, Inc., Wallingford CT, 2009.

[22] T. K. Zywietz, H. Jiao, P. v. R. Schleyer, A. de Meijere, *J. Org. Chem*. **1998**, 63, 3417-3422.

[23] Z. Chen, C. S. Wannere, C. Corminboeuf, R. Puchta, P. v. R. Schleyer, *Chem. Rev*. **2005**, 105, 3482.

[24] P. V. Schleyer, C. Maerker, A. Dransfeld, H. J. Jiao, N. J. R. V. Hommes, *J. Am. Chem. Soc*. **1996**, 118, 6317.

[25] D. Geuenich, K. Hess, F. Kohler, R. Herges, *Chem. Rev*. **2005**, 105, 3758.

[26] S. Cho, Z. S. Yoon, K. S. Kim, M. C. Yoon, D. G. Cho, J. L. Sessler, D. Kim, *J. Phys. Chem. Lett*, **2010**, 1, 895.

[27] B. K. Reddy, S. G. Gadekar, V. G. Anand, *Chem. Commun*, **2016**, 52, 3007-3009.

# Chapter III

# Synthesis, Characterization and Redox Properties of 20π S-Confused Antiaromatic Isophlorins

## III.1. Introduction:

Ever since the serendipitous discovery of N-confused porphyrins (NCP's)[1] or inverted porphyrins **I.12**, many synthetic methods have been developed for a variety of NCPs and their derivatives. These inverted-porphyrins are porphyrin-like macrocycles and display aromatic characteristics. Structural isomers of porphyrin such as NCP **I.12** and neo-confused porphyrin[2], **III.2**, have attracted significant interest for the synthesis of porphyrinoid organometallic complexes.[3] Both, **I.12** and **III.2**, (**Scheme-III.1**) represent isomeric porphyrin skeletons obtained by swapping the positions of a carbon and nitrogen in a single pyrrole ring. Confused porphyrin derivatives, **I.14a-c**, have also been synthesized by replacing a pyrrole by other heterocycles such as thiophene/furan/selenophene to yield core-modified NCP.[4] Even these macrocycles displayed aromatic characteristics and were able to bind metal ions. It can be envisaged that the nature of the macrocyclic ligand can be tuned if the nature of the co-ordinating atoms are modified in the core of this macrocycle. Doubly confused porphyrins have also been synthesized and were found to bind metal ions similar to porphyrin or NCP. Complete modification of a confused porphyrin have evaded the synthetic chemists till date.

Replacing all the four pyrrole rings of NCP **I.12**, with a different heterocycle such as thiophene leads to the formation of new class of inverted isophlorin, which can be coined as S-confused isophlorin **III.5**. This S-confused isophlorin **III.5**, bears structural resemblance to isophlorin **II.1** wherein one of the heterocycles is inverted and connected through α,β-linkage. This modification of isophlorin core **III.1** leads to the formation of new class of macrocycles known as carbaisophlorinoids **III.5**. As described earlier, it is obvious that replacing all the four pyrroles by furan or thiophene alters the conjugated pathway from the 18π to 20π network, with negligible change in its ring size and the same change is observed in S-confused isophlorin. In this chapter the synthesis, structural, electronic and redox properties of first generation confused isophlorin, a structural twin of isophlorin, such as S-confused isophlorin with one inverted heterocyclic ring will be described in detail.

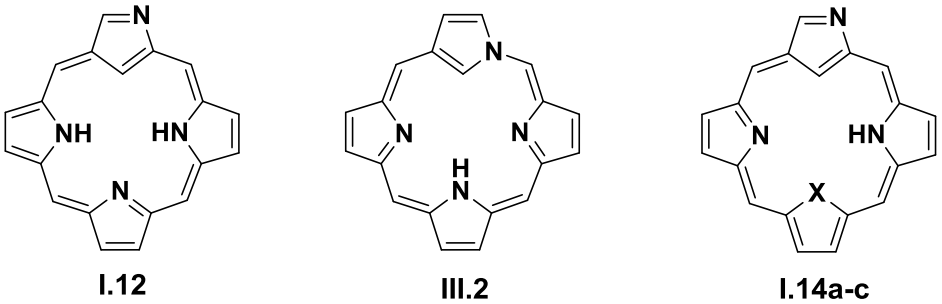


**Scheme-III.1:** Structural illustration for N-confused porphyrin **I.12**, Neo-confused porphyrin **III.2** and core-modified N-confused porphyrins, **I.14a-c**.

Latos-Grazynski and co-workers[5] reported a S-confused porphyrin, **III.4a (Scheme-III.2)**, in which a thiophene ring was inverted similar to the confused pyrrole of **I.12**. Its oxidation yielded an exocyclic keto

group on the alpha carbon of the confused thiophene, **III.4b**, with enhanced aromaticity **(Scheme-III.2)**. Replacing all the pyrrole units by thiophene in **I.12** should result in the formation of a S-confused anti-aromatic isophlorin, **III.5**. Unlike **III.4a**, oxidation of **III.5** to the corresponding exocyclic C=O should ideally yield a 19π electron radical, **III.6**. By virtue of antiaromatic property, the oxidation of **III.5** to its corresponding 18π macrocyclic dication, $[\mathbf{III.5}]^{2+}$ is a potential inhibitor to yield the macrocyclic radicaloid, **III.6**. An apparent resistance to oxidation by isoelectronic tetrathia porphycene[6] illustrates a solitary report on structure induced altered redox properties in antiaromatic macrocycles. In this chapter, the synthesis of a chlorinated derivative of S-confused 20π tetra-thiaisophlorin, **III.8**, with unique redox property to yield an aromatic porphyrin mono cation upon its oxidation will be described in detail.

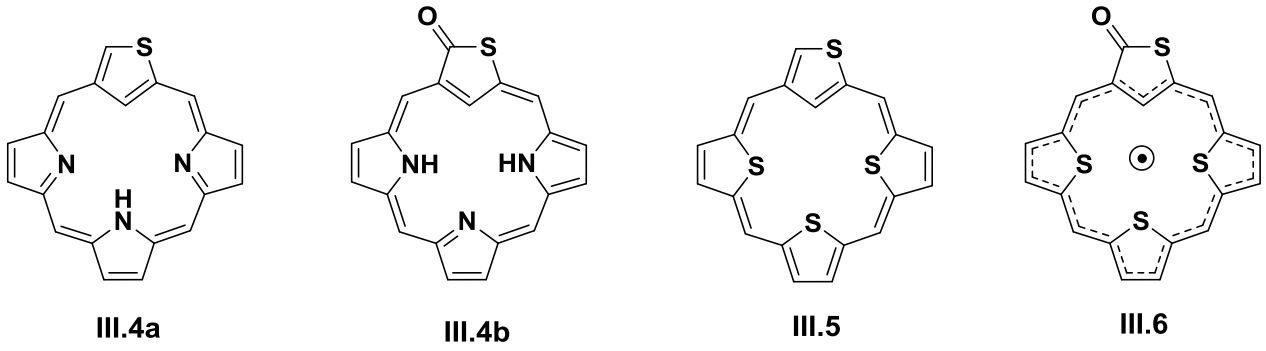


**Scheme-III.2:** Illustrative representation of S-confused porphyrin (**III.4a** and **III.4b**) and the proposed confused isophlorins (**III.5** and **III.6**).

## III.2. Synthesis of S-confused isophlorin (III.8b):

NCP **I.12** can be synthesized through a one-pot synthesis with commercially available precursors such as pyrrole and aryl aldehyde.[7] However, its anti-aromatic twin, namely the confused isophlorin has not been known till date. It can be envisaged that a synthetic procedure parallel to the synthesis of NCP could be possible with other heterocyclics such as thiophene/furan/selenophene. Yet, a similar methodology failed to yield **III.5** when thiophene was reacted with pentafluoro benzaldehyde under reaction conditions similar to the synthesis of NCP. The methodology failed even with furan and selenophene. Therefore, a rational approach to the synthesis of S-confused isophlorin was designed from appropriate precursors. Two different approaches were designed from thiophene diol. In principle, a 3+1 McDonald type condensation of a trithiophene (**III.7a**) unit with a 2,4-hydroxymethylthiophene (**III.7b**) appeared to be the ideal choice for synthesis of S-confused isophlorin (**Scheme-III.3**).

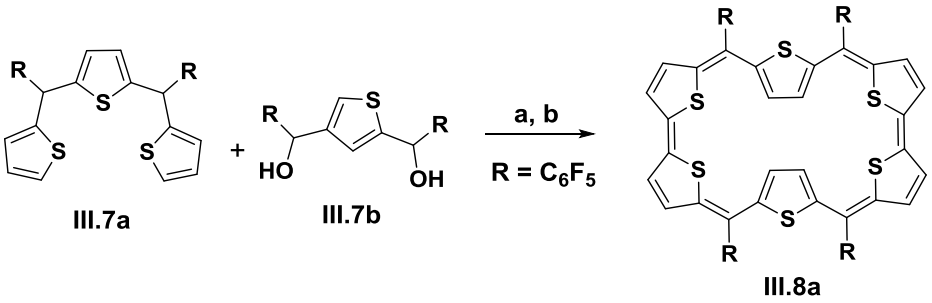


**Scheme-III.3:** Unsuccessful synthesis of S-Confused isophlorin. a) $BF_3.OEt_2$, b) $FeCl_3$

Surprisingly, this reaction did not yield the desired macrocycle (**III.5**). The MALDI-TOF/TOF mass spectrum of this reaction mixture displayed only the coupling of the trithiophene unit to yield a hexa thiophene macrocycle (**III.8a**). Therefore, the strategy was revised by synthesizing the trithiophene unit bearing the confused thiophene unit and further condensed with thiophene diol. An equimolar ratio of thiophene 2,5-bis(pentafluorophenylhydroxymethyl)thiophene[8], **III.7d**, and a confused 2,4-bis[(pentafluorophenyl)(thiophen-2-yl)methyl]thiophene[9], **III.7c**, was condensed in acidic medium under inert conditions[10]. It was followed by oxidation with $FeCl_3$ with continued stirring for an additional two hours in a flask open to the atmosphere (**Scheme-4**).

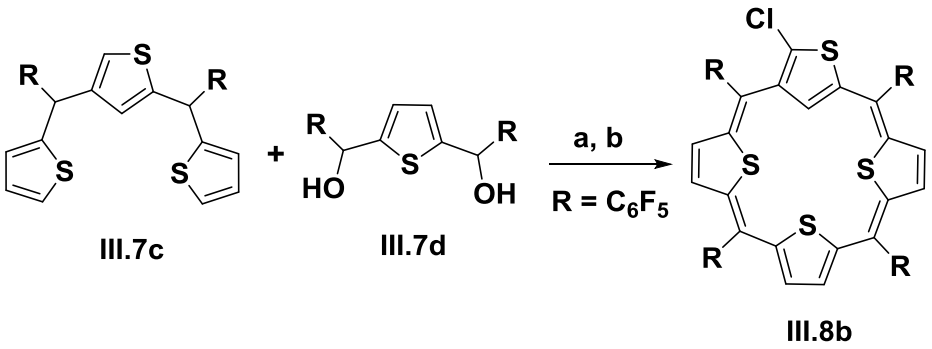


**Scheme-III.4:** Synthesis of S-Confused isophlorins **III.8b** a) $BF_3.OEt_2$, b) $FeCl_3$.

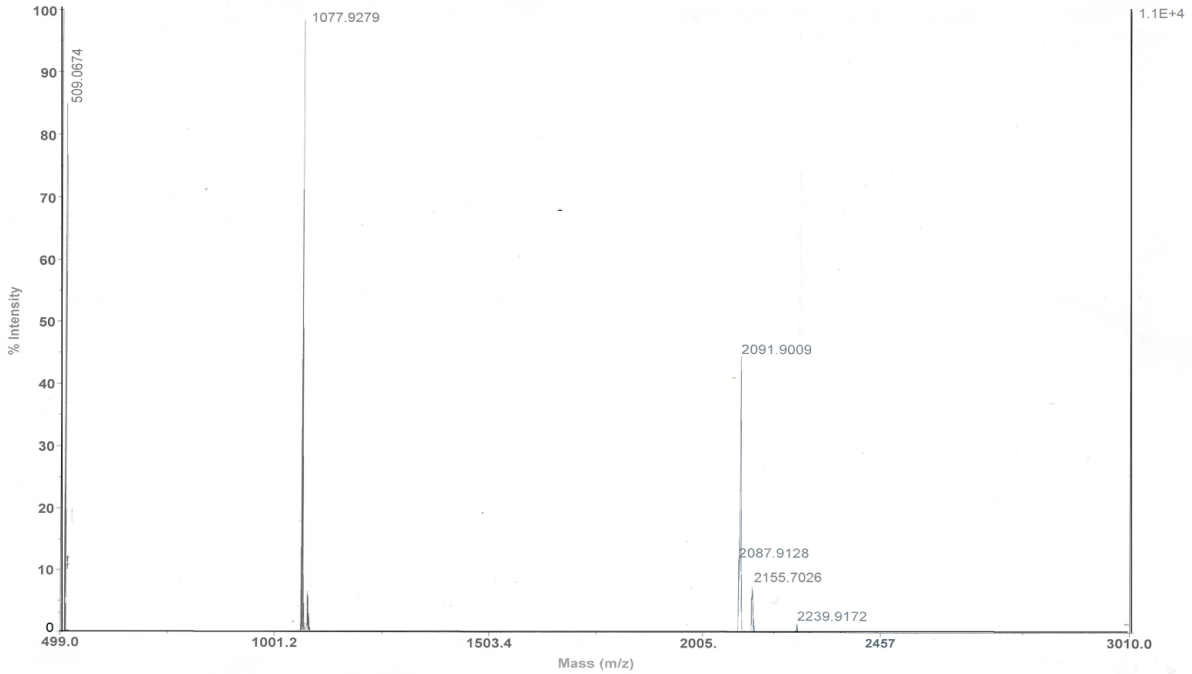


**Figure-III.1:** MALDI-TOF/TOF mass spectrum of reaction mixture.

## III.3. Isolation and characterization of S-confused Isophlorin (III.8b):

The reaction mixture was passed through a short pad of basic alumina column and concentrated under reduced pressure. MALDI-TOF/TOF mass spectrum confirmed the formation of a product with thirty six mass units greater than the expected macrocycle **III.5**, (**Figure-III.1**). Upon further purification through column chromatography on silica gel (100-120 mesh) a brown coloured band separated with $CH_2Cl_2$ / petroleum ether as eluent and the isolated band corresponded to the chlorinated derivative of the 20π electron S-confused isophlorin macrocycle **III.8b**, in 3.8% yield. In its high resolution mass spectrum (**Figure-III.2)**, the isolated product displayed an *m*/*z* value of 1077.8795, (anticipated for **III.5**: $C_{44}H_8F_{20}S_4$; 1043.9189). Molecular structure determined from single crystal X-ray diffraction studies (**Figure-III.3**) confirmed the chlorinated derivative, **III.8b**, of the expected confused thiophene isophlorin ($C_{44}H_7F_{20}S_4Cl$; 1077.8800) in support of the mass spectrometric analysis.

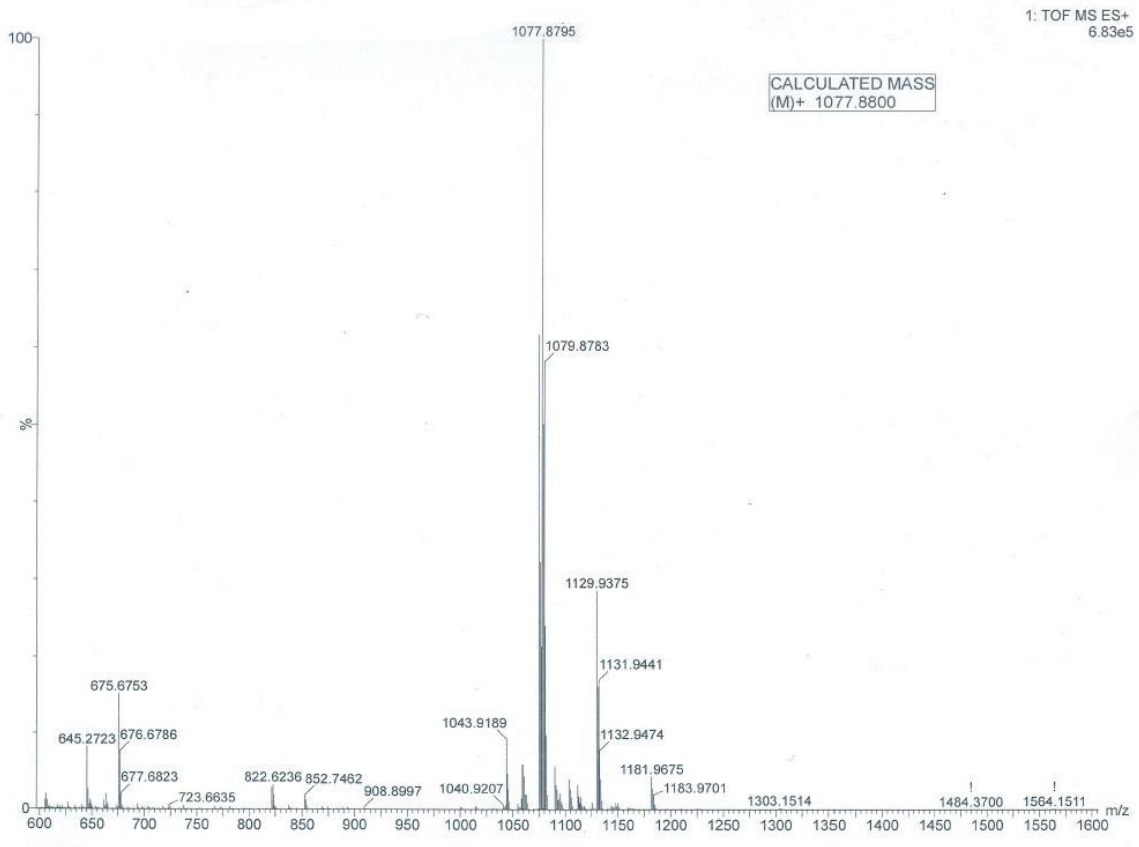


**Figure-III.2:** High resolution (ESI – TOF) mass spectrum of **III.8b**.

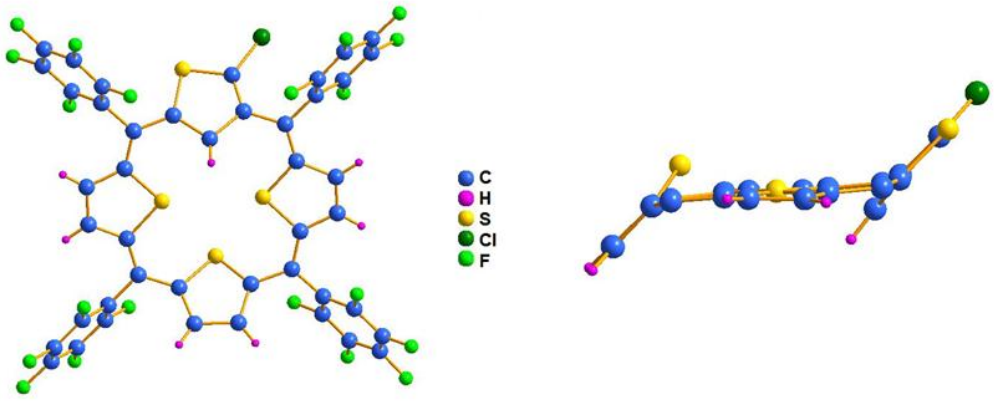


**Figure-III.3:** Molecular structure of **III.8b**, top view (left). In the side view (right) *meso*-pentafluorophenyl rings are omitted for clarity.

The formation of this confused isophlorin, **III.8b**, was successful only when $FeCl_3$ was employed as the oxidizing agent. Chlorination of **III.5** is contrary to the DDQ oxidation of a similar confused thiophene ring during the synthesis of S-confused porphyrin[5]. Identification of a semi-conjugated macrocycle confirmed through MALDI-TOF/TOF mass spectrometry of reaction mixture (**Figure-III.4)** suggests the formation of

**III.9** or any of its diastereomers, **(Scheme-III.4)**, when DDQ was employed as the oxidizing agent in the synthesis of **III.5**,

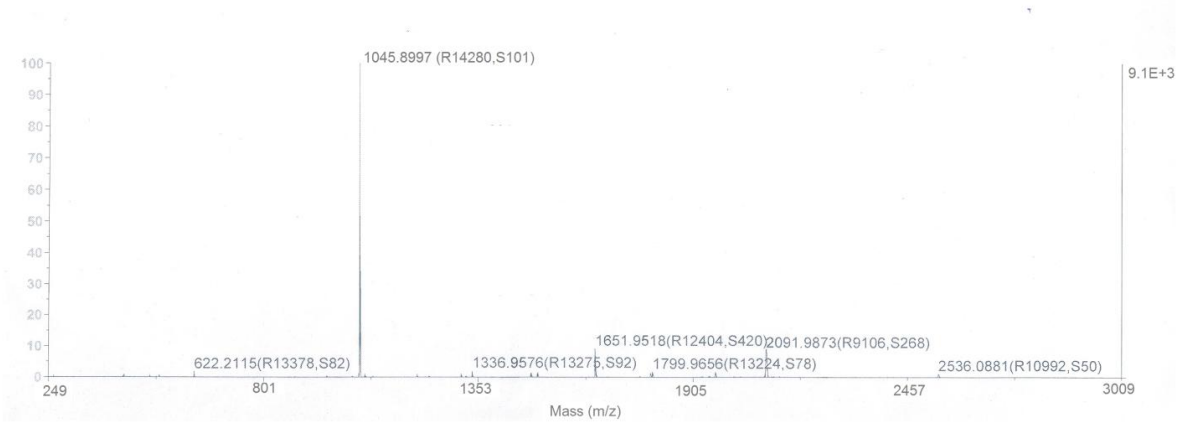


**Figure-III.4:** MALDI-TOF/TOF mass spectrum of semi-conjugated macrocycle, **III.9.**

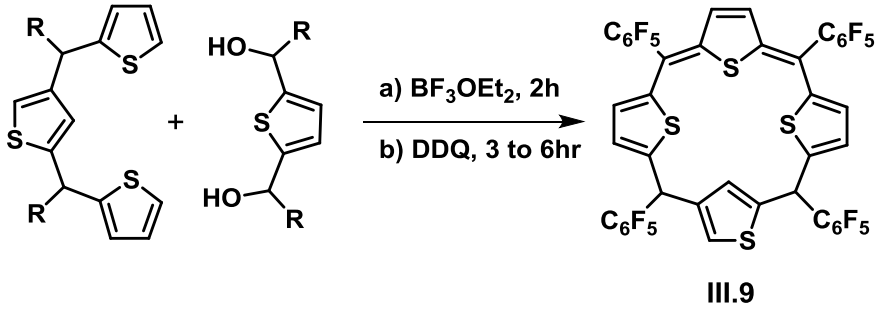


**Scheme-III.4**: Formation of semi-conjugated macrocycle, **III.9** (R = $C_6F_5$).

Despite undergoing substitution under reaction conditions, **III.8b** was found to be highly stable under ambient atmosphere. Efforts to de-chlorinate **III.8b** to yield the desired **III.5** went futile. **III.8b** forms brownish colored solutions in common organic solvents and displayed an intense absorption for the Soret-like band **(Figure-III.5)** at $\lambda_{max}$ = 412 nm (ε = 87,000).

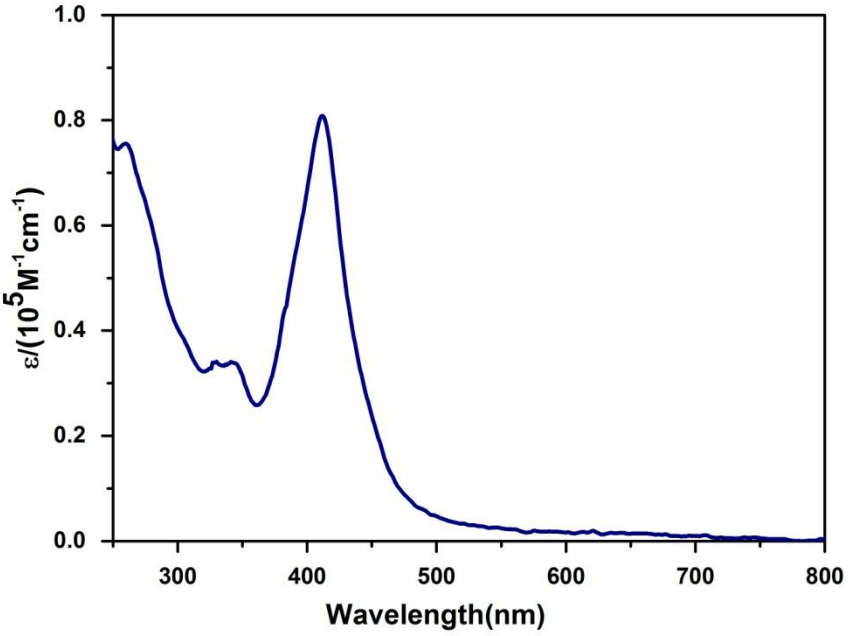


**Figure-III.5:** UV-Visible absorption spectrum of **III.8b**.

The unsymmetrical connectivity of the confused thiophene ring renders a decreased symmetry in comparison to the parent tetrathia isophlorin[11]. This was further reflected in the $^1$H NMR spectrum of **III.8b** recorded at room temperature. Six β-protons for the three normal thiophene rings were found to resonate in the region between δ 6.7 to 6.2 ppm. A singlet corresponding to the β-CH, of the inverted thiophene ring, in the macrocyclic core resonated at δ 9.4 ppm (**Figure-III.6)**. Further, it did not result in a well-resolved spectrum at room temperature as well as at variable low temperatures. A significant down field chemical shift for this proton can be attributed to the presence of significant paratropic ring current effect as expected of the 4nπ systems. However, these chemical shift values further suggest weak paratropic ring current effects in comparison to the mono pyrrole isophlorin **II.1**.[12]

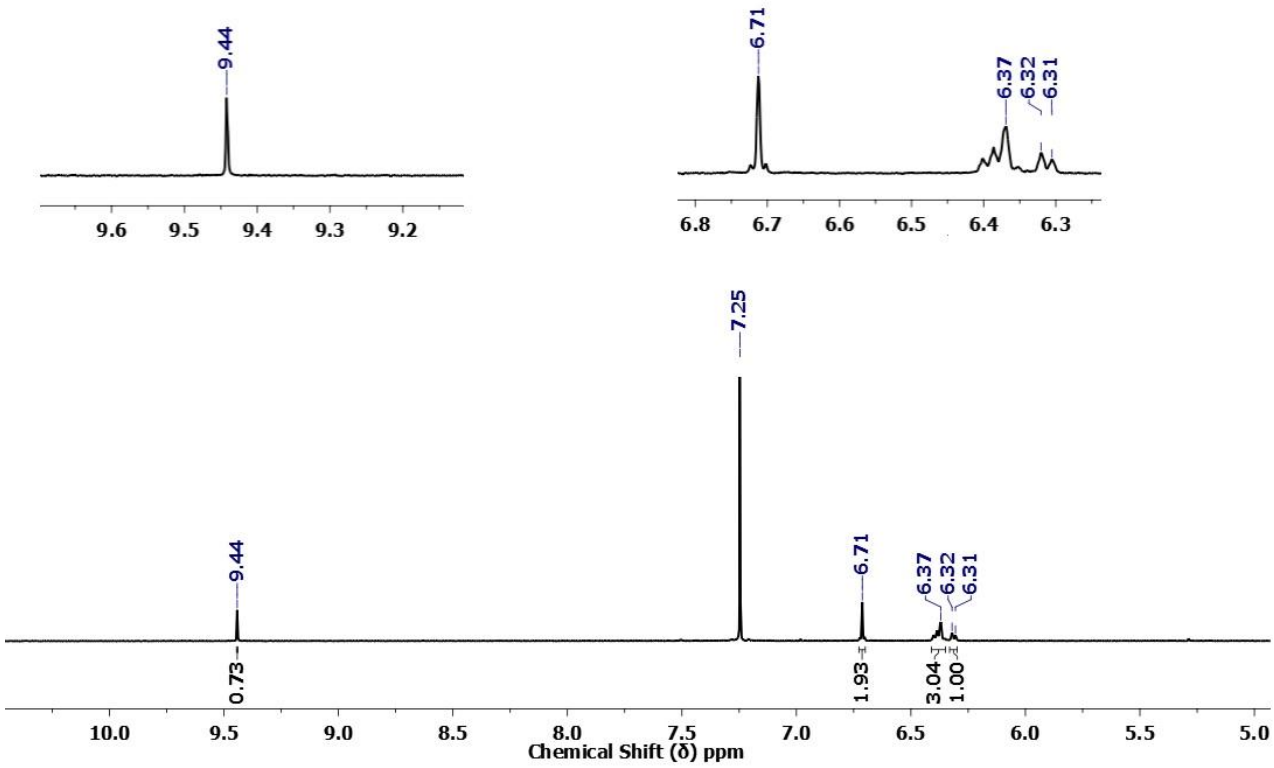


**Figure-III.6:** $^{1}$H NMR spectrum of **III.8b** in $CDCl_3$ at 298K.

The $^{19}$F NMR spectra displayed eight different signals from δ -159.98 to -161.30 ppm, -151.50 to 153.16 ppm and -137.81 ppm to 138.09 ppm corresponding to *ortho*, *meta* and *para* substituted fluorines of pentafluoro groups recorded at 298K **(Figure-III.7)**.

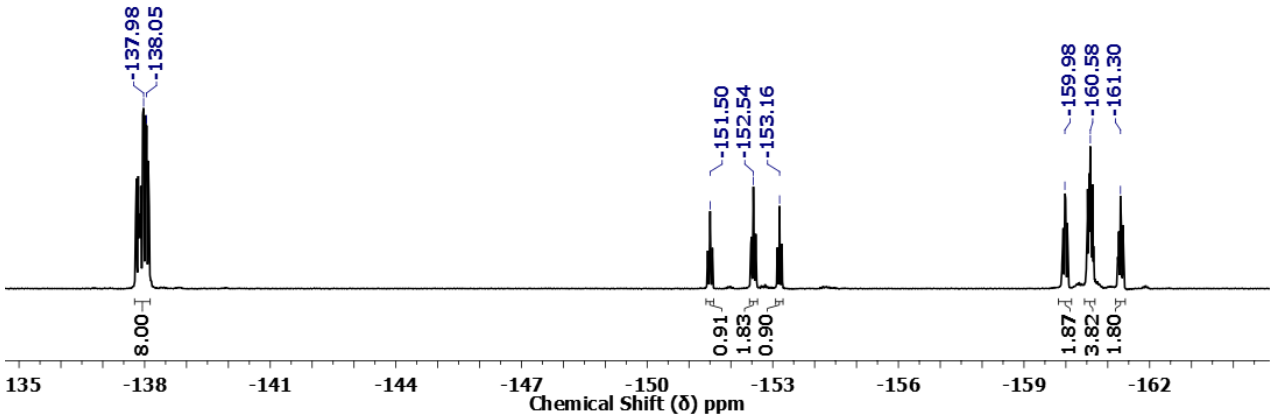


**Figure-III.7:** $^{19}$F NMR spectrum of **III.8b** in $CDCl_3$ at 298K.

To prevent the chlorination of confused thiophene ring in **III.8b**, a similar macrocycle was synthesized in 3.3% yields under similar reaction conditions with methyl substituted thiophene **III.10, (Scheme-III.5)**. An *m*/*z* value of 1057.9344 (Calcd. $C_{45}H_{10}F_{20}S_4$; 1057.9346) in its high resolution mass spectrum established the composition of the expected isophlorin with a methyl substituent on the confused thiophene ring (**Figure-III.8)** and its structure was confirmed from single crystal X-ray diffraction analysis (**Figure-III.9**).

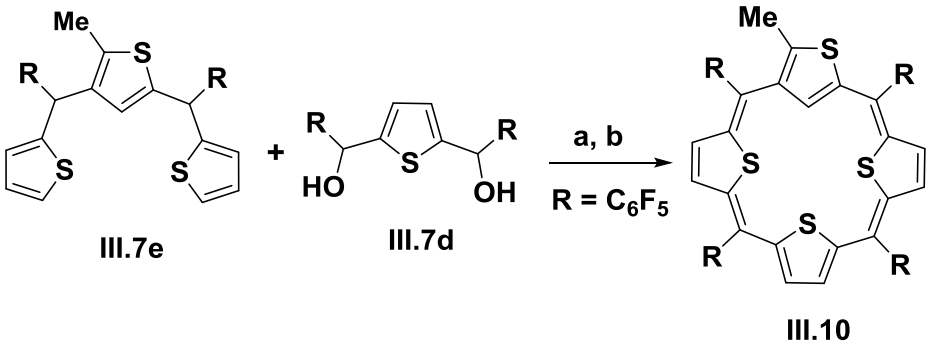


**Scheme-III.5:** Synthesis of methyl substituted S-Confused isophlorins, **III.10** a) $BF_3.OEt_2$, b) $FeCl_3$

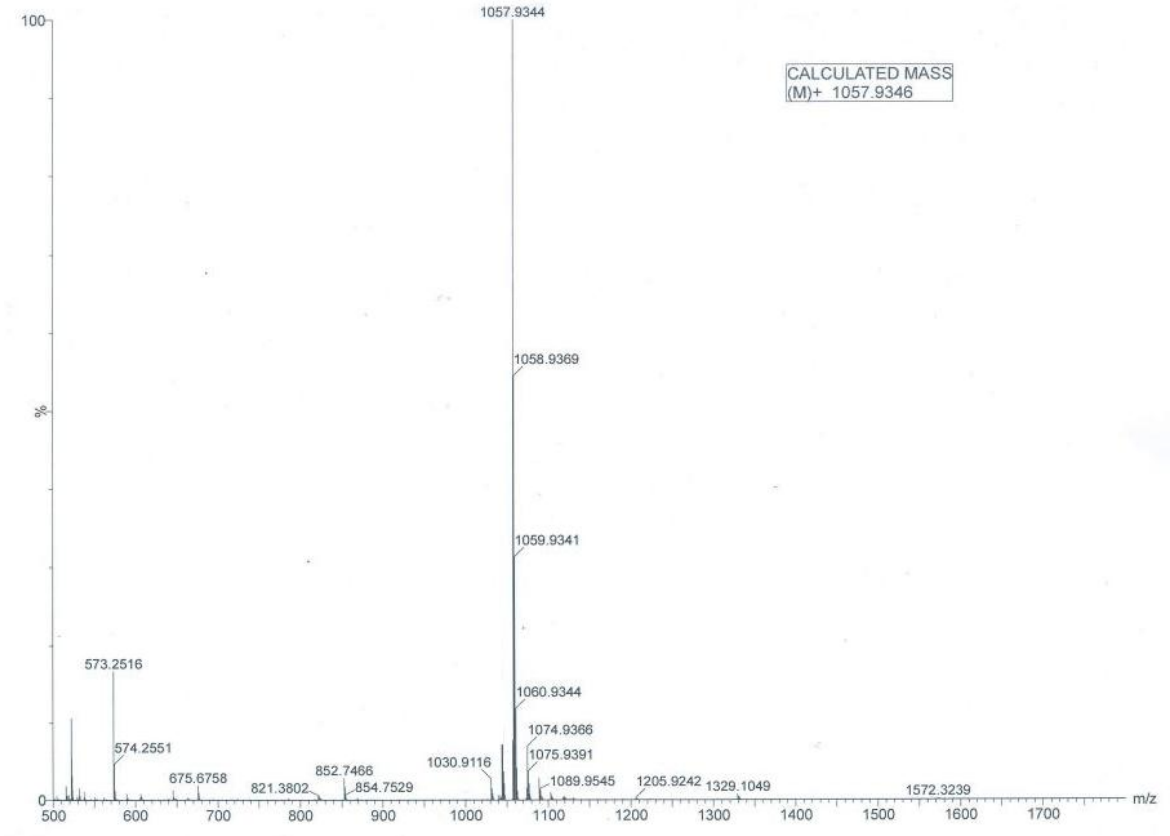


**Figure-III.8:** High resolution mass spectrum of **III.10**.

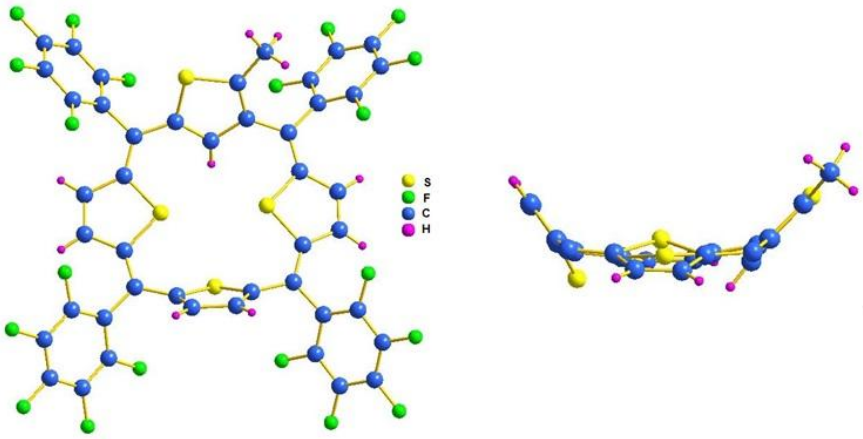


**Figure-III.9:** Molecular structure of **III.10**, top view (left) and side view (right) *meso*-pentafluorophenyl rings are omitted for clarity.

A $^{1}$H NMR pattern similar to that of **III.8b** was observed for **III.10 (Figure-III.10)**, in which the resonance for the peripheral methyl protons of confused thiophene ring was observed at 1.8ppm. Further, this significant loss of paratropic ring current effect is attributed to the reduced overlap of π orbitals due to the 2,4 link of the thiophene in the 20π electronic framework.

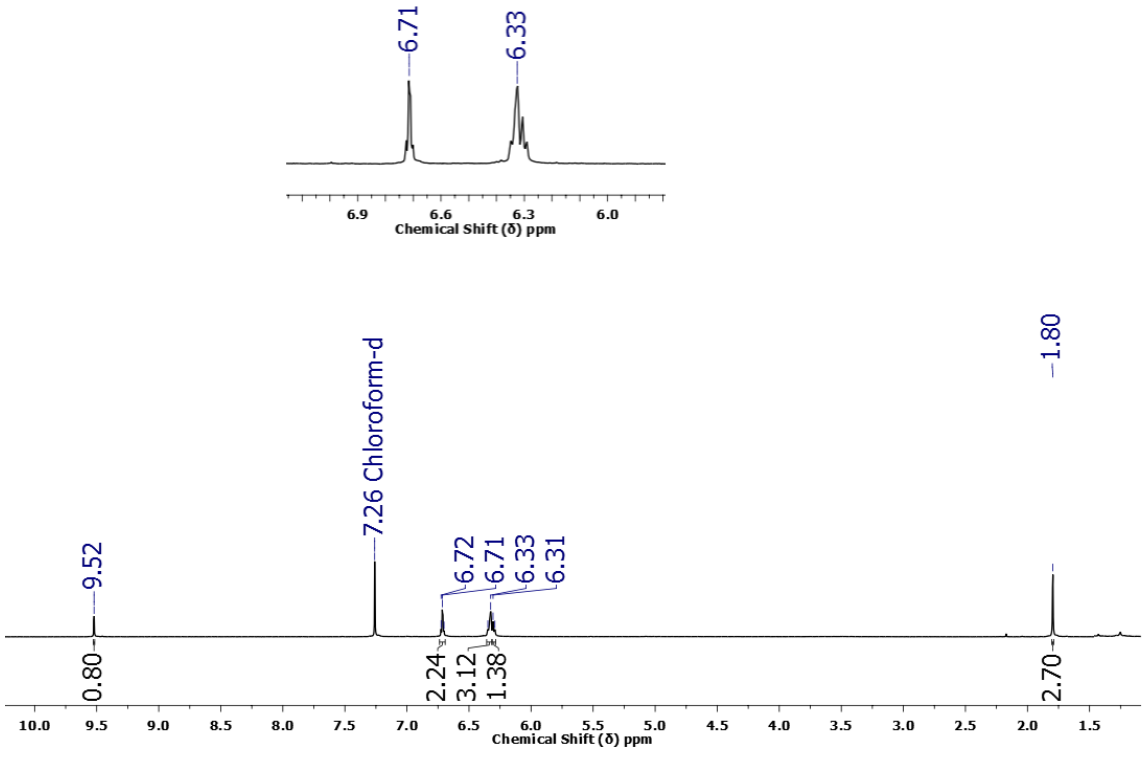


**Figure-III.10:** $^{1}$H NMR spectrum of **III.10** in $CDCl_3$ at 298K.

In both the macrocycles, **III.8** and **III.10**, inversion of confused thiophene ring forces the sulphur atom and its adjacent alpha substitution to the macrocyclic periphery. Structural uniqueness of **III.10**, is highlighted by tilt of the confused thiophene and its diagonal partner by [49.0º(9) and 56.7º(7)] on the same side of the macrocycle. In **III.8b**, both, the confused thiophene ring and its diagonally opposite thiophene ring were tilted by [44º(2) and 44º(1)] above and below the mean macrocyclic plane of the isophlorin. The co-planarity of the other two thiophene units and a near orthogonal orientation of the *meso* pentafluorophenyl rings with the macrocycle invoke a structural resemblance of **III.8b** to the earlier reported β-substituted tetrathia isophlorins.[11] Unsymmetrical connectivity of the confused thiophene ring rendered a decreased macrocyclic symmetry as reflected in the $^1$H NMR spectrum of **III.8b** recorded at room temperature (**Figure-III.6**). An estimated NICS(0)[13] value of +2.6 ppm buttressed the feeble antiaromaticity of **III.8b**.

### III.4. Two electron oxidation of S-confused isophlorin III.8b:

As isophlorin and its expanded congeners are susceptible to two-electron oxidation,[14] it was envisaged that **III.8b** and **III.10** would yield the corresponding 18π dication upon ring oxidation by appropriate reagents. Meerwein salt, $[Et_3O]^+[SbCl_6]^-$,[15] is a well known one-electron oxidant for organic donor species, which leads to the formation a radical cation (**Scheme-III.6**).

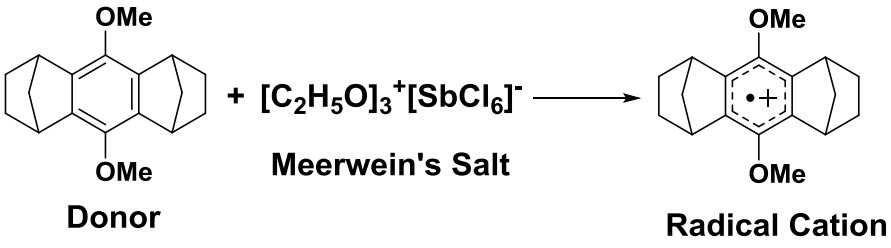


**Scheme-III.6:** One electron oxidation using Meerwein's salt.

Expecting the ring oxidation, Meerwein's salt was added to a dichloromethane solution of **III.8b** and stirred for thirty minutes followed by cooling (dry ice acetone bath). The solution was layered with diethyl ether and maintained at the same temperature for two more hours to yield a green colored solution suggestive of the expected ring oxidation to dication (**Scheme-III.7**).

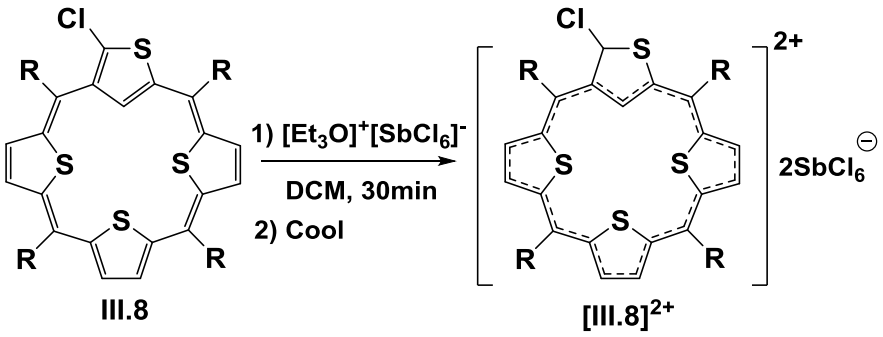


**Scheme-III.7:** Expected two electron oxidation of **III.8b**.

However, mass spectrometric analysis of this green colored solution displayed an unanticipated *m*/*z* value of 1058.9064 (**FIgure-III.11**). A similar product was identified from mass spectrometric analysis upon oxidizing **III.8b,** by $[NO]^+[BF_4]^+$ and $Br_2$. Usually, such two-electron ring oxidation display *m*/*2* value for the dication species (**Scheme-III.7**). Absence of such evidence strongly suggested a structural modification to the macrocyclic skeleton upon oxidation. Cooling the greenish solution to -70ºC yielded dark green crystals. These crystals were stable under ambient conditions and subjected to single crystal X-ray diffraction. Molecular structure obtained from single crystal X-ray diffraction analysis of these green crystals revealed the oxidation of C-Cl bond to C=O on the alpha carbon of the confused thiophene ring (**Figure-III.12**).

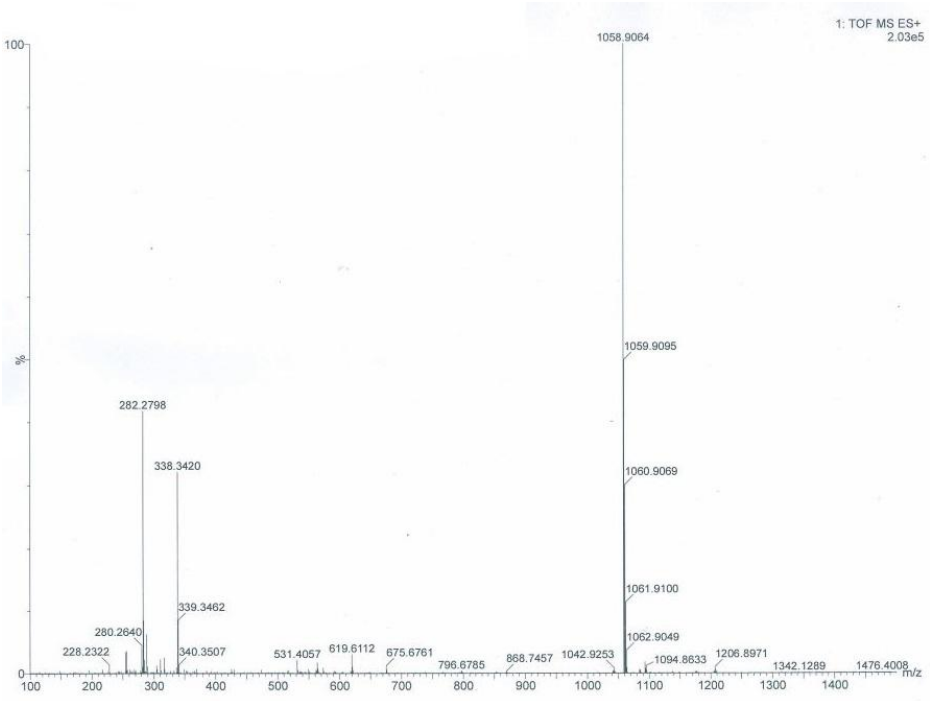


**FIgure-III.11:** High resolution mass spectrum of oxidized **III.8b**.

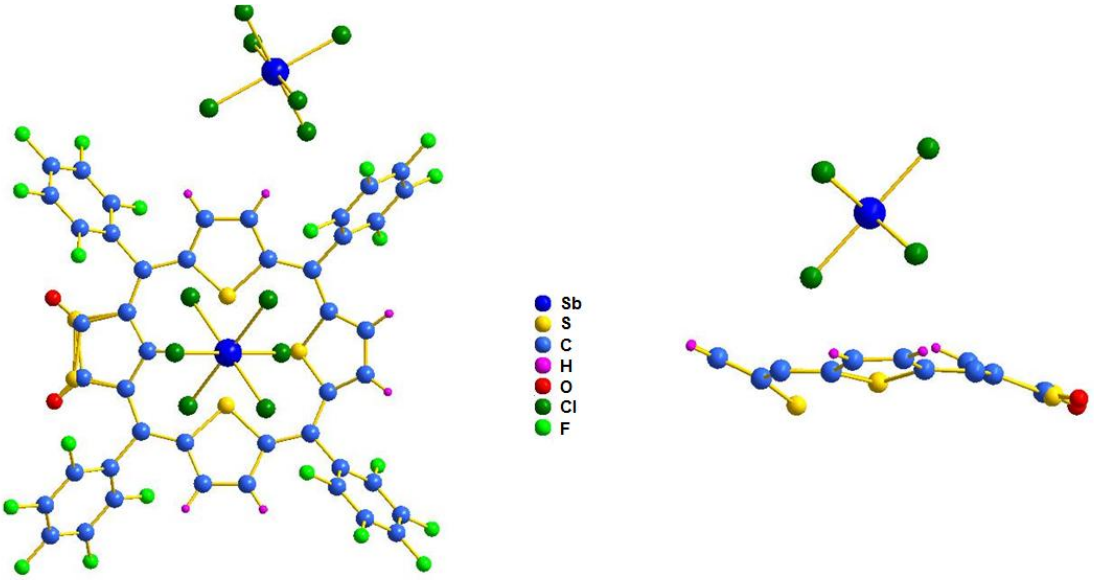


**FIgure-III.12:** Molecular structure of oxidised **III.8b**, top view (left). In the side view (right) *meso*-pentafluorophenyl rings are omitted for clarity

The composition (Cald. for $[C_{44}H_7F_{20}S_4O]^+$: 1058.9060) of the macrocycle was validated from the observed *m*/*z* value in its high resolution mass spectrum (**FIgure-III.11)**. IR spectrum of this macrocycle displayed a carbonyl stretching frequency at (1690-1650 $cm^{-1}$) for the observed exocyclic C=O in the confused thiophene ring (**FIgure-III.13**). In addition, the macrocycle was associated with a $[SbCl_6]^-$ counter anion, suggesting oxidation of the macrocycle to a mono cationic species, [**III.8b**]$^+$ **(Scheme-III.8)**. However, the confused thiophene ring and its diagonally opposite thiophene ring were found to deviate from the mean macrocyclic plane by [16.7°(2) and 16.2$^o$(3)] as observed in the parent isophlorin, **III.8b**.

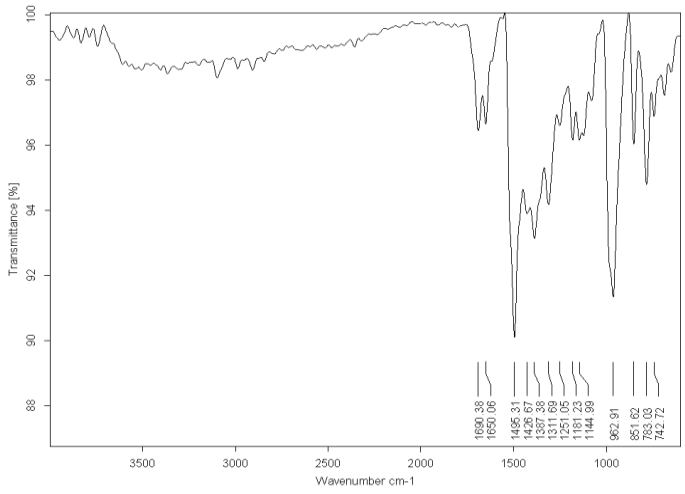


**FIgure-III.13:** Infrared (IR) spectrum of [**III.8b**]$^+$

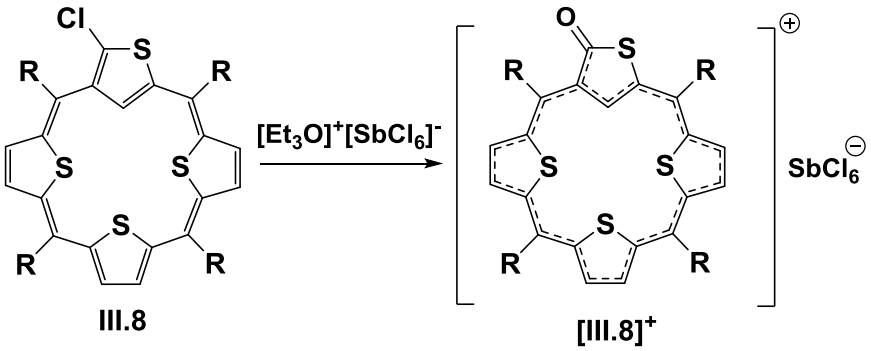


**Scheme-III.8:** Two electron oxidation to monocation, [**III.8b**]$^{+}$

A well resolved $^{1}$H NMR spectrum in deuterated acetonitrile of [**III.8b**]$^{+}$ recorded at room temperature displayed remarkable up field and down field chemical shift values implying the significant ring current effects upon oxidation (**FIgure-III.14**). Even though the number of signals remained the same as observed for **III.8b**, it distinctly separated the hydrogen of the confused thiophene ring from the other hydrogens of the macrocycle. Six doublets corresponding to β-hydrogen atoms of the three normal thiophene rings resonated in the down field region between 10.3 – 9.3 ppm.

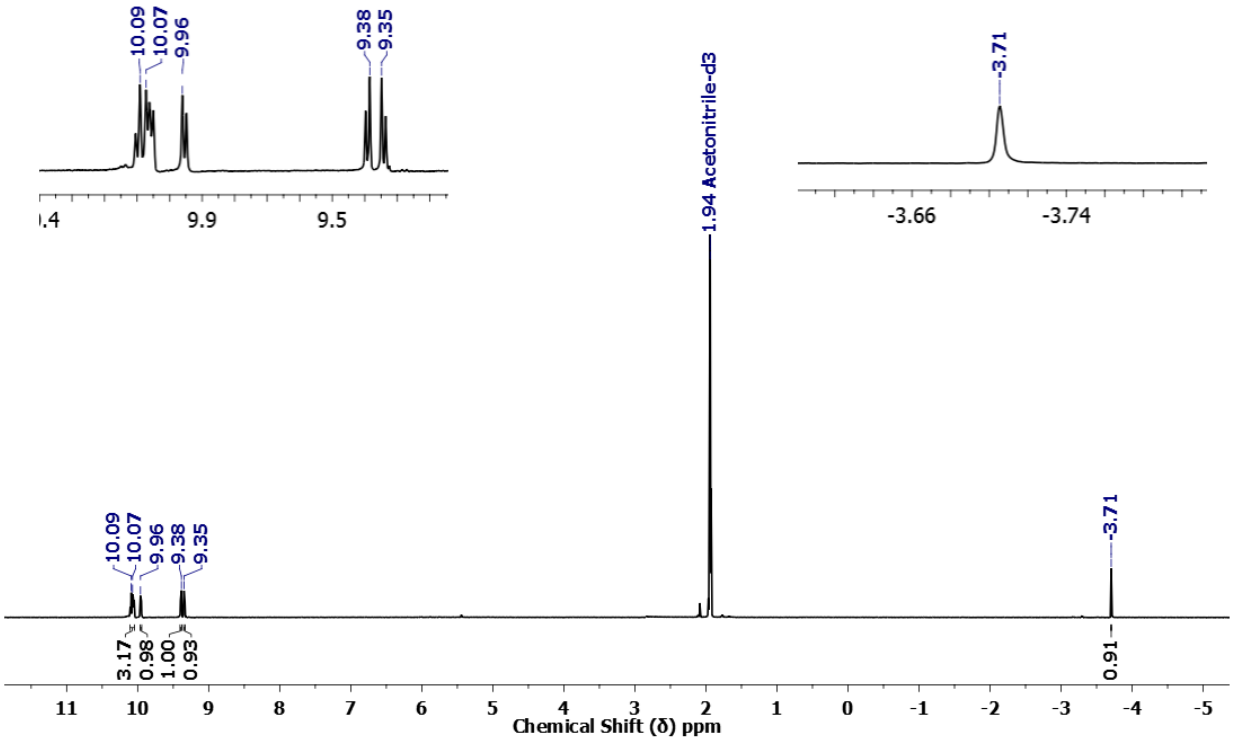


**FIgure-III.14:** $^{1}$H NMR of [**III.8b**]$^{+}$ in acetonitrile-$d_3$ at 298K

The cross coupling of these doublets were confirmed from $^{1}$H-$^{1}$H COSY spectrum (**FIgure-III.15**). A solitary singlet for the inner CH resonated at -3.7 ppm to demonstrate substantial diatropic ring current effects for the oxidized macrocycle.

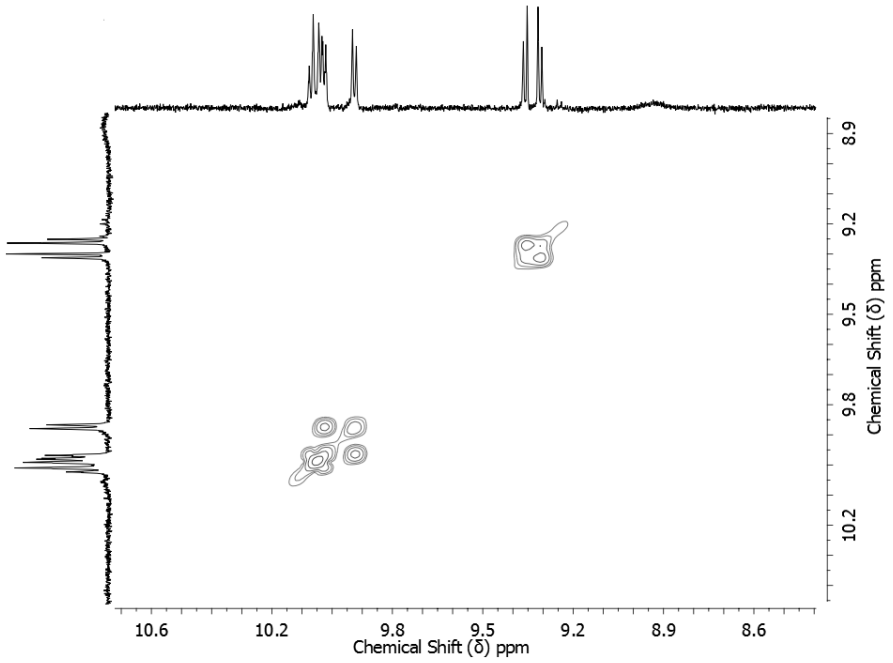


**FIgure-III.15:** Partial $^{1}$H-$^{1}$H COSY spectrum of [**III.8b**]$^{+}$ in Acetnitrile-$d_3$ at 298K.

The calculated NICS(0) value of -12.9 ppm lend further justification for the aromatic characteristics of **[III.8b]**$^{+}$. Ring oxidation by two electrons should have ideally yielded 18π dicationic species, **[III.8b]**$^{2+}$. Isolation of the mono cationic species, **[III.8b]**$^{+}$, suggested either an unfavourable thermodynamic pathway to yield **[III.8b]**$^{2+}$ or the kinetic instability of the supposed cation radical, **[III.8b]**$^{\bullet+}$, as an oxidized intermediate **(Scheme-III.9)**. Hence, two different pathways **(Scheme-III.9)** could be envisaged for the oxidative transformation of **III.8b** to **[III.8b]**$^{+}$.

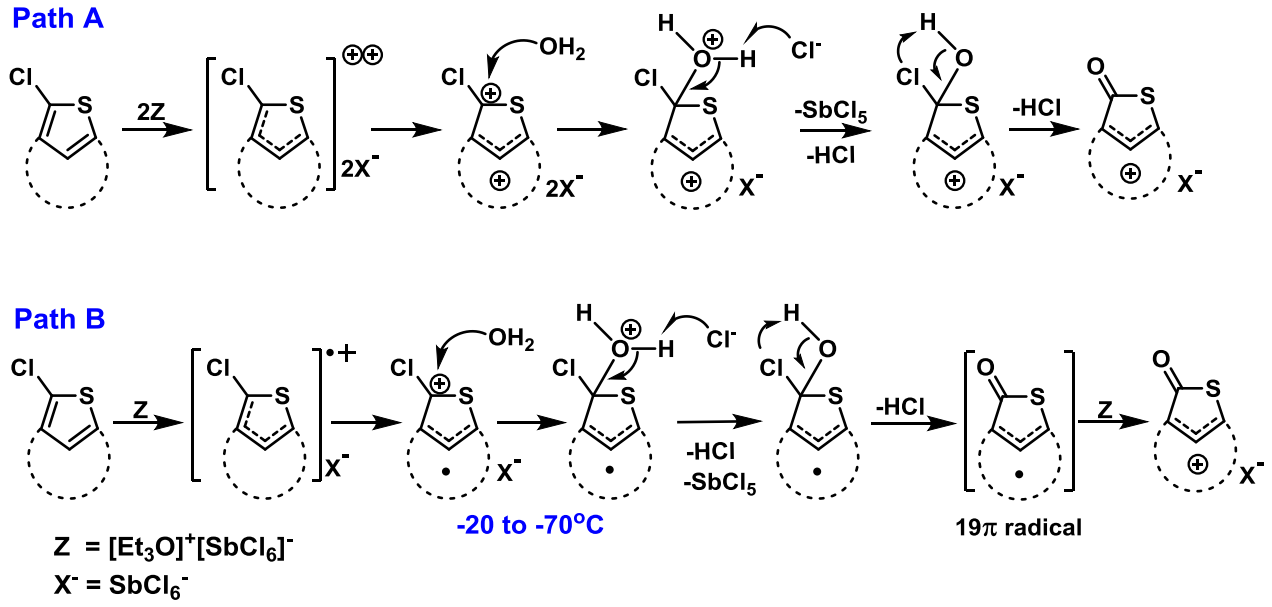


**Scheme-III.9:** Plausible mechanisms for the transformation **III.8b** into **[III.8b]**$^{+}$. Z = $[Et_3O]^+[SbCl_6]^-$ ; $X^-$ = $[SbCl_6]^-$.

In path A, the expected hypothetical dication, **[III.8b]**$^{2+}$ seems to be highly reactive under ambient moisture, resulting in the formation of 18π mono cation. Alternatively, in path B the unstable mono cation radical, **[III.8b]**$^{\bullet+}$, reacts with ambient moisture to yield the 19π macrocyclic radical, **III.6**. Subsequent one-electron oxidation of **III.6** yields the 18π mono cation, **[III.8b]**$^{+}$. The fleeting life time of the proposed cation radical should be the ideal precursor for the observed dicationic species, similar to oxidation of expanded isophlorins. Invariably, their stability within the limited time is sustained by the absence of reactive functional groups. The distinct changes in this irreversible redox process were monitored by electronic spectroscopy **(Figure-III.16)**. **III.8b** forms brownish colored solutions in common organic solvents and displays an intense absorption band (black) at 412 nm (ε = 87000). Addition of oxidizing agent at room temperature did not induce any color change. However, it displayed an uncharacteristic blue shifted featureless absorption at 275 nm suggestive of a cation radical species, **[III.8b]**$^{\bullet+}$ (blue). Upon cooling in dry ice acetone bath, the brownish solution turned green and its absorption was red shifted by more than 60 nm compared to **III.8**. The greenish mono cationic species, **[III.8b]**$^{+}$, displayed a typical porphyrin like spectrum with Soret-like absorption at 475 nm (ε = 67200) followed by low energy absorptions between 600 and 720 nm (red). No low energy absorptions were observed for the 20π isophlorin, **III.8b**.

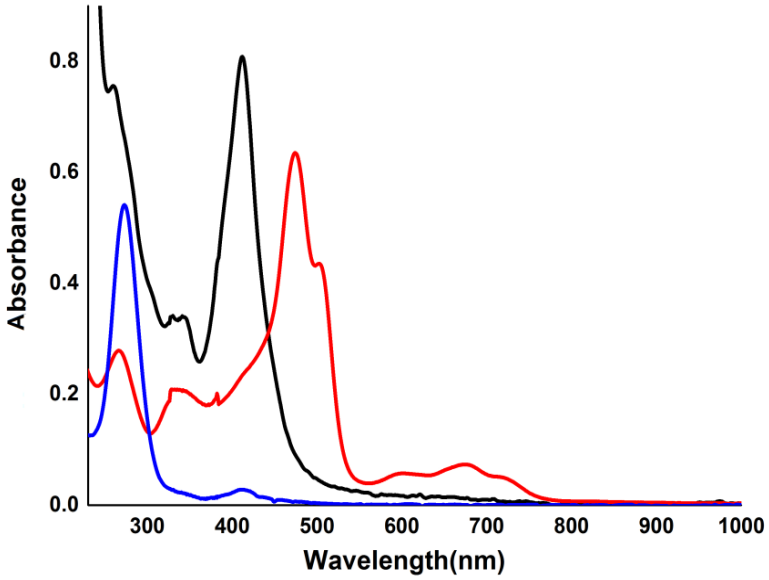


**FIgure-III.16:** UV-Visible absorption spectrum of **[III.8b]**$^{\bullet+}$ (blue), **III.8b** (black) and **[III.8b]**$^{+}$ (red).

Further support for this understanding came from the unforeseen resistance of **III.10** towards two-electron oxidation under similar conditions. Even though it displays a blue shifted featureless absorption (**Figure-III.17**) akin to **III.8b**, upon oxidation (red), no further reaction could be detected over long periods of time either at room or at low temperatures. High resolution mass spectrometric analysis did not establish the expected two-electron oxidized macrocycle, either (**Figure-III.18**).

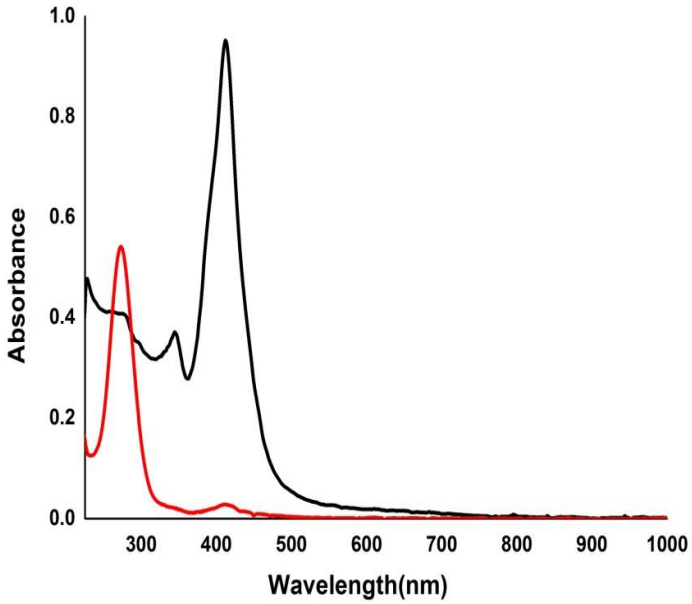


**Figure-III.17:** UV-Visible absorption spectrum of **[III.10]** (black) and **[III.10]**$^{\bullet+}$ (red).

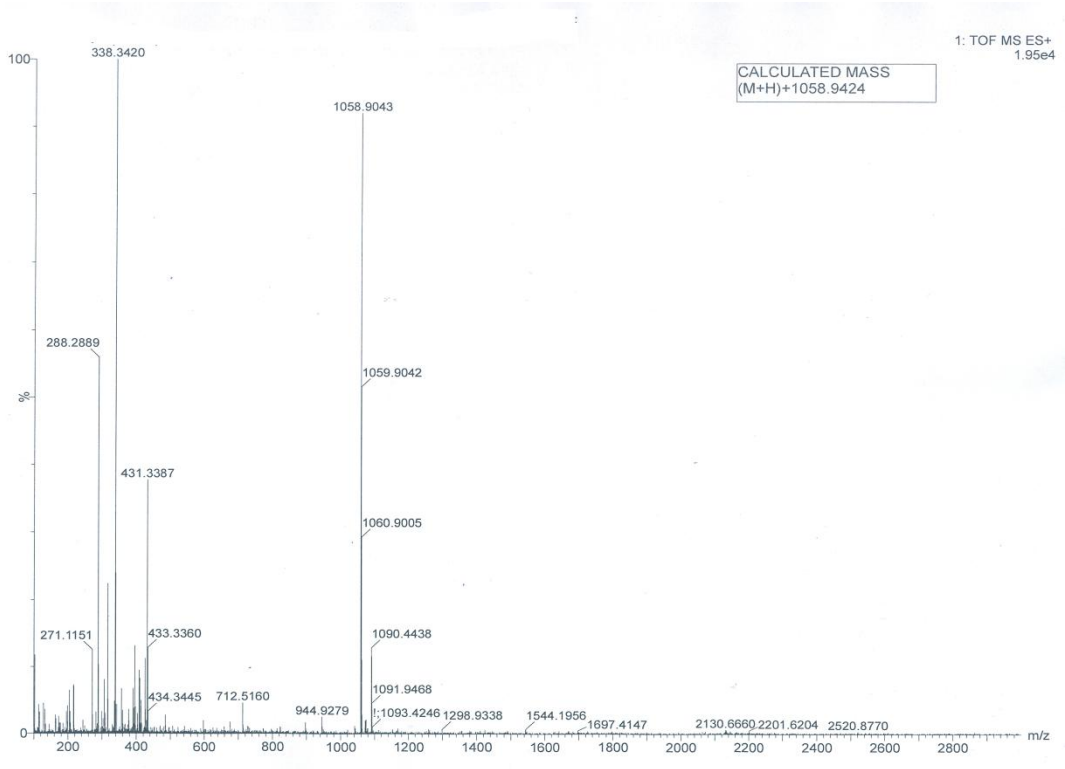


**Figure-III.18:** : High resolution mass spectrum of **III.10**, after oxidation with **$[Et_3O]^+[SbCl_6]^-$**.

These observations establish the formation of an uncharacteristic cation radical upon oxidation of a confused isophlorin. Therefore, it can be considered that a good leaving group, such as Cl, in the macrocyclic cation radical reacts with moisture leading to a highly unstable 19π radical, **III.6**, which undergoes subsequent one-electron oxidation to yield the 18π cationic species, **$[III.8b]^+$**. The formation of the radical cation, **$[III.8b]^{+\bullet}$** was established through ESR spectroscopy (**Figure-III.19**) upon the addition of meerwein salt at room temperature. Hence path B (**Scheme-III.9**) seems to be the most appropriate route for transmutation of **III.8b** to the mono cationic species, **$[III.8]^+$**.

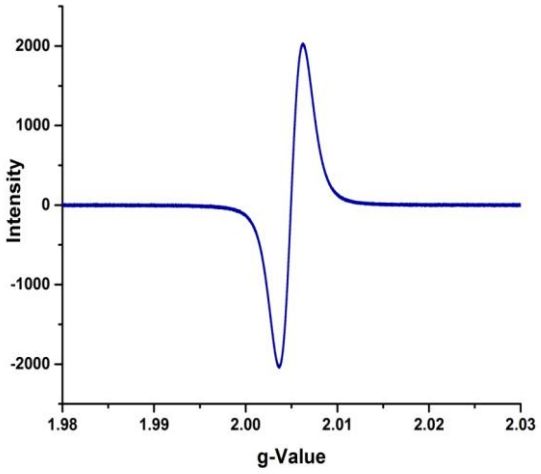


**Figure-III.19:** EPR spectrum of **$[III.8b]^{+\bullet}$**.

It was also observed that **[III.8b]**$^{+}$ exhibited significant emission at $\lambda_{max}$ = 517 and 551 nm and weak emission at 747 nm when excited at $\lambda$ = 474 nm (**Figure-III.20**).

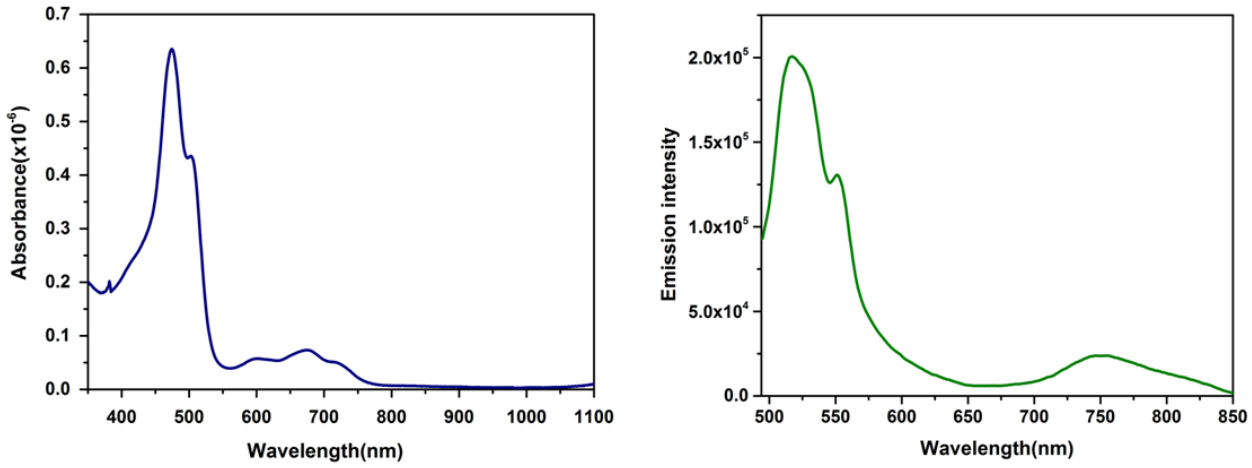


**Figure-III.20:** Absorption (left) and emission (right) spectrum for **[III.8b]**$^{+}$.

This shift in signal from low field, $\delta$ = +9.4 ppm in **III.8b** to high field $\delta$ = -3.7ppm in **[III.8b]**$^{+}$ for the inner CH, by nearly $\Delta\delta$ = 13 ppm confirms the aromatic character of the cationic macrocycle **[III.8b]**$^{+}$ **(Figure-III.21)**.

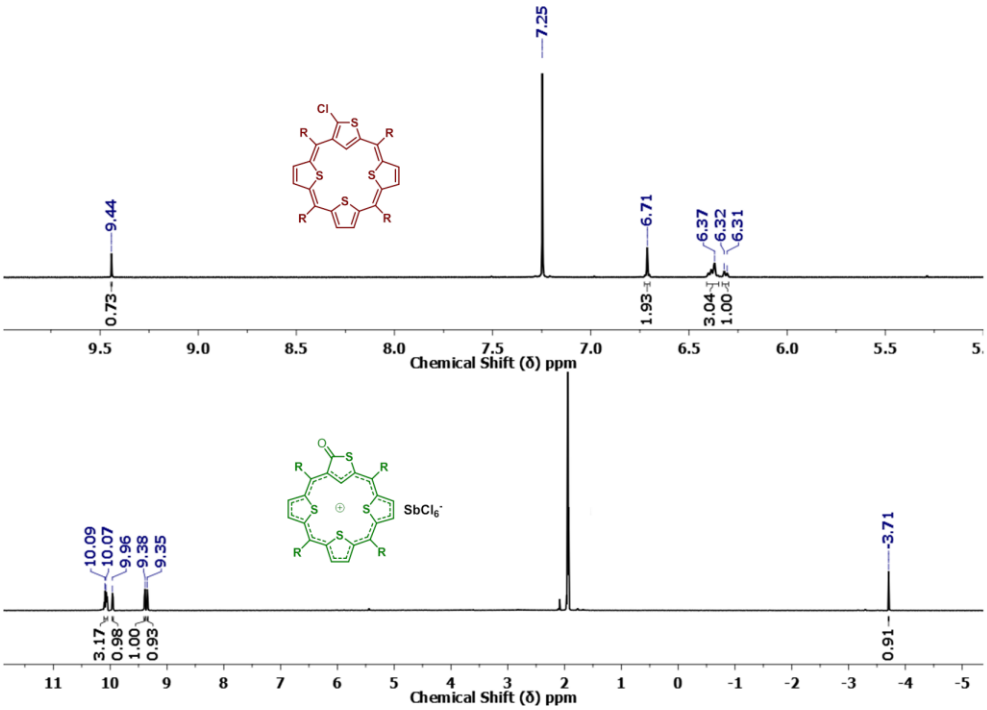


**Figure-III.21:** $^{1}$H NMR of **III.8b** (above) and **[III.8b]**$^{+}$ **(**below**)** at 298K.

## III.5. Quantum mechanical calculations:

The confirmation of aromaticity and antiaromaticity of obtained macrocycles was also determined by employing DFT calculations as mentioned in chapter II, such as nucleus independent chemical shift (NICS) and anisotropy of the induced current density (AICD) for both **III.8b** and **[III.8b]$^+$ (Figure-III.22)**. The antiaromatic character of 20π electron S-confused isophlorin **III.8b** calculated using NICS was found to be δ = +2.6 ppm NICS(0) which confirms its weak [4n]π electron antiaromatic character and δ = -12.9 ppm NICS(0) for its monocation aromatic 18π electron **[III.8b]$^+$**. This large negative value of NICS suggested its strong [4n+2] π electron aromatic character. Further, it suggested that this change in the NICS values from positive to large negative values clearly confirms the formation of its aromatic monocationic species by its two electron oxidation of neutral macrocycle **III.8b** to its monocation **[III.8b]$^+$**.

### III.5a. NICS calculations for III.8b and [III.8b]$^+$.

| Molecule | NICS | Ring Current | Aromaticity | HOMO-LUMO (eV) |
|---|---|---|---|---|
| **III.8b** | **+2.6 ppm** | **Paratropic** | **Weakly antiaromatic** | **2.01** |
| **[III.8b]$^+$** | **-12.9 ppm** | **Diatropic** | **Aromatic** | **2.24** |

**Figure-III.22**: NICS and HOMO-LUMO band for **III.8b** and **[III.8b]$^+$**, calculated at B3LYP/6-31G (d,p) level.

**III.5b. HOMO-LUMO band gap for III.8b and [III.8b]$^{+}$.**

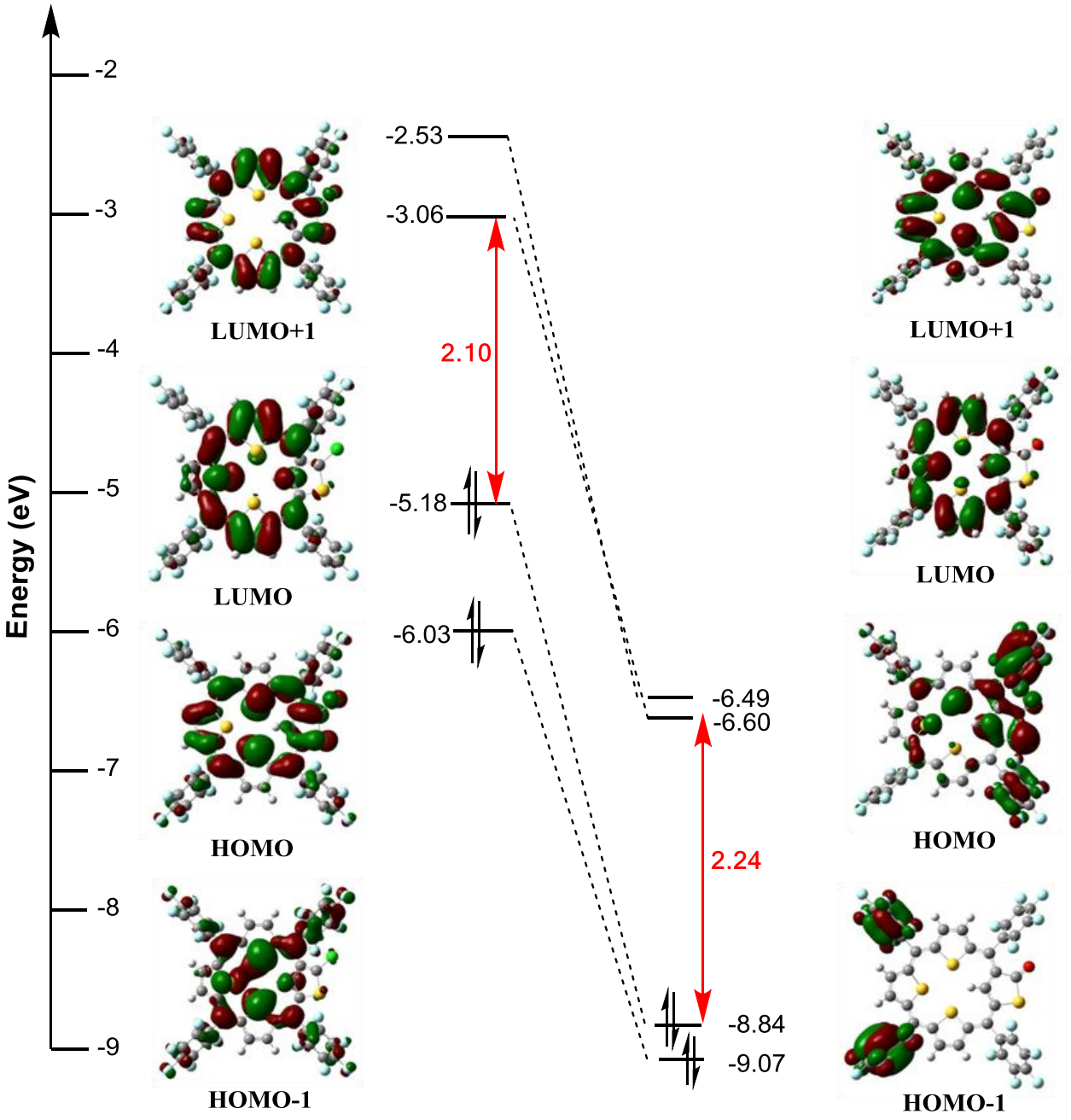


**Figure-III.23**: Selected frontier molecular orbitals of **III.8b** and **[III.8b]$^{+}$**, calculated at B3LYP/6-31G (d,p) level.

### III.5c. TD-DFT calculations for III.8b and [III.8b]$^{+}$.

Further to understand the electronic absorption properties of theses macrocycles the TD-DFT calculations were performed on the optimized structures of **III.8b** and **[III.8b]$^{+}$ (Figure-III.24, 25 and 26)**. The computed electronic absorptions are in agreement with the experimental results. The small HOMO-LUMO gap corresponding to the 2.10 eV for **III.8b** supported the antiaromatic character and relatively larger HOMO-LUMO gap of 2.24 for **[III.8b]$^{+}$** are in complete agreement with the aromatic character **(Figure-III.23)**.

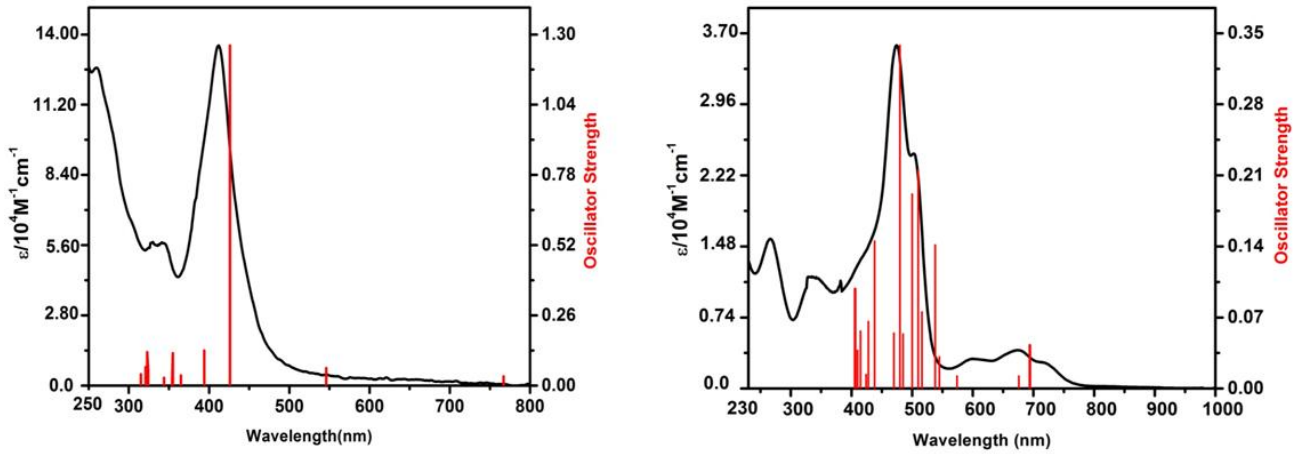


**Figure-III.24:** The steady state absorption spectras along with the theoretical vertical excitations energies (red bar) obtained from TD-DFT calculations which were carried out using B3LYP/6-31G(d,p) level of **III.8b** (left) and **[III.8b]$^{+}$** (right).

| Energy (cm-1) | Wavelength(nm) | Osc. Strength | Major contributions |
|---|---|---|---|
| 13031.58992 | 767.3660744 | 0.0349 | HOMO→LUMO (99%) |
| 18324.23664 | 545.7253252 | 0.0651 | H-1→LUMO (33%), HOMO→L+1 (66%) |
| 23479.76816 | 425.8985835 | 1.2587 | H-1→LUMO (63%), HOMO→L+1 (32%) |
| 24304.87904 | 411.4400234 | 0.0141 | H-2→LUMO (30%), H-1→L+1 (67%) |
| 25373.57104 | 394.1108638 | 0.1305 | H-2→LUMO (55%), H-1→L+1 (23%), HOMO→L+2 (12%) |
| 27410.13504 | 364.8285565 | 0.0377 | H-3→LUMO (10%), HOMO→L+2 (68%), HOMO→L+3 (11%) |
| 28168.30144 | 355.0089813 | 0.1199 | HOMO→L+3 (12%), HOMO→L+4 (75%) |
| 28250.57056 | 353.9751517 | 0.0199 | H-3→LUMO (11%), HOMO→L+3 (40%), HOMO→L+4 (22%) |
| 29043.41904 | 344.3120793 | 0.0293 | HOMO→L+5 (77%) |
| 29462.83024 | 339.4107056 | 0.0193 | H-5→LUMO (25%), H-2→L+1 (49%) |
| 30864.63152 | 323.9954442 | 0.0565 | H-12→LUMO (15%), H-10→LUMO (34%), H-9→LUMO (11%), H-3→L+1 (13%) |
| 30950.12688 | 323.1004525 | 0.1241 | HOMO→L+6 (83%) |
| 31198.54736 | 320.527744 | 0.0691 | H-12→LUMO (34%), H-10→LUMO (29%), H-3→L+1 (12%) |
| 31722.81136 | 315.2305729 | 0.042 | H-11→LUMO (27%), H-9→LUMO (59%) |

**Figure-III.25:** Selected TD-DFT (B3LYP/6-31g (d, p)) calculated energies, oscillator strengths and compositions of the major electronic transitions for **III.8b**.

| Energy (cm-1) | Wavelength (nm) | Osc. Strength | Major contributions |
|---|---|---|---|
| 14414.03376 | 693.768321 | 0.0427 | H-1→L+1 (21%), HOMO→LUMO (70%) |
| 14785.85792 | 676.3219324 | 0.0124 | H-1→LUMO (36%), HOMO→L+1 (56%) |
| 17408.79104 | 574.422427 | 0.0123 | H-2→LUMO (82%), H-1→L+1 (10%) |
| 18334.72192 | 545.4132353 | 0.0312 | H-2→L+1 (86%) |
| 18588.78832 | 537.9586785 | 0.1415 | H-4→LUMO (27%), H-2→LUMO (13%), H-1→L+1 (32%) |
| 19393.7352 | 515.6304289 | 0.0754 | H-3→LUMO (75%) |
| 19604.24736 | 510.0935433 | 0.2152 | H-4→L+1 (12%), H-3→LUMO (15%), H-3→L+1 (29%), H-1→LUMO (19%), HOMO→L+1 (11%) |
| 20008.33392 | 499.7917388 | 0.1915 | H-4→L+1 (12%), H-3→L+1 (62%), H-1→LUMO (12%) |
| 20618.09328 | 485.0109011 | 0.0537 | H-5→LUMO (63%), H-4→LUMO (20%) |
| 20821.3464 | 480.2763379 | 0.3381 | H-5→LUMO (22%), H-4→LUMO (28%), H-1→L+1 (15%) |
| 21297.2168 | 469.5449219 | 0.0545 | H-4→L+1 (58%) |
| 22822.42176 | 438.1655946 | 0.1452 | H-7→LUMO (73%) |
| 23357.9776 | 428.1192564 | 0.0661 | H-9→LUMO (15%), H-8→LUMO (26%), H-7→L+1 (43%) |
| 23610.43088 | 423.5416139 | 0.0138 | H-8→LUMO (66%), H-7→L+1 (30%) |
| 24112.91776 | 414.7154691 | 0.0566 | H-10→LUMO (12%), H-9→LUMO (39%), H-8→L+1 (16%) |
| 24378.276 | 410.2012792 | 0.0375 | H-11→LUMO (17%), H-10→LUMO (29%), H-8→L+1 (38%) |
| 24609.75872 | 406.3428705 | 0.0981 | H-11→LUMO (17%), H-10→L+1 (12%), H-9→LUMO (20%), H-8→L+1 (27%) |

**Figure-III.26:** Selected TD-DFT (B3LYP/6-31g (d, p)) calculated energies, oscillator strengths and compositions of the major electronic transitions for **[III.8b]**$^{+}$.

### III.5d. ACID calculations for III.8b and [III.8b]$^{+}$.

Anisotropy of Induced-Current Density (AICD)[9] further supported the anticlockwise and clockwise ring current effects for the corresponding weakly antiaromatic[10] and significant aromatic behaviour of **III.8b** and **[III.8b]**$^{+}$ macrocycles. The AICD plot did not show clear ring current effects corresponding to the antiaromatic behaviour **III.8b**, which indicates weak antiaromatic character **(Figure-III.27)**. But the monocation **[III.8b]**$^{+}$ displayed a clear clockwise direction of ring current effects which affirmed the aromatic character **(Figure-III.27)**. The magnitude and the direction of the induced ring current in the systems can directly displayed by AICD plots when an external magnetic field is applied orthogonal to the macrocycle plane.

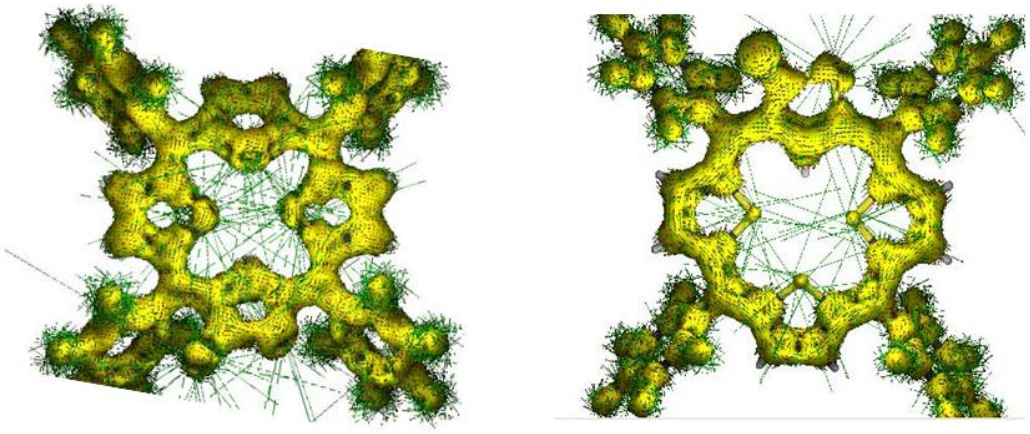

**Figure-III.27:** AICD plot of **III.8b** (left) and **[III.8b]**$^{+}$ (right). The external magnetic field if applied orthogonal to the macrocyclic plane.

## III.7. Conclusion:

The successful synthesis of first stable derivative of S-confused antiaromatic macrocycle was achieved by replacing all the pyrrole 'N' atoms of NCP with sulphur atoms. Condensation of an equimolar ratio of 2,4-connected trithiophene with 2,5-thiophene diol under acidic media by MacDonald-type condensation, followed by oxidation with anhydrous $FeCl_3$ yielded 20π electron S-confused antiaromatic macrocycle. $^1$H NMR studies strongly supported the weakly antiaromatic behaviour of neutral macrocycle. In contrast to the normal tetrathia isophlorin, a confused tetrathia isophlorin can undergo an irreversible two-electron ring oxidation to yield the 18π aromatic mono cation with exocyclic carbonyl group at α-position of confused thiophene ring. $^1$H NMR analysis provided a distinct evidence of the altered electronic characteristics through typical paratropic and diatropic ring current effects for the [4n] and the [4n+2]π electrons systems, respectively. The two-electron oxidation of the antiaromatic macrocycle to the aromatic mono cation has been uniquely proven and these observations were studied through experimental studies including $^1$H NMR, EPR, UV-Vis and single crystal X-ray crystallography and computational studies using TD-DFT, NICS and AICD. These results represent a macrocycle with a structural resemblance to the parent tetrathia isophlorin, which undergoes a reversible two-electron oxidation. Despite the structural resemblance to a confused porphyrin, spectroscopic and computational studies reveal weak paratropic ring current effects in these 20π macrocycles. Unlike the parent isophlorin, the π circuit of 20π confused isophlorin enigmatically dampens the oxidation into its corresponding dication and they display redox properties atypical of parent tetrathia isophlorins. Yet, it does display uncharacteristic irreversible two one-electron oxidations through a typical neutral radical intermediate for the formation of a unique 18π aromatic mono cationic species with exocyclic C=O on the confused thiophene ring, experimental evidence supports the oxidation of an unstable 19π neutral radical, as a transient intermediate. Spectroscopic and structural characterization revealed the substituent dependent macrocycle oxidation unfamiliar to the chemistry of anti-aromatic isophlorinoids.

## III.8: Experimental Section:

An equimolar concentration of S-confused trithiophene and the corresponding thiophene diol were dissolved in 100 ml dry dichloromethane and degassed with Nitrogen for ten minutes. Then, a catalytic amount of boron trifluoride diethyl etherate ($BF_3.OEt_2$) was added under dark using a syringe. After stirring for an hour, fifteen equivalents of $FeCl_3$ were added and stirring was continued for an additional 2 h. Then few drops of triethyl amine were added and the resultant solution was passed through a short basic Alumina column. This mixture was concentrated and further purified by silica gel column chromatography using $CH_2Cl_2$/hexane as eluent. The monocation was generated by two electron oxidation using meerwein salts $[Et_3O]^+[SbCl_6]^-$ to a solution of the free base macrocycle in dry dichloromethane solution. Evaporation of the solvent gave the monocation as a green metallic solid. Monocationic salt of hexachloroantimonate was prepared as per earlier report.

.

### Synthetic procedure for confused isophlorin III.8b:

S-confused trithiophene, **III.7c** (608 mg, 1 mmol ) and thiophene 2,5-diol, **III.7d** (476 mg, 1 mmol ) were dissolved in dry 100 ml $CH_2Cl_2$ and stirred for ten minutes under $N_2$ atmosphere. Catalytic amount of $BF_3.OEt_2$ (0.12mL, 1 mmol ) was added as described above and after oxidation with $FeCl_3$ (2.43g, 15mmol ) for 2 hours. The reaction mixture was passed through short pad of basic alumina column. This crude mixture was purified by silica gel column chromatography gives **III.8b** as brown solid. The resulting solid was recrystallized from $CH_2Cl_2$/hexane. Yield (3.6%).

**$^1$H NMR :** (400 MHz, $CDCl_3$, 298K) δ 9.46 (s, 1H), 6.74-6.72 (m, 2H), 6.41-6.32 (m, 4H). **HRMS:** *m/z*= 1077.8800 (calculated for $C_{44}H_7ClF_{20}S_4$); Observed: 1077.8795 (100.0%). **UV/Vis ($CH_2Cl_2$)**: $\lambda_{max}(\varepsilon)$L mol$^{-1}$cm$^{-1}$ = 412 nm (87092.704). **Crystal data:** $C_{46}H_{11}Cl_5F_{20}S_4$ ($M_r$ = 1249.04), triclinic, space group *P* 1 (no. 1), *a* = 8.198(3), *b* = 10.441(4), *c* = 13.934(5) Å, *α* = 101.832(7)°, *β* = 96.687(9)°, γ = 104.041(8)°, *V* =1115.0(7) Å$^3$, *Z* = 1, *T* = 100 K , $\rho_{cald}$ = 1.860 Mg/m$^3$, $R_{int}$ (all data) = 0.0843, $R_1$ (all data) = 0.1227, $R_w$ (all data) = 0.2298, GOOF = 1.342.

### Synthetic procedure for confused isophlorin, III.10:

The synthetic procedure for **III.10**, is similar to **III.8b**. Yields (3.3%)

**$^1$H NMR:** (400 MHz, $CDCl_3$, 298K) δ 9.52 (s, 1H), 6.72-6.70 (m, 2H), 6.35-6.29 (m, 4H). **HRMS:** *m/z*= 1057.9346 (calculated for $C_{45}H_{10}F_{20}S_4$); Observed: 1057.9344 (100.0%). **UV/Vis ($CH_2Cl_2$)**: $\lambda_{max}$ = 412 nm. **Crystal data:** $C_{49}H_{17}F_{20}S_4$ ($M_r$ = 1113.87), triclinic, space group *P -1*, *a* = 9.507(7), *b* = 16.556(12), *c* = 27.301 (19) Å, *α* = 87.915 (12)°, *β* = 89.873 (14)°, γ = 89.924 (13)°, *V* = 4294 (5) Å$^3$, *Z* = 4, *T* = 100 K , $\rho_{cald}$ = 1.723 Mg/m$^3$, $R_{int}$ (all data) = 0.0822, $R_1$ (all data) = 0.2482, $R_w$ (all data) = 0.2524, GOOF = 0.930

## Synthetic procedure for aromatic monocation $[III.8b]^+$:

The monocation **[III.8b]**$^+$ was obtained, by the addition of $[Et_3O]^+[SbCl_6]^-$ to a solution of the free base macrocycle, **III.8b** (10 mg) in dichloromethane and stirred for 30 minutes under nitrogen atmosphere. Cooling of the solution (-20 to -70 $^\circ$C) in dry ice-acetone bath and layering it with diethyl ether and kept for additional two hour which gave green colored crystals. These obtained green coloured crystal directly submitted to NMR.

**$^1$H NMR**: (400 MHz, Acetonitrile-$d_3$, 293 K) δ -3.71 (s, 1H), 9.35-9.34 (d, $J$ = 4.0 Hz, 1H), 9.40-9.38 (d, $J$ = 8.0 Hz, 1H), 9.96-9.95 (d, $J$ = 4.0 Hz, 1H), 10.10-10.05 (m, 3H). **HRMS:** $m/z$ = 1058.9055 calculated for $(C_{44}H_7F_{20}OS_4)^+$; Observed: 1058.9064 (100.0%). **UV/Vis ($CH_3CN$):** $\lambda_{max}(\varepsilon)$L mol$^{-1}$cm$^{-1}$ = 475nm (67196), 503nm (46062) and Q Bands at 600nm, 674nm and 720nm. **Crystal data:** $C_{52}H_{19}Cl_6F_{20}N_4OS_4Sb$ ($Mr$ = 1558.41), triclinic, space group P -1 (no. 1), $a$ = 13.599(2), $b$ = 14.523(2), $c$ = 15.318(2) Å, $\alpha$ = 90.915(4)°, $\beta$ = 105.079(4)°, $\gamma$ = 92.619(3)°, V =2916.8(7)Å$^3$, Z = 2, T = 100 K , $\rho_{cald}$ = 1.774 Mg/m$^3$, $R_{int}$ (all data) = 0.0332, $R_1$ (all data) = 0.0446, $R_w$ (all data) = 0.0883, GOF = 1.026

## III.9. References:


[1] (a) H. Furuta. T. Asano. T. Ogawa. *J. Am. Chem. Soc*. **1994**, 116, 767−768. (b) P. J. Chmielewski, L. Latos-Grazynski, K. Rachlewicz, T. Glowiak, *Angew. Chem. Int. Ed*. **1994**, 33, 779−781.

[2] T. D. Lash, A. D. Lammer, G. M. Ferrence, *Angew. Chem., Int. Ed*. **2011**, 50, 9718−9721.

[3] T. D. Lash, *Chem. - Asian J*. **2014**, 9, 682−705.

[4] (a) S. K. Pushpan, A. Srinivasan, V. G. Anand, T. K. Chandrashekar, A. Subramanian, R. Roy, K. Sugiura, Y. Sakata, *J. Org. Chem*. **2001**, 66, 153−161. (b) P.-Y. Heo, C.-H. Lee, *Tetrahedron Lett*. **1996**, 37, 197−200. (c) C.-H. Lee, H.-J. Kim, *Tetrahedron Lett*. **1997**, 38, 3935−3938.

[5] (a) N. Sprutta, L. Latos-Grazynski, *Tetrahedron Lett*. **1999**, 40, 8457−8460. (b) I. Schmidt, J. C. Piotr, *Tetrahedron Lett*. **2001**, 42, 6389−6392. (c) T. D. Lash, A. L. Von Ruden, *J. Org. Chem*. **2008**, 73, 9417−9425.

[6] Z. Hu, J. L. Atwood, M. P. Cava, *J. Org. Chem*. **1994**, 59, 8071−80875.

[7] G. R. Geier, III, J. S. Lindsey, *J. Org. Chem*. **1999**, 64, 1596−1603.

[8] (a) C. H. Lee, H. J. Kim, D. W. Yoon, *Bull. Korean Chem. Soc*. **1999**, 20, 276−280. (b) J. S. Reddy, V. G. Anand, *Chem. Commun*. **2008**, 1326−1328.

[9] (a) J. A. Hong, R. Kim, H. J. Yun, J. M. Park, S. C. Shin, Y. H. Kim, *Bull. Korean Chem. Soc*. **2013**, 34, 1170−1174. (b) Y. L. Gol'dfarb, Y. Vol'kenshtein, B. Lopatin, *Zhurnal Obshchei Khimii*. **1964**, 34, 969−77. (c) J. A. Ewen, M. J. Elder, R. L. Jones, A. L. Rheingold, L. M. Liable-Sands, R. D. Sommer, *J. Am. Chem. Soc*. **2001**, 123, 4763−4773.

[10] T. D. Lash, M. A. Muckey, M. J. Hayes, D. Liu, J. D. Spence, G. M. Ferrence, *J. Org. Chem*. **2003**, 68, 8558−8570.

[11] E. Vogel, M. Phol, A. Herrmann, T. Wiss, C. Konig, J. Lex, M. Gross, J. P. Gisselbrecht, *Angew. Chem. Int. Ed.* **1996**, 35, 1520−1524.

[12] S. P. Panchal, S. C. Gadekar, V. G. Anand, *Angew. Chem., Int. Ed*. **2016**, 55, 7797−7800.

[13] P. V. R. Schleyer, C. Maerker, A. Dransfeld, H. J. Jiao, N. J. R. V. Hommes, *J. Am. Chem. Soc*. **1996**, 118, 6317−6318.

[14] (a) B. K. Reddy, A. Basavarajappa, M. D. Ambhore, V. G. Anand, *Chem. Rev*. **2017**, 117, 3420−3443. (b) T. Y. Gopalakrishna, J. S. Reddy, V. G. Anand, *Angew. Chem., Int. Ed*. **2013**, 52, 1763−1767.

(c) M. kon-no, J. Mack, N. Kobayashi, M. Suenaga, K. Yoza, T. Shinmyozu, *Chem. - Eur. J*. **2012**, 18, 13361−13371.

[15] R. A. Rathore, S. Kumar, S. V. Lindeman, J. K. Kochi, *J. Org. Chem*. **1998**, 63, 5847−5856.

# Chapter IV

# Synthesis, Characterization and Redox Properties of 28π Azulene Appended Antiaromatic Expanded Isophlorins

## IV.1. Introduction:

Synthesis of pyrrole based isophlorin[1] and the S-confused derivative revealed contrasting two-electron oxidation of 4nπ systems. It can be perceived that the components of the antiaromatic system are crucial to the macrocyclic oxidation. However, not many examples of such modified isophlorins have been studied to arrive at an empirical understanding of the redox process. In contrast to the unique metal co-ordination properties of the carba porphyrins, electronic properties of antiaromatic carba-isophlorin are atypical of a porphyrinoid due to the unsymmetrical connectivity of the heterocyclic units. In this regard, the presence of one or more carbon atoms in the core of isophlorinoid macrocycles induces contrasting π conjugation and the resulting ring current effects. This was clearly observed with 20π mono-benzene and 30π dibenzo expanded isophlorinoids[2]. It was observed that the 20π system resisted the global conjugation effect in support of a strong 6π diatropic ring current of the benzene. On the other hand, the 30π expanded isophlorin displayed significant diatropic ring current effects. Therefore, it can be envisaged that the connectivity between the benzene rings are crucial to the stabilization of globalized ring current effects in such isophlorin macrocyclic network. In this chapter, the objective is to synthesize azulene appended expanded isophlorin because of its redox active nature and its utility in the construction large number of redox active molecules. Exploration of this concept led to the synthesis of azuliporphyrins and its heteroanalogues, which exhibit borderline macrocyclic aromaticity and unusual reactivity pathways.[3,4] These azuliporphyrins have unique electronic features, such as near-infrared absorptions, high extinction coefficients, or small HOMO-LUMO gaps[5-11].

Latos-Grazynski and co-workers reported the dithiadiazuliporphyrin[12] and dioxadiazuliporphyrin[13] **(Scheme-IV.1)**. It was observed that azulene reacted with thiophene diol or furan diol leading to the formation of azulene appended porphyrins.

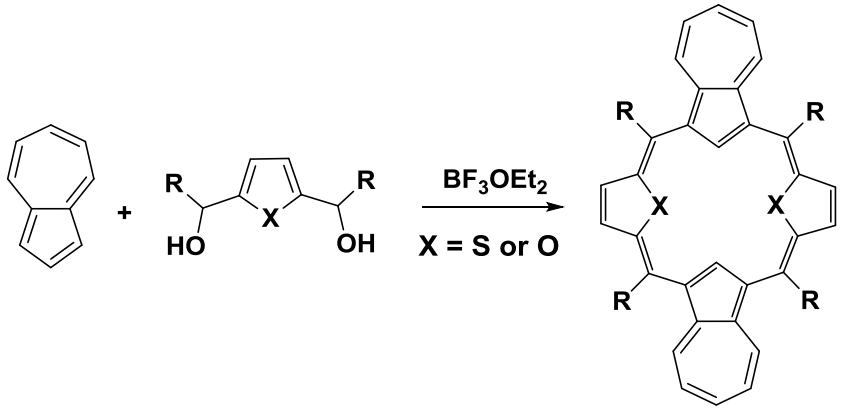


**Scheme-IV.1:** Synthesis of azuliporphyrins.

Further, this non-nitrogenous azuliporphyrins are easily oxidized to its radical cation and dication species. Addition of excess DDQ exclusively lead to the formation of its dication, which was further reduced back to its neutral macrocycle using $SnCl_2$ **(Scheme-IV.2)**.

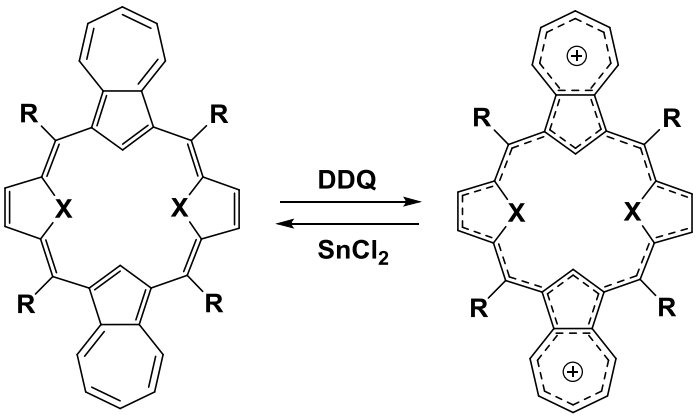


**Scheme-IV.2**: Dication formation of azuliporphyrins.

It is very well known that expanding the π network of isophlorin is an ideal strategy to synthesize large and stable 4nπ macrocycles. Molecules containing extended π-electron chromophores are of interest because of their potential for applications in optoelectronics, electrochromic, or molecular conductivity.[14,15] These systems are expected to have different properties compared to the aromatic counterparts and if the parent azulene appended porphyrin is expanded by inserting an additional two other heterocycles other than pyrrole, the formed macrocycle will be expected to form a 28π electron expanded isophlorin. Unlike the nitrogen, the chalcogens are not capable of sustaining a double bond with α carbons in the heterocyclic unit, and hence, the π circuit is forced to flow only through the carbon atoms.

## IV.2. Synthesis:

Anticipating analogous macrocycles under identical reaction conditions, a catalytic amount of boron trifluoride etherate was added to an equimolar ratio of bithiophene diol[16] and azulene in dichloromethane solvent **(Scheme-IV.3)**. After stirring this solution under dark for one hour, DDQ was added to the reaction mixture with continued stirring for additional two hours. MALDI-TOF/TOF mass spectrum of reaction mixture confirmed the formation of expected macrocyclic composition containing two bithiophene units connected to two azulene rings **(Figure-IV.1)**.

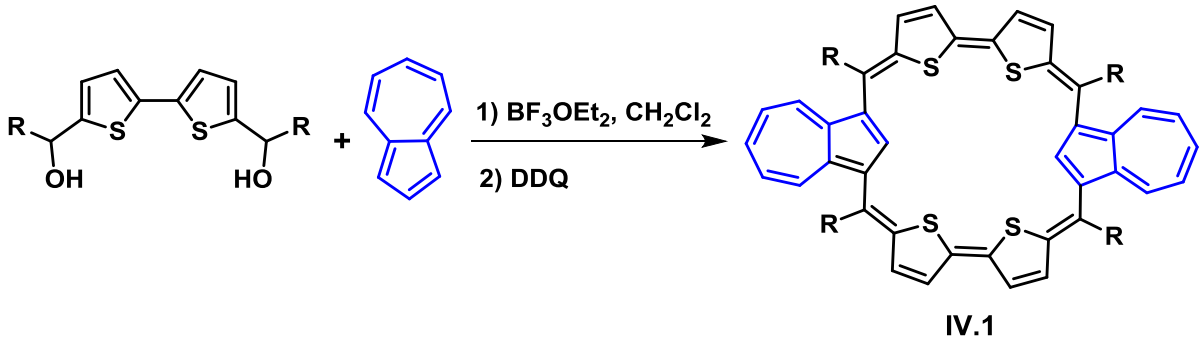


**Scheme-IV.3:** One pot synthesis of azulene appended expanded isophlorin.

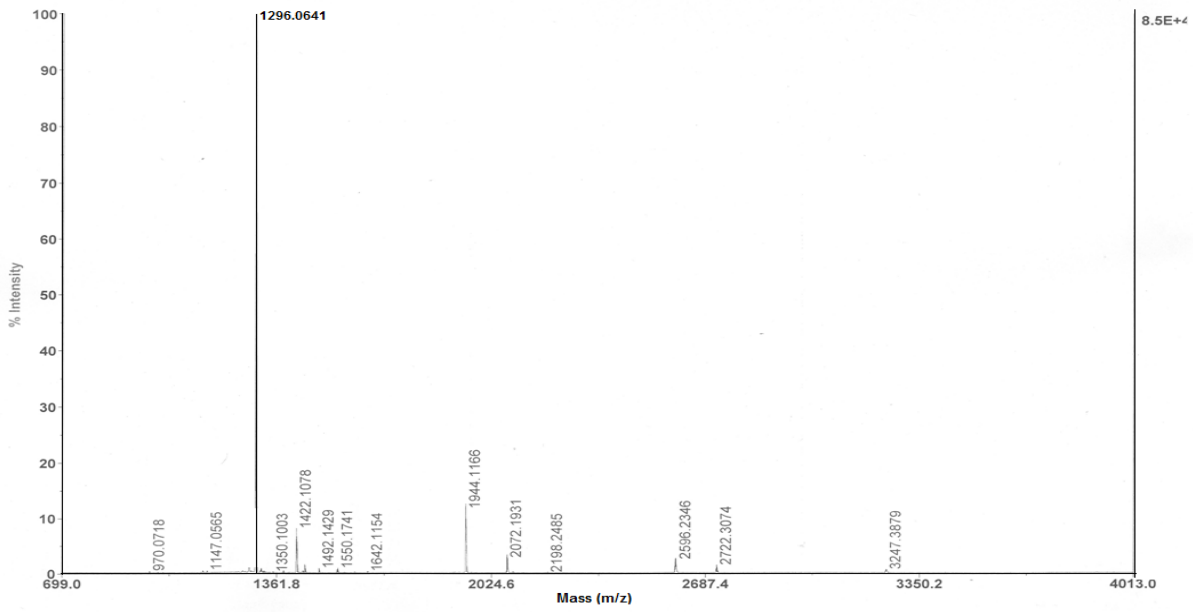


**Figure-IV.1:** MALDI-TOF/TOF mass spectrum of reaction mixture **(Scheme-IV.3)**.

## Results and Discussions:

### IV.3. Spectral Characterization:

The above separated molecule was analyzed by analytical tools such as, high resolution mass spectrometry, UV-Vis, NMR spectroscopy and single-crystal X-ray crystallography. High resolution mass spectroscopy displayed the exact compositions of formed macrocycle.

### IV.4. Isolation and characterization:

The reaction was stopped after two hours and the solution was passed through short pad of basic alumina and further purification through basic alumina column chromatography led to the isolation of expected

macrocycle. This 28π electron azulene appended macrocycle **(IV.1)** was isolated as a brown coloured solution eluted with $CH_2Cl_2$/Petrolium ether (4%) which displayed a sharp and an intense absorption band at 498nm (ε = 77800) **(Figure-IV.2)**. In its high resolution mass spectrum **(Figure-IV.3)**, the molecule displayed its molecular ion peak at *m/z* value of 1296.0140 ($C_{64}H_{20}F_{20}S_4$: Cald: 1296.0128).

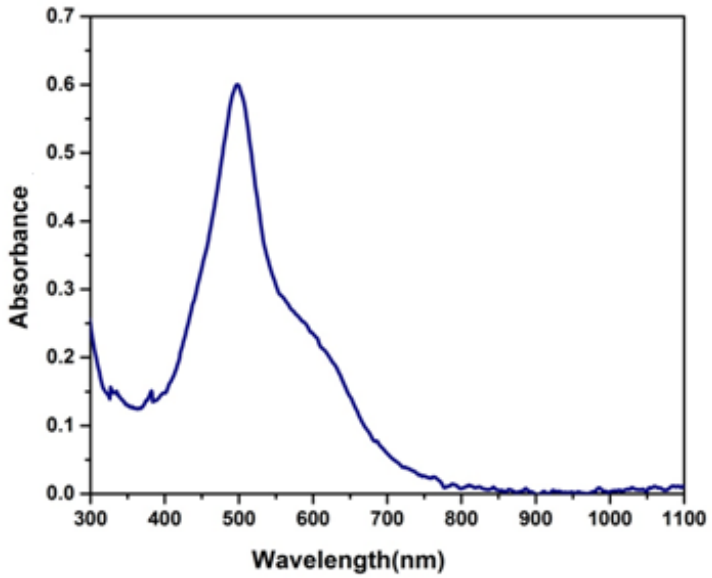


**Figure-IV.2:** UV-Visible spectrum of **IV.1**.

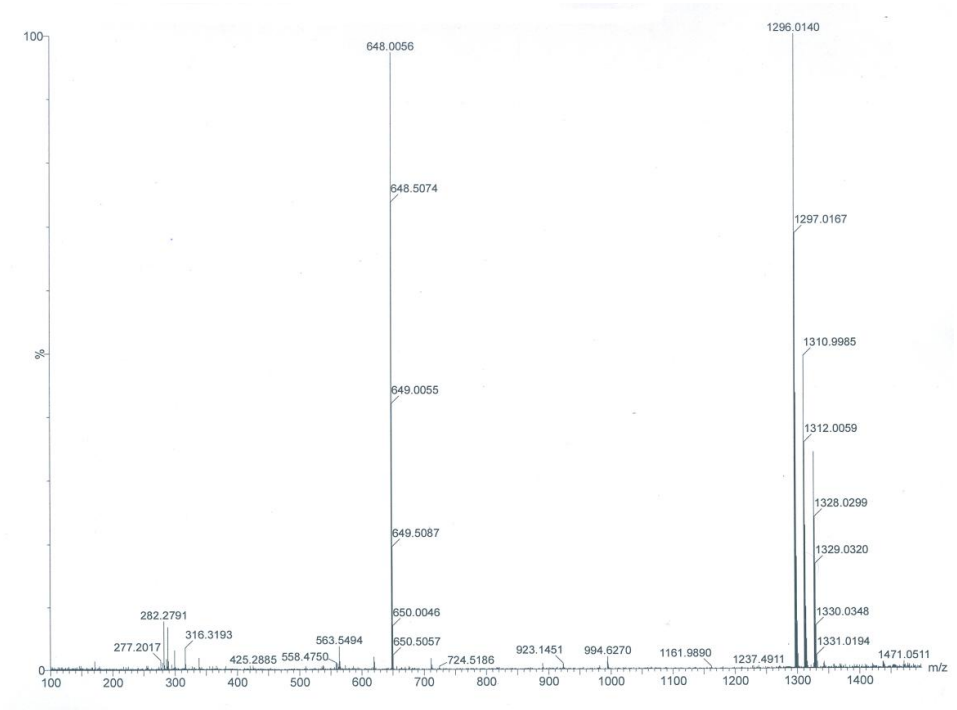


**Figure-IV.3:** High-resolution mass spectrum of **IV.1**.

## IV.5. NMR Characterization of IV.1:

The formed macrocycle, **IV.1** consists of 28π electron conjugated expanded isophlorin. In its $^{1}$H NMR the molecule displayed a total of six different signals and out of these, five signals corresponded to two β-protons of thiophene ring and azulene's seven membered ring protons **(Figure-IV.4)**. Three doublets at 7.81, 7.50 and 6.83 ppm and two triplets at 7.60 and 7.11 ppm corresponds to two thiophene protons and one azulene protons. The inner CH proton in this case was observed at 9.45 ppm. Further, this small difference between peripheral and inner protons was reflective of its weak antiaromatic character of **IV.1**. $^{1}$H-$^{1}$H 2D COSY spectrum **(Figure-IV.5)** recorded at 298K clearly displayed expected correlations amongst the peripheral protons of thiophene and azulene.

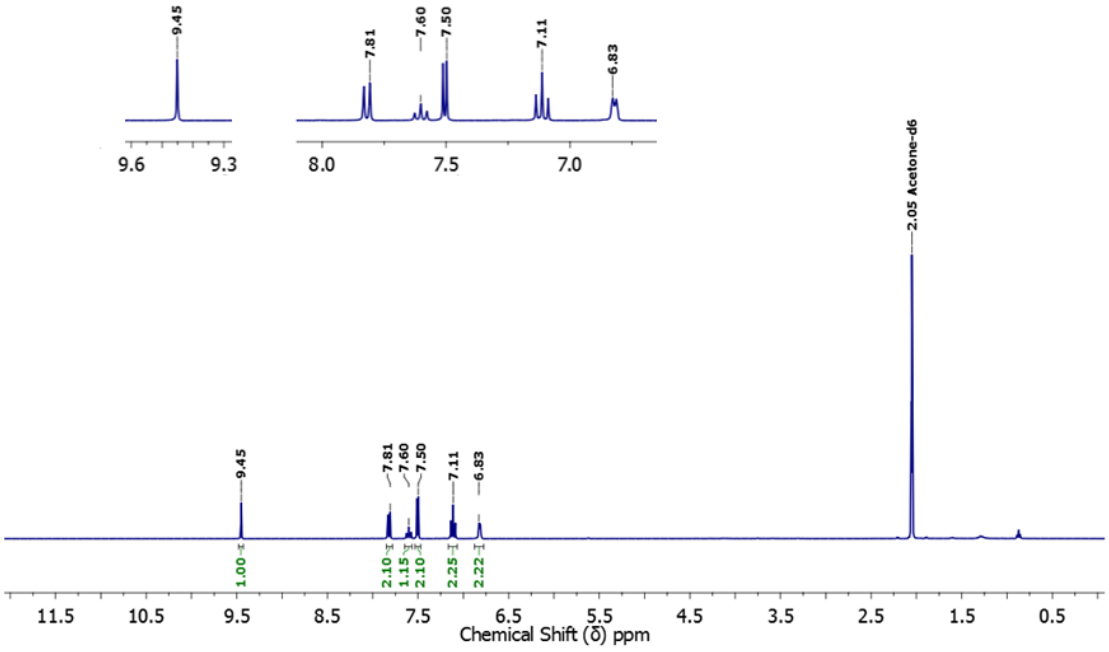


**Figure-IV.4:** $^{1}$H NMR spectrum of **IV.1** in Acetone-$d_6$ at 298K.

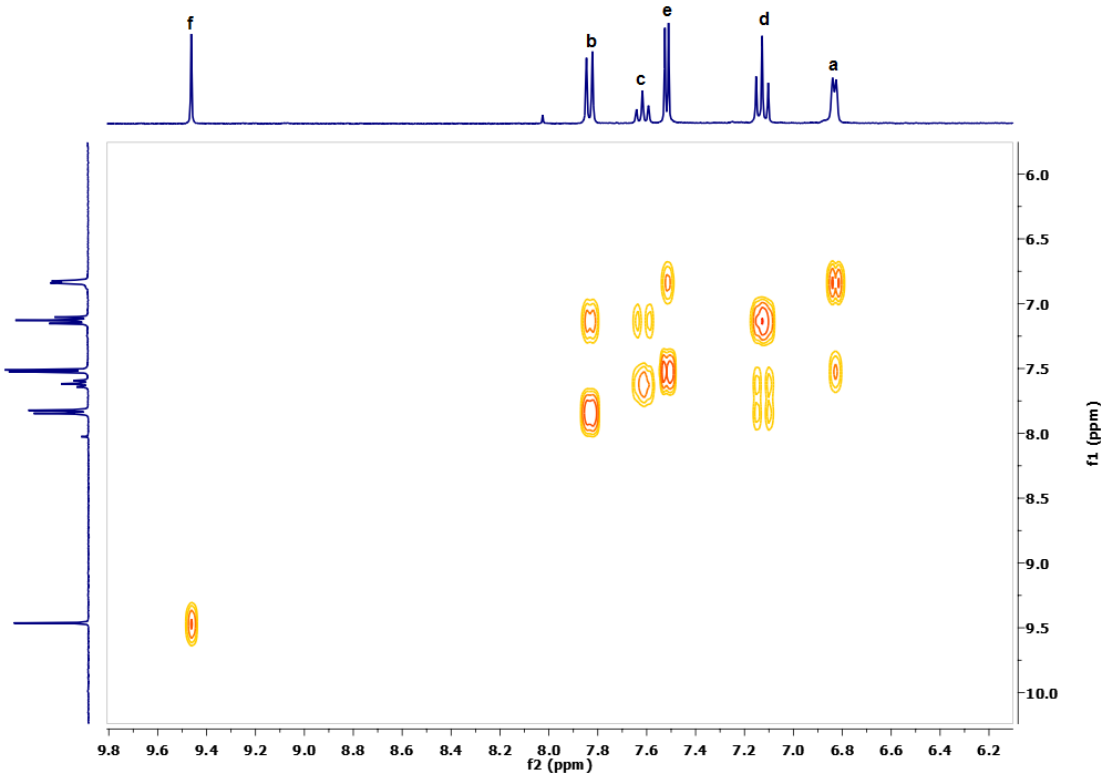


**Figure-IV.5:** $^{1}$H-$^{1}$H 2D COSY spectrum of **IV.1** in Acetone-$d_6$ at 298K.

## IV.6. Two electron oxidation of IV.1:

Antiaromatic compounds are known to undergo two electron oxidation leading to the formation of corresponding dicationic aromatic species. Hence **IV.1** was subjected to oxidation by employing Meerwein's salts as the oxidizing agent[17]. Addition of meerwein's salts to the brown coloured dichloromethane solution of **IV.1** immediately induced the colour change from brown to purple coloured solution indicative of its oxidation **(Scheme-IV.4)**. This purple coloured solution displayed a red shifted UV-Vis absorption at $\lambda_{max}$ = 640nm (ε = 92500) with increased intensity, followed by two weak and broad absorptions **(Figure-IV.6)** at 414nm (ε = 41200) and 777m (ε = 13100), indicating its aromatic character of dicationic, **IV.2** species.

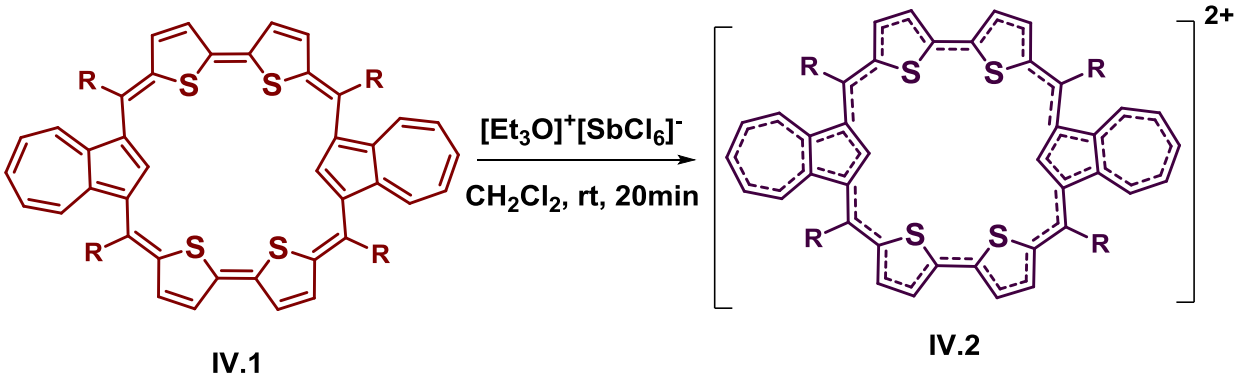


**Scheme-IV.4:** Two electron oxidation of **IV.1**.

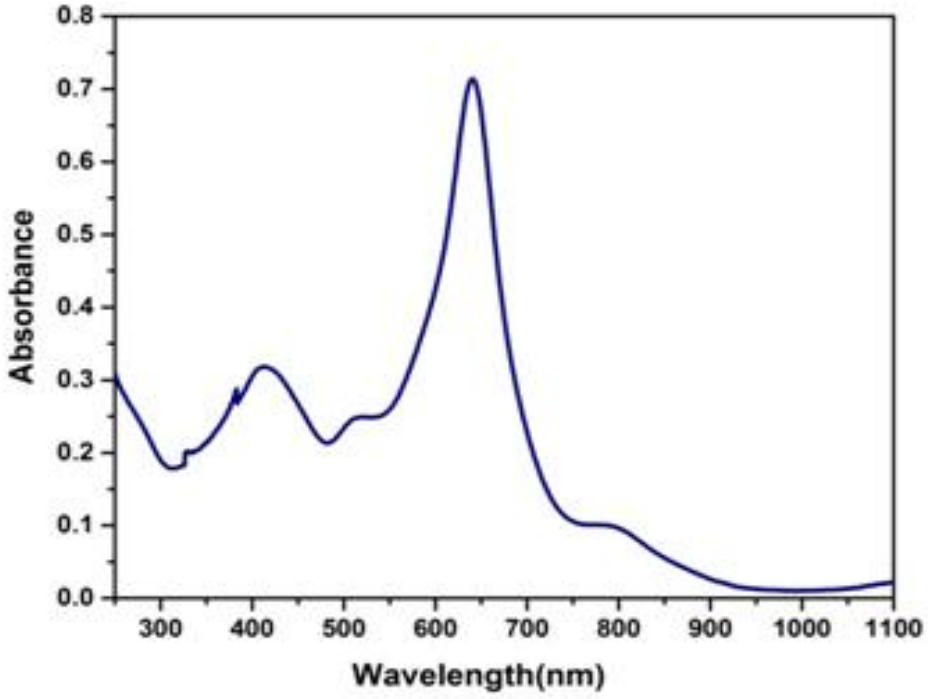


**Figure-IV.6:** UV-Vis absorption spectrum of **IV.2**.

The formed purple coloured solution after oxidation was cooled (dry ice acetone bath) and layered with diethyl ether which yielded dark purple coloured crystals of **IV.2 (Scheme-IV.4)**. The ESI-TOF high-resolution mass spectrum of these purpled coloured crystals displayed an *m/z* value of 648.0060 (Cald. for $[C_{64}H_{20}F_{20}S_4]^{2+}$: 648.0070) corresponding to the dication species of the macrocycle **IV.2 (Figure-IV.7)**. Interestingly, this value suggested an oxidative process without altering the chemical composition of the macrocycle. The oxidation of the macrocycle by two electrons suggested the formation of 26π aromatic dication **IV.2**.

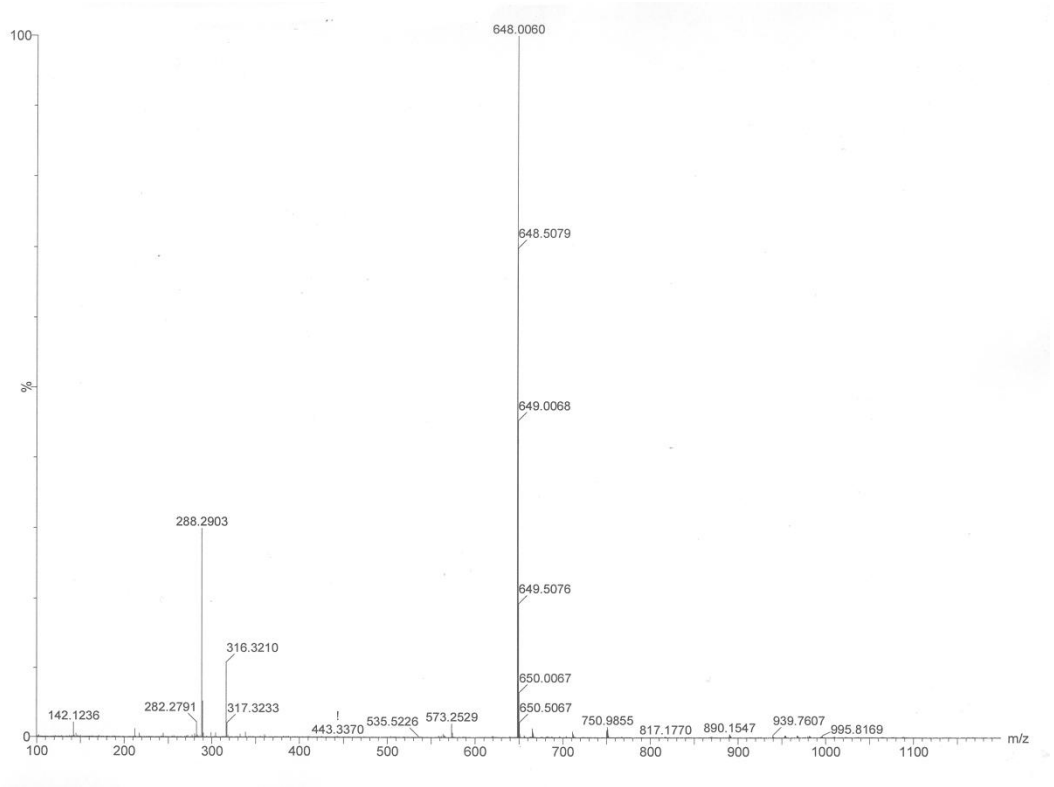


**Figure-IV.7:** High-resolution mass spectrum of **IV.2**.

## IV.7. NMR Characterization of IV.2:

After the oxidation the purple coloured solution was cooled in dry ice acetone bath and layered with diethyl ether which yielded golden coloured crystals. The $^{1}H$ NMR spectrum recorded at 298K obtained by dissolving these crystals of **IV.2**, in deuterated acetonitrile ($CD_3CN$) the macrocycle displayed a singlet in the up field region at -1.99 ppm and the peripheral protons corresponding to thiophene and azulene protons were found to be resonated in the down field region between 10.5 to 8.5 ppm **(Figure-IV.8)**. Such a downfield shift of peripheral protons and upfield shift of inner CH proton confirmed the presence of diatropic ring current effect expected for 26π aromatic dication upon two electron oxidation of the antiaromatic macrocycle. All efforts to grow good quality crystals of dication **IV.2** for single crystal X-ray diffractometer went futile.

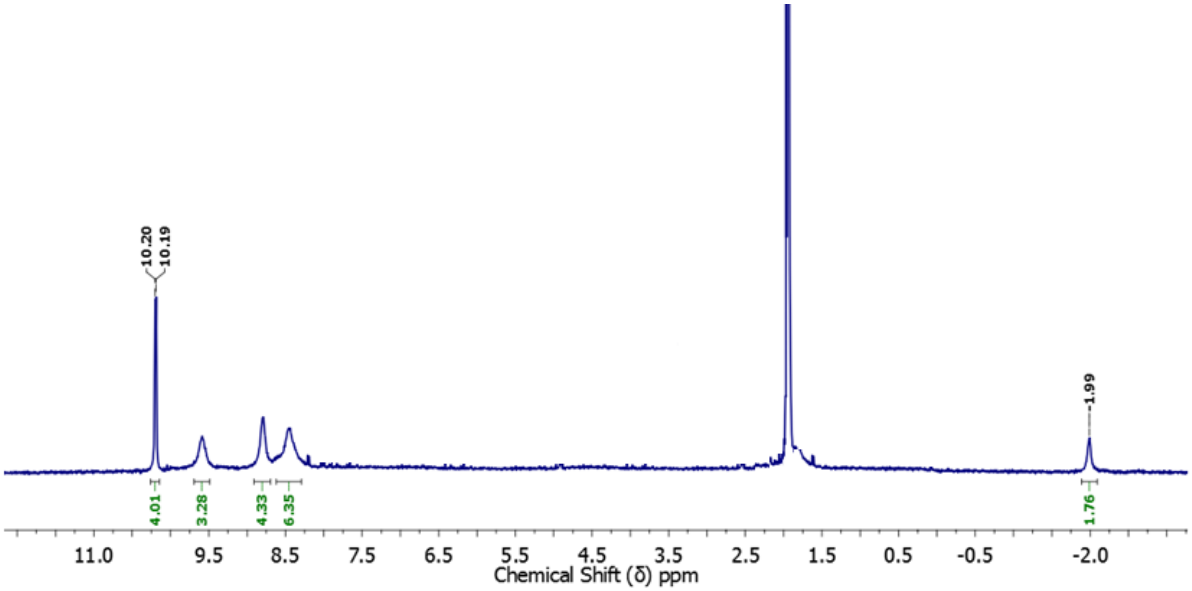


**Figure-IV.8:** $^{1}$H NMR spectrum of **IV.2** in Acetonitrile-$d_3$ at 298K.

## IV.8. Chemical reversibility:

The oxidation of 28π electron macrocycle **IV.1** to the 26π dicationic species **IV.2** was achieved either by addition of $[Et_3O]^+[SbCl_6]$ or $[NO]^+[BF_4]^-$ as a one-electron oxidant. The subtle change in the colour of the solution from brown to purple colour upon oxidation was observed with both the oxidants. This purple coloured solution displayed an absorption at $\lambda_{max}$ = 640 nm which is red shifted compared to neutral species in **IV.2** confirmed the formation of dicationic species. Further we were curious to check its chemical reversibility by adding zinc powder to the dicationic solution. After addition of zinc powder, the colour of the solution changed from purple to brown **(Scheme-IV.5)** and this redox change was observed by electronic absorption spectroscopy. The brown coloured solution displayed a blue shifted absorption which resembled and overlapped with free base macrocycle **IV.1**, indicating its complete chemical reversibility from dication **IV.2** to free base **IV.1**. It was observed that both the states of **IV.1** and **IV.2** were found to stable at ambient temperature.

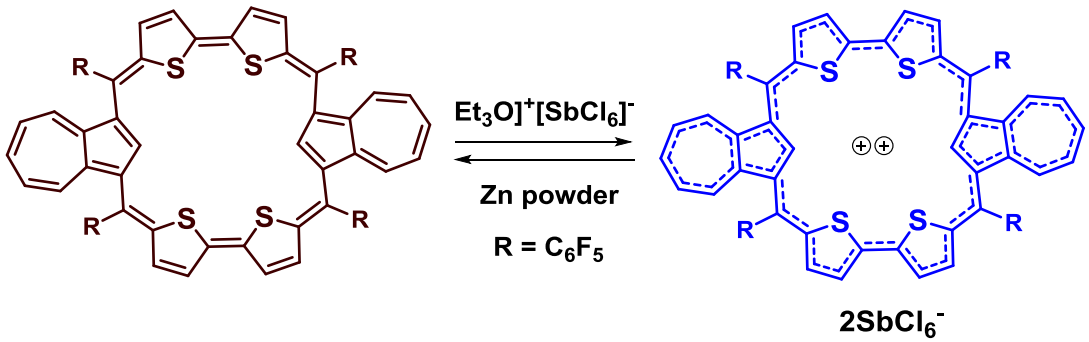


**Scheme-IV.5:** Chemical reversibility of **IV.2** to **IV.1**.

To confirm the molecular structure of **IV.1**, good quality crystals were grown by using solvent diffusion method. The molecule crystallizes in triclinic system with P -1 space group and it shows bowl shaped conformation in which four opposite thiophene rings are in near plane with all the sulphur atoms are pointed towards the centre of the macrocycle **(Figure-IV.9)**. Two opposite azulene rings form a dihedral angle of 39.78° with the plane of macrocycle consisting of four thiophene rings.

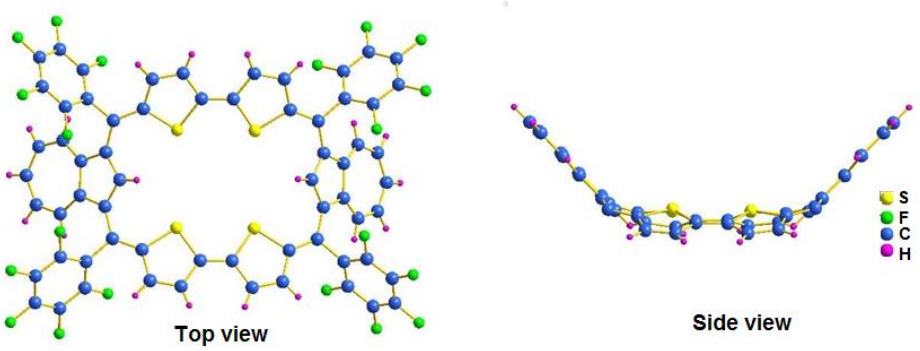


**Figure-IV.9:** Molecular structure for IV.1

## IV.9. Quantum mechanical calculations:

The antiaromatic character of the formed 28π electron expanded isophlorin was further confirmed by Nucleus Independent Chemical shift (NICS) calculations[18]. The calculated NICS value at ring centre for **IV.1** was found to be 1.31 ppm indicating its weak antiaromatic nature **(Table-IV.1)**. Further, the dication **IV.2** displayed a NICS value at -6.95 ppm calculated at the ring centre suggesting significant aromatic character for **IV.2** and this equally matched with diatropic ring current effects in its $^{1}$H NMR spectrum **(Figure-IV.8).**

| NICS | Ring Current | Aromaticity |
|---|---|---|
| **-6.95 ppm (IV.2)** | **Diatropic** | **Aromatic** |
| **+1.31 ppm (IV.1)** | **Weakly paratropic** | **Weakly antiaromatic** |

**Table-IV.1:** NICS and ring currents.

## IV.10. Conclusion:

When bithiophene diol reacts with azulene under acidic conditions followed by oxidation with DDQ lead to the formation of azulene appended expanded isophlorin which is a 28π macrocycle. This molecule displayed a weakly antiaromatic character which was confirmed through its $^{1}$H NMR spectroscopy and by using theoretical studies such as NICS values. After two electron oxidation using meerwein's salt, the molecule displayed significant diatropic ring current effect confirmed by the resonance of its inner CH proton in the up field region of its $^{1}$H NMR spectrum. In support of the observation, the estimated NICS value suggested a significant aromatic character for the dicationic species. The chemical reversibility of the dication to its antiaromatic neutral state was established and found that the dication is completely reversible to its free base macrocycle upon addition of a reducing agent such as zinc powder. The confirmation of this reversibility was obtained through electronic absorption spectroscopy. Both the states of the macrocycles were found to be stable at ambient temperature. Single crystal X-ray diffraction studies revealed a non planar structure for freebase macrocycle and the molecule adopted a bowl shaped structure in which four thiophene rings are in near plane of the macrocycle and two opposite azulene rings were tilted from mean plane of the macrocycle. These observations clearly suggest that extension of the π conjugation of azuliporphyrins by the addition of two thiophene rings inside the macrocyclic core does not significantly alter the ring current effects. However, upon oxidation the molecule displayed significant ring current effects and these observations suggest the possibility of fine tuning the properties of azulene appended expanded isophlorin.

## IV.11. Experimental Section:

**General synthetic procedure for IV.1:** Azulene (25.02mg, 0.195mmol) and bithiophene diol (109.00mg, 0.195mmol) were dissolved in dry dichloromethane solution (300mL) and degassed with nitrogen for ten minutes. Then catalytic amount $BF_3OEt_2$ (0.024mL, 0.195mmol) was added under dark using syringe. After stirring the reaction mixture for an hour was added DDQ (132.93mg, 0.585mmol) and further continued stirring for an additional 2 h. Then few drops of triethyl amine was added and the resultant solution was passed through the short pan of basic alumina column. Further concentration of reaction mixture under reduced pressure and purified by basic alumina column chromatography using $CH_2Cl_2$/hexane as eluent isolated a brown solid corresponding to free base macrocycle in yield 4%.

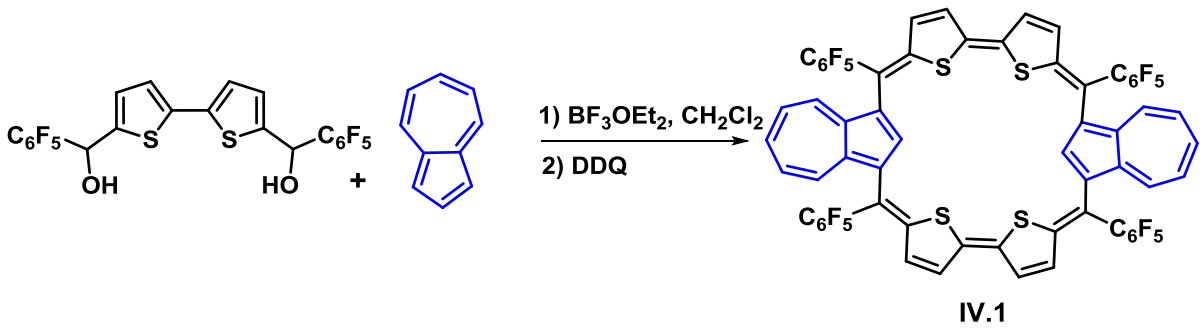


**IV.1**

**$^1$H NMR**: (400 MHz, Acetone-$d_6$, 298 K) δ 9.45 (s, 1H), 7.83-7.81 (d, *J* = 8.0 Hz, 2H), 7.63-7.58 (t, *J* = 8.0 Hz, *J* = 12.0 Hz 1H), 7.51-7.50 (d, *J* = 4.0 Hz, 2H), 7.14-7.09 (t, *J* = 12.0 Hz, *J* = 8.0 Hz 2H), 6.83-6.81 (d, *J* = 8.0 Hz, 2H). **HRMS** (ESI-TOF): *m/z* = 1296.0128 calculated for ($C_{64}H_{20}F_{20}S_4$) **IV.1**; Observed: 1296.0140 (100.0%). **UV/Vis** ($CH_2Cl_2$): $\lambda_{max}$ (ε) L mol$^{-1}$cm$^{-1}$ = 498 nm (77800). **Crystal data:** $C_{64}H_{20}F_{20}S_4$ (*Mr* = 1573.82), triclinic, space group P -1, *a* = 12.034 (4), *b* = 16.046 (5), *c* = 17.758 (5) Å, *α* = 72.188 (7)°, *β* = 80.299 (7)°, *γ* = 70.456 (7)°, V = 3068.2 (17)Å$^3$, Z = 2, T = 100 K , $D_{calcd}$ = 1.704 g cm$^{-3}$, $R_{int}$ (all data) = 0.0894, $R_1$ (all data) = 0.1586, $R_w$ (all data) = 0.2554, GOF = 1. 328.

### Synthetic procedure for IV.2:

The dication **IV.2**, was generated by the addition of $[Et_3O]^+[SbCl_6]^-$ or $NOBF_4$ to a solution of the macrocycle, **IV.1** (10 mg) in dry dichloromethane and the resulting solution was stirred for 10 minutes under nitrogen atmosphere at room temperature. The brown coloured solution immediately changes to purple colour and this solution was further stirred for additional 20min and the solution was cooled in dry ice-acetone bath. This cooled solution then layered with diethyl ether and kept for additional two hour. The golden coloured crystals were obtained after keeping this solution undisturbed. These purple colored crystals directly submitted to NMR.

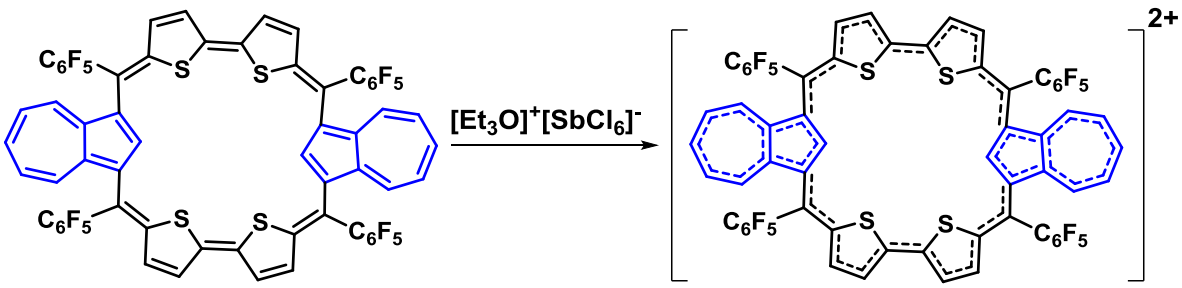


**IV.1** **IV.2**

**$^1$H NMR**: (400 MHz, Acetonitrile-$d_3$, 298 K) δ -1.99 (s, 1H), 10.20-10.19 (d, *J* = 4.0 Hz, 2H), 9.59 (broad, 2H), 8.79 (broad, 2H), 8.44 (broad, 3H). **HRMS** (ESI-TOF): *m/z* = 648.0064 calculated for ($C_{64}H_{20}F_{20}S_4$) **IV.1**; Observed: 648.0060 (100.0%). **UV/Vis** ($CH_2Cl_2$): $\lambda_{max}$ (ε) L $mol^{-1}cm^{-1}$ = 640 nm (92480) and 777nm (13110).

## IV.12. References:


[1] S. P. Panchal, V. G. Anand, *Angew. Chem. Int. Ed.* **2016**, 55, 7797-7800

[2] J. S. Reddy, V. G. Anand. *Chem. Commun*, **2008**, 1326-1328.

[3] D. A. Colby, T. D. Lash, *Chem. Eur. J*. **2002**, 8, 5397-5402.

[4] (a) S. R. Graham, G. M. Ferrence, T. D. Lash, *Chem. Commun*. **2002**, 894-895. (b) T. D. Lash, S. T. Chaney, *Angew. Chem., Int. Ed.* **1997**, 36, 839-840. (c) T. D. Lash, *Chem. Commun*. **1998**, 1683-1684. (d) S. R. Graham, D. A. Colby, T. D. Lash, *Angew. Chem. Int. Ed*. **2002**, 41, 1371-1374. (e) T. D. Lash, D. A. Colby, S. R. Graham, G. M. Ferrence, L. F. Szczepura, *Inorg. Chem*. **2003**, 42, 7326-7338. (f) D. A. Colby, G. M. Ferrence, T. D. Lash, *Angew. Chem. Int. Ed*. **2004**, 43, 1346-1349. (g) T. D. Lash, D. A. Colby, S. R. Graham, S. T. Chaney, *J. Org. Chem*. **2004**, 69, 8851-8864

[5] S. H. Gill, M. Harmjanz, J. Sanyamara, I. Finger, M. J. Scott, *Angew. Chem. Int. Ed*. **2004**, 43, 485.

[6] R. Kumar, R. Misra, T. K. Chandrashekar, E. Suresh, *Chem. Commun*. **2007**, 43.

[7] C. Lambert, G. Noll, M. Zabel, F. Hampel, E. Schmalzlin, C. Brauchle, K. Meerholz, *Chem.-Eur. J.* **2003**, 9, 4232.

[8] K. Kurotobi, K. S. Kim, S. B. Noh, D. Kim, A. Osuka, *Angew. Chem. Int. Ed*. **2006**, 45, 3944.

[9] J.-H. Chou, H. S. Nalwa, M. E. Kosal, N. A. Rakow, K. S. Suslick. In *The Porphyrin Handbook*, K. M. Kadish, K. M. Smith, R. Guilard, Eds. Academic Press: San Diego, CA, **2000**, 43.

[10] D. H. Yoon, S. B. Lee, K.-H. Yoo, J. Kim, K. J. Lim, N. Aratani, A. Tsuda, A. Osuka, D. Kim, *J. Am. Chem. Soc*. **2003**, 125, 11062.

[11] D. Seidel, V. Lynch, J. L. Sessler, *Angew. Chem. Int. Ed.* **2002**, 41, 1422.

[12] N. Sprutta, M. Swiderska, L. Latos-Grazynski, *J. Am. Chem. Soc*. **2005**, 127, 13108-13109.

[13] N. Sprutta, M. Siczek, L. Latos-Grazynski, M. Pawlicki, L. Szterenberg, and T. Lis. *J. Org. Chem*. **2007**, 72, 9501-9509.

[14] P. M. S. Monk, R. J. Mortimer, D. R. Rosseinsky, *Electrochromism: Fundamentals and Applications*, VCH: Weinheim, Germany **1995**.

[15] E. Coronado, J. R. Galan-Macaros, *J. Mater. Chem*. **2005**, 15, 66

[16] A. Srinivasan, V. M. Reddy, S. J. Narayanan, B. Sridevi, S. K. Pushpan, M. Ravikumar, T. K. Chandrashekar, *Angew. Chem. Int. Ed.* **1997**,36, 2598

[17] R. A. Rathore, S. Kumar, S. V. Lindeman, J. K. Kochi, *J. Org. Chem*. **1998**, 63, 5847−5856.

[18] P. V. R. Schleyer, C. Maerker, A. Dransfeld, H. J. Jiao, N. J. R. V. Hommes, *J. Am. Chem. Soc*. **1996**, 118, 6317−6318.

# Summary of the thesis

This thesis describes the synthesis, characterization and redox properties of a stable pyrrole derivative isophlorin, first generation confused isophlorin and azulene appended expanded isophlorin which were synthesized from easy to make and air stable precursors. Even though all the macrocycles are classified as antiaromatic systems, they displayed different structural, electronic and redox properties. Detailed analyses and spectroscopic characterization of these isolated macrocycles distinguished the properties of the macrocycles in terms of their structural features, electronic properties and redox potential. The most significant aspect of this thesis is in the discovery of first stable pyrrole based 20π antiaromatic isophlorin and confused isophlorin macrocycle and their dicationic species. These novel reports could have been more attractive with higher synthetic yields of the isolated macrocycles. Nevertheless, they can attract significant attention for their diverse redox behaviour as exemplified by the nature of oxidized product obtained from these antiaromatic macrocycles. Irrespective of the structural features, all of them underwent two electron oxidations leading to the formation of (4n+2)π electrons dications and monocation. The 18π dication and monocation derived from oxidation of 20π macrocycles was found to be aromatic from their $^{1}$H NMR spectrum and also form the estimated NICS values. Further, the azulene appended expanded 28π macrocycle displayed it's weakly antiaromatic character and significant aromatic character upon oxidation to its dication. The azulene containing expanded isophlorins differ in structure and photo physical properties in comparison to their parent 20π macrocycle. Both pyrrole based and azulene isophlorin macrocycle underwent reversible two electron reduction to its free base macrocycles. This change was confirmed through electronic absorption spectroscopy indicating its ability to sustain reversible oxidation. The 20π tetrathia-confused isophlorin displayed an irreversible two electron oxidation to its aromatic cation which does not undergo its two electron reduction to its free base macrocycle. Further, experimental and computational studies confirmed its antiaromatic and aromatic character for the neutral and oxidized states respectively. In conclusion, this thesis reveals the unexplored aspects of isophlorin and confused isophlorin. In support of earlier reports on isophlorin's redox properties, it establishes that antiaromatic molecules possess redox characteristics dissimilar to the aromatic counterparts. More importantly, their variable oxidation states are stable enough to be isolated and characterized comprehensively. Since they possess reversible and active redox stable states compared to aromatic molecules, it is expected that the findings described in this thesis would encourage the role of isophlorin and its expanded derivatives as potential candidates for applications in organic electronics.